

Rochester Institute of Technology

RIT Digital Institutional Repository

Theses

4-2-2014

Optical Heterodyne Detection of Phase-Shifted Signals

Daria Permeneva

Follow this and additional works at: <https://repository.rit.edu/theses>

Recommended Citation

Permeneva, Daria, "Optical Heterodyne Detection of Phase-Shifted Signals" (2014). Thesis. Rochester Institute of Technology. Accessed from

This Thesis is brought to you for free and open access by the RIT Libraries. For more information, please contact repository@rit.edu.



Optical Heterodyne Detection of Phase-Shifted Signals

Daria Permeneva

Thesis Prepared for the Degree of
Master of Science in Telecommunications Engineering Technology

Thesis Advisor

Drew N. Maywar, Ph.D.

Electrical, Computer and Telecommunications Engineering Technology
College of Applied Science and Technology

Rochester Institute of Technology

Rochester, NY

4/2/2014

Optical Heterodyne Detection of Phase-Shifted Signals

Daria Permeneva

MS Telecommunications Engineering Technology Program
Electrical, Computer, and Telecommunications Engineering Technology
College of Applied Science and Technology
Rochester Institute of Technology
Rochester, New York

MS Thesis Supervisor: Drew Maywar

MS Thesis Defense: 2 April 2014

Approved by

Dr. Drew N. Maywar, Assistant Professor
Electrical, Computer, and Telecommunications Engineering Technology

Dr. Miguel Bazdresch, Assistant Professor
Electrical, Computer, and Telecommunications Engineering Technology

Mark J. Indelicato, Associate Professor
Electrical, Computer, and Telecommunications Engineering Technology

Abstract

Optical Heterodyne Detection of Phase-Shifted Signals

Daria Permeneva

My thesis investigates whether abrupt changes in optical phase (i.e., phase shifts) can be measured using optical heterodyne detection (OHD), a method commonly used to measure gradual changes in the temporal phase. I developed analysis software in MATLAB to consider and quantify the success of three different phase-shift measurement methods: non-split signal method, split signal method and split signal with zero-out method. I also explored whether spectral information can be used to access temporal phase shifts; this is a new area, as OHD typically deals with temporal information. My work identified both spectral and temporal phase assessment methods that provide high precision results.

Acknowledgements

I would like to express enormous gratitude to my thesis adviser Prof. Drew Maywar. His guidance and motivation gave me desire to continue my education and confidence to pursue thesis. Prof. Maywar spent endless hours working with me on the research and answering all my questions. I would never have been able to complete my thesis without his continuous support, immense knowledge and enthusiasm.

Special thanks go to Dr. David Aronstein for providing ideas about Fourier Shift Theorem.

Thank you to Prof. Mark Indelicato and Prof. Miguel Bazdresch for taking the time to be on my thesis committee.

I also want to thank all faculty and staff of the TET department who continuously helped and supported me through my education and made my time at RIT enjoyable and exciting.

I especially thank my family who provided unconditional love, support, care and encouragement. I love them so much and deeply appreciate all they do for me.

Contents

Table of Contents	i
1 Introduction	1
1.1 Background	1
1.2 Phase detection	3
1.2.1 Temporal mixed signal	3
1.2.2 Spectral mixed signal	4
1.2.3 Filtered spectral mixed signal	6
1.2.4 Filtered temporal mixed signal	7
1.2.5 Phase of filtered temporal mixed signal	8
1.3 Details on Coupling and Mixing	10
1.4 Summary of Optical Heterodyne Detection	14
2 Numeric Computations	15
2.1 Temporal mixed signal	15
2.2 Spectral mixed signal	17
2.2.1 Filtered spectral mixed signal	20
2.3 Filtered temporal mixed signal	22
2.4 Phase of filtered temporal mixed signal	22
2.5 Impact of zero padding	25
3 Important conditions for optical heterodyne phase detection	32
3.1 Frequency difference Δf & δf	33

3.2	Frequency difference Δf & $\delta t N$	33
3.3	Number of points N & δt	36
3.3.1	Number of points and zero padding	38
3.4	Conclusion	43
3.5	Summary of Optical Heterodyne Detection	45
4	OHD of Phase-Shifted Signals: Non-Split Signal	46
4.1	Phase shift of π	47
4.2	Phase shift of $\frac{\pi}{2}$	51
4.3	Phase shift of $-\frac{\pi}{2}$	53
4.4	Phase shift of 0	55
4.5	Conclusion	56
4.6	Summary of OHD of Phase-Shifted Signals: Non-split Signal	59
5	OHD of Phase-Shifted Signals: Split Signal	60
5.1	Impact of time vector zero position	60
5.2	Split of phase-shifted signal at equal parts	64
5.3	Split of phase-shifted signal at not even parts	71
5.4	Summary of OHD of Phase-Shifted Signals: Split Signal	79
6	OHD of Phase-Shifted Signals: Split Signal with Zero Out	80
6.1	Split signal with zero out	80
6.2	Temporal phase split	85
6.3	Summary of Optical Heterodyne Detection: Split Signal with Zero Out	89
7	Conclusion	90

List of Figures

1.1	Basic set-up of optical heterodyne detection.	2
1.2	Temporal mixed signal.	4
1.3	Spectral power and phase of the spectral mixed signal.	6
1.4	Filtered spectral mixed signal.	7
1.5	Real part of the filtered temporal mixed signal.	8
1.6	Temporal phase of filtered temporal mixed signal.	9
1.7	Temporal phase of filtered temporal mixed signal with linear part removed.	10
1.8	3-dB directional coupler.	11
2.1	Temporal mixed signal.	16
2.2	Spectral power of mixed signal analytic expression and numeric examples.	17
2.3	Wrapped and unwrapped spectral phase of mixed signal.	19
2.4	Spectral phase of mixed signal analytic expression (a) and numeric (b).	20
2.5	Filtered spectral mixed signal analytic expression and numeric.	21
2.6	Filtered spectral mixed signal.	21
2.7	Real part of the filtered temporal mixed signal.	22
2.8	Temporal phase of filtered mixed signal.	23
2.9	Phase without linear portion.	24
2.10	Temporal mixed signal with (B) and without (A) zero padding.	25
2.11	Spectral power of mixed signal with (B) and without (A) zero padding.	26
2.12	Phase of spectral mixed signal with (B) and without (A) zero padding.	28
2.13	Filtered spectral mixed signal with (B) and without (A) zero padding.	28

2.14	Real part of filtered temporal mixed signal with (B) and without (A) zero padding.	29
2.15	Phase of temporal mixed signal with (B) and without (A) zero padding. .	29
2.16	Phase of temporal mixed signal with (B) and without (A) zero padding with linear part removed.	30
3.1	Spectral power of mixed signal when $\Delta f = 0$	33
3.2	Temporal power for A. $\Delta f = 0.1$ MHz, $Range\ t_{sig} = 10000$ ns; B. $\Delta f = 0.5$ MHz, $Range\ t_{sig} = 2000$ ns.	34
3.3	Spectral power for A. $\Delta f = 0.1$ MHz, $Range\ t_{sig} = 10000$ ns; B. $\Delta f = 0.5$ MHz, $Range\ t_{sig} = 2000$ ns.	35
3.4	Temporal and spectral mixed signal, $N = 2^{12}$	37
3.5	Temporal and spectral mixed signal, $N = 2^{16}$	37
3.6	Power of spectral mixed signal $N_{sig} = 2^{12}$ without and with zero padding respectively.	39
3.7	Power of spectral mixed signal $N_{sig} = 2^{16}$ without and with zero padding respectively.	39
3.8	Phase of spectral mixed signal $N_{sig} = 2^{12}$ without (A) and with (B) zero padding.	40
3.9	Phase of spectral mixed signal $N_{sig} = 2^{16}$ without (A) and with(B) zero padding.	40
3.10	Phase of temporal mixed signal $N_{sig} = 2^{12}$ without (A) and with(B) zero padding.	41
3.11	Phase of temporal mixed signal $N_{sig} = 2^{16}$ without (A) and with(B) zero padding.	41

3.12	Phase of temporal mixed signal with linear part removed and 3-dB coupler correction for $N_{sig} = 2^{12}$ without (A) and with(B) zero padding.	42
3.13	Phase of temporal mixed signal with linear part removed and 3-dB coupler correction for $N_{sig} = 2^{16}$ without (A) and with(B) zero padding.	42
3.14	Assessed phase versus actual input phase, for spectral and temporal phase assessment techniques.	44
4.1	Temporal mixed signal with a phase shift of π at t=0, with (B) and without (A) padding.	47
4.2	Power of spectral mixed signal, with (B) and without (A) padding. . . .	48
4.3	Phase of spectral mixed signal, with (B) and without (A) padding. . . .	49
4.4	Filtered spectral mixed signal, with (B) and without (A) padding. . . .	49
4.5	Filtered temporal mixed signal, with (B) and without (A) padding. . . .	50
4.6	Temporal phase of the mixed signal, with (B) and without (A) padding. .	50
4.7	Phase of filtered temporal signal, having the linear part removed, with (B) and without (A) padding.	51
4.8	Temporal mixed signal with the phase shift of $\frac{\pi}{2}$	52
4.9	Power and phase of the spectral mixed signal.	52
4.10	Filtered spectral and temporal signals.	53
4.11	Phase of temporal mixed signal.	53
4.12	Power of temporal (A) and spectral (B) mixed signal.	54
4.13	Phase of spectral (A)and temporal (B) mixed signal.	54
4.14	Assessed spectral phase shift with (B) and without (A) padding.	56
4.15	Assessed temporal phase shift with (B) and without (A) padding.	57
4.16	Δ difference error.	58

5.1	Temporal mixed signal for case A and B.	61
5.2	Power of spectral mixed signal for case A and B.	61
5.3	Phase of spectral mixed signal for case A and B.	62
5.4	Adjusted phase of spectral mixed signal for case A and B.	63
5.5	Temporal phase of filtered spectral mixed signal for case A and B.	63
5.6	Phase of temporal mixed signal with linear part removed and 3-dB coupler correction for case A and B.	64
5.7	Temporal mixed signal before split.	65
5.8	Temporal mixed signal, before and after phase shift.	66
5.9	Power of spectral mixed signal, before and after phase shift.	66
5.10	Phase of spectral mixed signal, before and after phase shift.	67
5.11	Filtered spectral mixed signal, before and after phase shift.	67
5.12	Filtered temporal mixed signal, before and after phase shift.	68
5.13	Phase of temporal mixed signal, before and after phase shift.	69
5.14	Phase of temporal mixed signal with linear part removed and 3-dB coupler correction.	69
5.15	Assessed phase shift.	70
5.16	Δ difference error.	71
5.17	Temporal mixed signal before split.	72
5.18	Temporal mixed signal after split at the phase shift.	72
5.19	Power of spectral mixed signal after split at the phase shift.	73
5.20	Phase of spectral mixed signal after split at the phase shift.	73
5.21	Filtered spectral mixed signal after split at the phase shift.	74
5.22	Filtered temporal mixed signal after split at the phase shift.	74

5.23	Phase of filtered temporal mixed signal after split at the phase shift. . . .	75
5.24	Phase of filtered temporal mixed signal after split at the phase shift. . . .	75
5.25	Phase of filtered temporal mixed signal with linear part removed and 3-dB coupler correction.	76
5.26	Assessed phase.	77
5.27	Δ difference error.	78
6.1	Temporal mixed signal.	81
6.2	Temporal mixed signal.	81
6.3	Power of spectral mixed signal before (A) and after (B) shift.	82
6.4	Phase of spectral mixed signal before (A) and after (B) shift.	82
6.5	Filtered power of spectral mixed signal before (A) and after (B) shift. . .	83
6.6	Filtered power of temporal mixed signal before (A) and after (B) shift. .	83
6.7	Phase of temporal mixed signal before (A) and after (B) shift.	84
6.8	Temporal phase with linear part removed and 3-dB coupler correction, before (A) and after (B) shift.	84
6.9	Split signal temporal phase, before (A) and after (B) shift.	85
6.10	Split signal temporal phase with linear part removed and 3-dB coupler correction, before (A) and after (B) shift.	86
6.11	Assessed temporal phase shift.	86
6.12	Assessed phase.	87
6.13	Δ difference error.	88

List of Tables

2.1	Phase shift	24
2.2	Phase shift	31
4.1	Spectral $\phi(f)$ and temporal $\phi(t)$ phase shift assessment of $\Delta\phi = 0$ [rad] .	55
4.2	Spectral $\phi(f)$ phase shift assessment [rad] with and without padding . . .	57
4.3	Temporal $\phi(t)$ phase shift assessment [rad] with and without padding . .	58
5.1	Spectral $\phi(f)$ and temporal $\phi(t)$ phase shift assessment [rad]	70
5.2	Spectral $\phi(f)$ and temporal $\phi(t)$ phase shift assessment [rad]	77
6.1	Spectral $\Delta\phi(f)$ and temporal $\Delta\phi(t)$ phase shift assessment [rad]	87
7.1	Summary of phase shift assessment	91

Chapter 1

Introduction

1.1 Background

Optical heterodyne detection is an interferometric technique measuring the phase of a temporal signal [1]. The principle of optical heterodyne measurement is based on two independent monochromatic lasers as depicted in Figure 1.1. An incoming signal with angular frequency ω_s is mixed with a local-oscillator signal with angular frequency ω_o by means of a 3-dB coupler. One port of the coupler goes into a photodiode. Two signals interfere with each other which allows for analyzing and performing phase detection in the photodiode. The photo current at the angular frequency difference $\Delta\omega = \omega_s - \omega_o$ is recovered at the output.

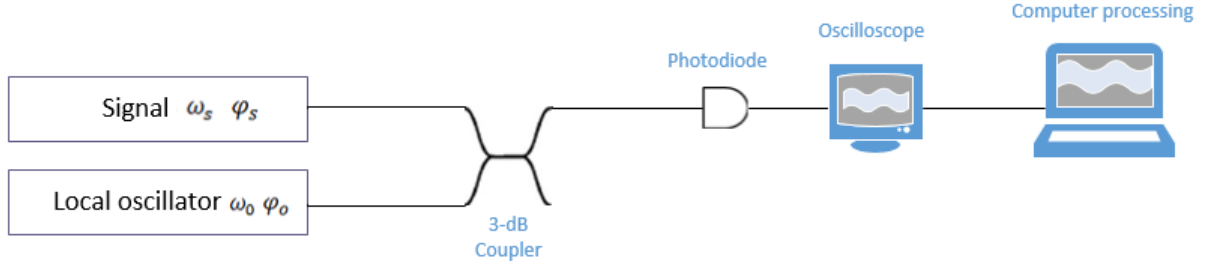


Figure 1.1: Basic set-up of optical heterodyne detection.

It is important to be able to detect the temporal phase because it can vary during the period of transmission (commonly referred to as chirp in fiber optics applications). When it does so, the instantaneous frequency changes, representing an increase in the spectral content of the signal. This larger spectral content (larger signal bandwidth), in turn, may impair signal quality through processes such as chromatic dispersion and signal clipping. Moreover, the phase is used to encode data in phase-shift-keying (PSK) and quadrature amplitude modulation (QAM) data formats, and so a variation in temporal phase would mean a potential corruption of data. Optical heterodyne detection for phase shift assessment can be used in research and device-characterization laboratories, where components and optical processes are being characterized; such a technique would be useful for phase modulators, intensity modulators, and directly modulated light sources, to name a few.

Generally a set up with two balanced photodiodes was preferred for phase detection as the laser phase noise can be strong [2]. However, it is possible to mend this problem by the use of filtering.

The next section will discuss the principle of operation for phase extraction using the optical heterodyne detection method.

1.2 Phase detection

1.2.1 Temporal mixed signal

In order to extract the phase of the signal, multiple steps should be performed. First, the power detected at the photodiode is given as:

$$P(t) = P_a + P_b \cos(\Delta\omega t + \Delta\Phi), \quad (1.1)$$

where $\Delta\omega = \omega_s - \omega_o$ is the angular frequency difference between the signal and the local-oscillator, $\Delta\Phi = \phi_s - \phi_o$ is the phase difference between phase offset of the signal ϕ_s and the local-oscillator ϕ_o , and P_a and P_b are two power levels (to be specified later). The cosine is the natural result of the electric fields beating together.

The power can also be expressed as:

$$P(t) = P_a + P_b \cos(\Delta\omega t + \Delta\Phi) = P_a + \frac{P_b}{2} \{e^{i(\Delta\omega t + \Delta\Phi)} + e^{-i(\Delta\omega t + \Delta\Phi)}\}. \quad (1.2)$$

In terms of temporal frequencies, this power expression becomes

$$P(t) = P_a + \frac{P_b}{2} \{e^{i(2\pi\Delta f t + \Delta\Phi)} + e^{-i(2\pi\Delta f t + \Delta\Phi)}\}, \quad (1.3)$$

where $\Delta f = f_s - f_o$, the temporal frequency of the signal $f_s = \omega_s/2\pi$, and the temporal frequency of the local oscillator $f_o = \omega_o/2\pi$.

An example of $P(t)$ is shown in Figure 1.2, for the case of $P_a = 1$ mW, $P_b = 1$ mW, $\Delta f = 1$ MHz, and $\Delta\Phi = \frac{\pi}{2}$.

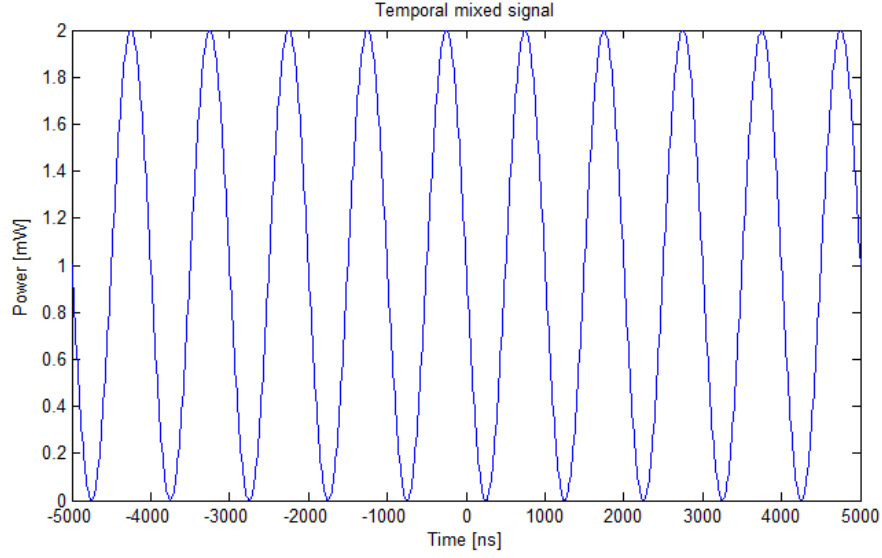


Figure 1.2: Temporal mixed signal.

1.2.2 Spectral mixed signal

The next stage is to decompose the time domain signal into low and high frequencies with the help of the Fourier transform. The Fourier Transform is defined as

$$\mathcal{F}\{\tilde{g}(t)\} = \int_{-\infty}^{\infty} \tilde{g}(t)e^{-i2\pi ft}dt. \quad (1.4)$$

The Fourier transform of an exponential function is:

$$\mathcal{F}\{e^{i(2\pi\Delta f t)}\} = A\delta(f - \Delta f). \quad (1.5)$$

The Fourier transform on the power signal is performed as

$$P(t) \xrightarrow{\mathcal{F}} \tilde{S}(f), \quad (1.6)$$

$$P_a + P_b \cos(2\pi\Delta f t + \Delta\Phi) \xrightarrow{\mathcal{F}} P_a\delta(f) + \frac{P_b}{2}[e^{i\Delta\Phi}\delta(f - \Delta f) + e^{-i\Delta\Phi}\delta(f + \Delta f)]. \quad (1.7)$$

Strictly speaking, most mathematical operations are not directly applicable to the Dirac delta functions. However, for the purpose of illustrating the spectral power and phase,

we assume that δ is a narrow Gaussian function.

$$\tilde{S} = P_a\delta(f) + \frac{P_b}{2}[e^{i\Delta\Phi}\delta(f - \Delta f) + e^{-i\Delta\Phi}\delta(f + \Delta f)]. \quad (1.8)$$

The spectral power is given by $|\tilde{S}|^2 = \tilde{S} \times \tilde{S}^*$:

$$\begin{aligned} |\tilde{S}|^2 &= [P_a\delta(f) + \frac{P_b}{2}e^{i\Delta\Phi}\delta(f - \Delta f) + \frac{P_b}{2}e^{-i\Delta\Phi}\delta(f + \Delta f)] \\ &\times [P_a\delta(f) + \frac{P_b}{2}e^{-i\Delta\Phi}\delta(f - \Delta f) + \frac{P_b}{2}e^{i\Delta\Phi}\delta(f + \Delta f)]. \end{aligned} \quad (1.9)$$

Any term having the product of two different delta functions, such as $\delta(f) \cdot \delta(f - \Delta f)$, is zero, leaving the following:

$$|\tilde{S}|^2 = P_a^2\delta(f)^2 + \frac{P_b^2}{4}\delta(f - \Delta f)^2 + \frac{P_b^2}{4}\delta(f + \Delta f)^2. \quad (1.10)$$

The graphical representation of the spectral mixed signal \tilde{S} is represented in Figure 1.3.

The spectral mixed signal \tilde{S} is a set of three peaks. $P_a\delta(f)$ is the central peak at the zero frequency, and $\frac{P_b}{2}e^{-i\Delta\Phi}\delta(f + \Delta f)$ and $\frac{P_b}{2}e^{i\Delta\Phi}\delta(f - \Delta f)$ are negative and positive side peaks at $-\Delta f$ and Δf , respectively. The spectral phase $\phi(f)$ can be identified using the real and imaginary parts as follows:

$$\tan\{\phi(f)\} = \frac{Im\{\tilde{S}\}}{Re\{\tilde{S}\}}, \quad (1.11)$$

$$\begin{aligned} \tilde{S} &= P_a\delta(f) + \frac{P_b}{2}\cos(\Delta\Phi)\delta(f - \Delta f) + \frac{P_b}{2}\cos(-\Delta\Phi)\delta(f + \Delta f) \\ &+ i\left\{\frac{P_b}{2}\sin(\Delta\Phi)\delta(f - \Delta f) + \frac{P_b}{2}\sin(-\Delta\Phi)\delta(f + \Delta f)\right\}, \end{aligned} \quad (1.12)$$

$$\tilde{S} = P_a\delta(f) + \frac{P_b}{2}\cos(\Delta\Phi)[\delta(f - \Delta f) + \delta(f + \Delta f)] + i\frac{P_b}{2}\sin(\Delta\Phi)[\delta(f - \Delta f) - \delta(f + \Delta f)], \quad (1.13)$$

$$\tan\{\phi(f)\} = \frac{Im\{\tilde{S}\}}{Re\{\tilde{S}\}} = \frac{\frac{P_b}{2}\sin(\Delta\Phi)[\delta(f - \Delta f) - \delta(f + \Delta f)]}{P_a\delta(f) + \frac{P_b}{2}\cos(\Delta\Phi)[\delta(f - \Delta f) + \delta(f + \Delta f)]}. \quad (1.14)$$

If $f = 0$, $\tan\{\phi(f)\} = 0$. In this case, $\phi(f = 0) = 0$.

If $f = \Delta f$, $\tan\{\phi(f)\} = \frac{\frac{P_b}{2}\sin(\Delta\Phi)}{\frac{P_b}{2}\cos(\Delta\Phi)} = \tan(\Delta\Phi)$. In this case, $\phi(f = \Delta f) = \Delta\Phi$.

If $f = -\Delta f$, $\tan\{\phi(f)\} = \frac{-\frac{P_b}{2} \sin(\Delta\phi)}{\frac{P_b}{2} \cos(\Delta\phi)} = -\tan(\Delta\Phi)$. In this case, $\phi(f = -\Delta f) = -\Delta\Phi$.

These values are shown in Figure 1.3

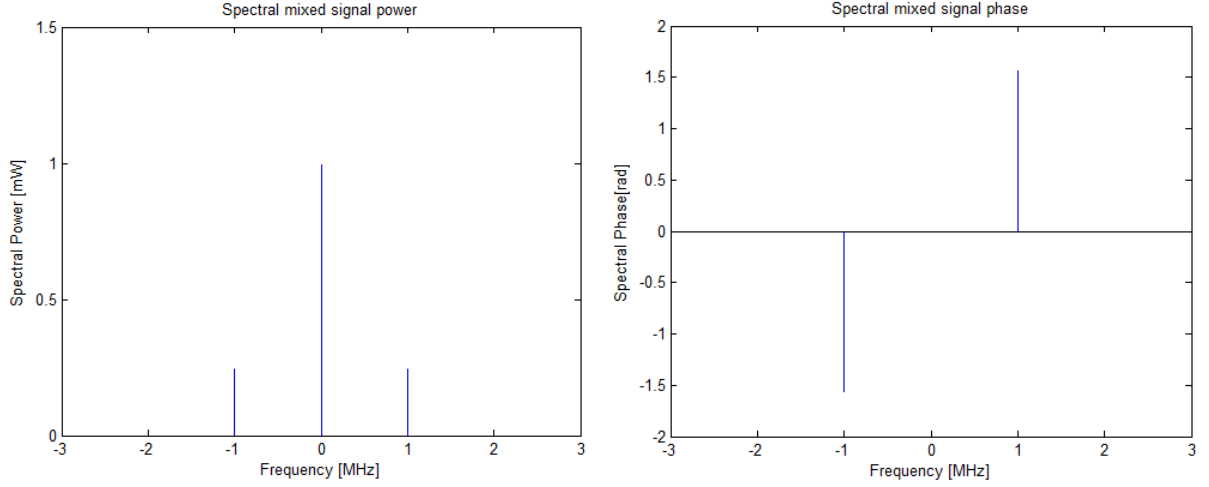


Figure 1.3: Spectral power and phase of the spectral mixed signal.

Note that the phase difference $\Delta\Phi$ can be determined for the analytic expression case simply by reading off the spectral phase value at the frequency of the right spectral power peak, or by the negative spectral phase of the left spectral power peak.

1.2.3 Filtered spectral mixed signal

In order to isolate the phase offset difference $\Delta\Phi$, the highest frequency peak is filtered out as depicted in Figure 1.4. The filter width is given by α , and the filtered spectral mixed signal is given by \tilde{S}_f :

$$\tilde{S}(f) \xrightarrow{\text{Filter}} \tilde{S}_f(f), \quad (1.15)$$

$$\tilde{S}_f(f) = \frac{P_b}{2} e^{i\Delta\Phi} \delta(f - \Delta f). \quad (1.16)$$

The filtering process can be considered to be the multiplication of the initial function $\tilde{S}(f)$ by a rectangular function $\Pi(\frac{f-f_0}{\alpha})$ centered at $f = f_0$, and having the width α :

$$\tilde{S}_f(f) = \tilde{S}(f) \times \Pi\left(\frac{f-f_0}{\alpha}\right). \quad (1.17)$$

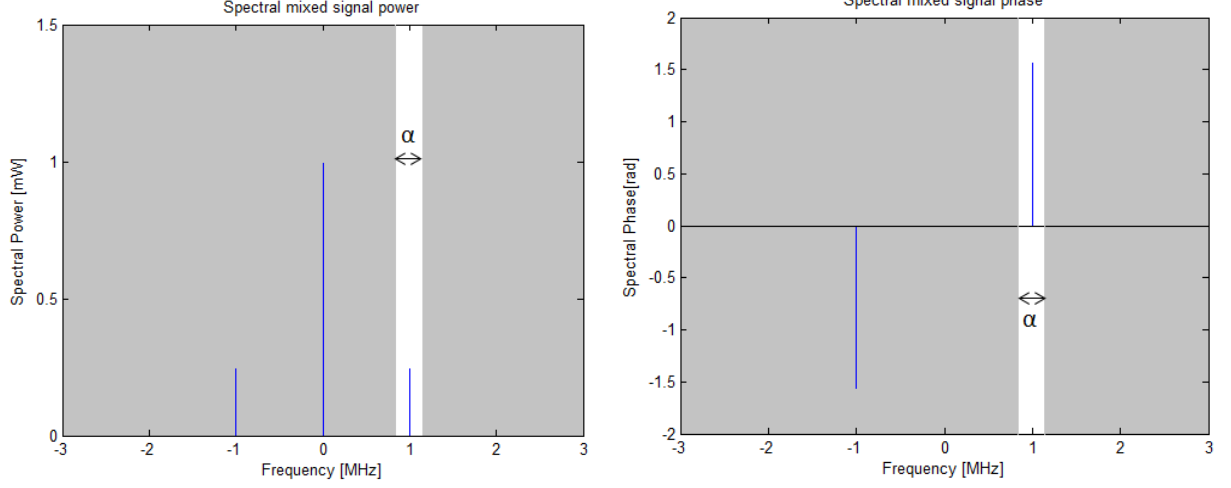


Figure 1.4: Filtered spectral mixed signal.

1.2.4 Filtered temporal mixed signal

The filtered spectral mixed signal is brought back to the temporal domain by applying the inverse Fourier transform:

$$\tilde{S}_f(f) \xrightarrow{\mathcal{F}^{-1}} \tilde{P}_f(t). \quad (1.18)$$

The inverse Fourier transform is defined as

$$\mathcal{F}^{-1}\{\tilde{h}(f)\} = \int_{-\infty}^{\infty} \tilde{h}(f) e^{i2\pi ft} df. \quad (1.19)$$

The inverse Fourier transform of a delta function is given by

$$\mathcal{F}^{-1}\{B\delta(f - \Delta f)\} = B e^{i2\pi \Delta f t}. \quad (1.20)$$

The filtered temporal mixed signal can be written as:

$$\tilde{P}_f(t) = \frac{P_b}{2} e^{i(2\pi \Delta f t + \Delta \Phi)} = \frac{P_b}{2} \cos(2\pi \Delta f t + \Delta \Phi) + i \frac{P_b}{2} \sin(2\pi \Delta f t + \Delta \Phi). \quad (1.21)$$

Note that $\tilde{P}_f(t)$ is a complex quantity. $|\tilde{P}_f(t)|^2 = 0.25 P_b^2$, and the real part $\text{Re}\{\tilde{P}_f(f)\} = \frac{P_b}{2} \cos(2\pi \Delta f t + \Delta \Phi)$ and is plotted in Figure 1.5 for the case of $P_b = 1$ mW, $\Delta f = 1$ MHz, and $\Delta \Phi = \frac{\pi}{2}$.

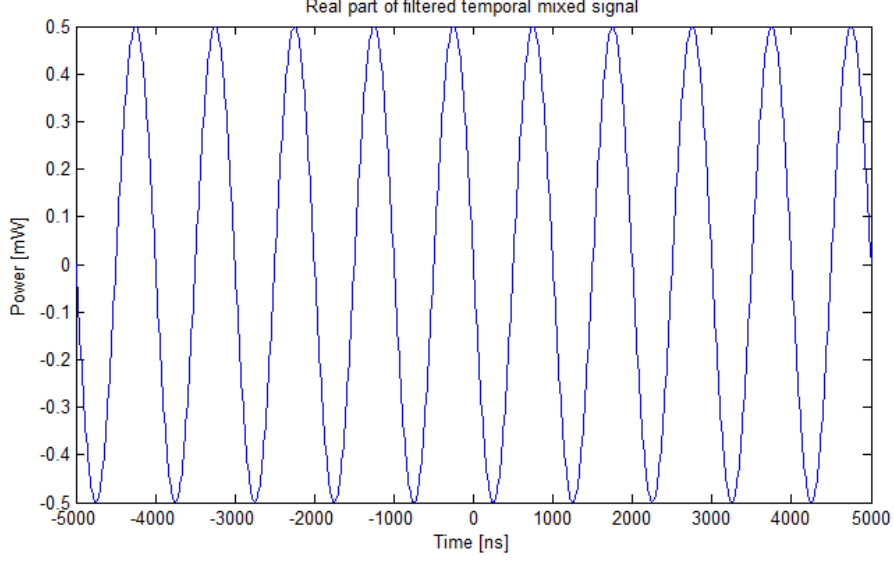


Figure 1.5: Real part of the filtered temporal mixed signal.

1.2.5 Phase of filtered temporal mixed signal

The filtered temporal signal $\tilde{P}_f(t)$ can be thought of as

$$\tilde{P}_f(t) = |\tilde{P}_f(t)|e^{i\phi_f(t)}. \quad (1.22)$$

The phase of $\tilde{P}_f(t)$ is $\phi_f(t) = 2\pi\Delta ft + \Delta\Phi$, which is the relationship of phase difference in time between the original signal and local oscillator, and is depicted in Figure 1.6 for the case where $\Delta f = 1$ MHz and $\Delta\Phi = \frac{\pi}{2}$. The phase can be determined as follows:

$$\phi_f(t) = \tan^{-1} \left\{ \frac{\text{Im}\{\tilde{P}_f\}}{\text{Re}\{\tilde{P}_f\}} \right\}, \quad (1.23)$$

$$\phi_f(t) = \tan^{-1} \left\{ \frac{\frac{P_b}{2} \sin(2\pi\Delta ft + \Delta\Phi)}{\frac{P_b}{2} \cos(2\pi\Delta ft + \Delta\Phi)} \right\}, \quad (1.24)$$

$$\phi_f(t) = \tan^{-1} \{ \tan(2\pi\Delta ft + \Delta\Phi) \}, \quad (1.25)$$

$$\phi_f(t) = 2\pi\Delta ft + \Delta\Phi. \quad (1.26)$$

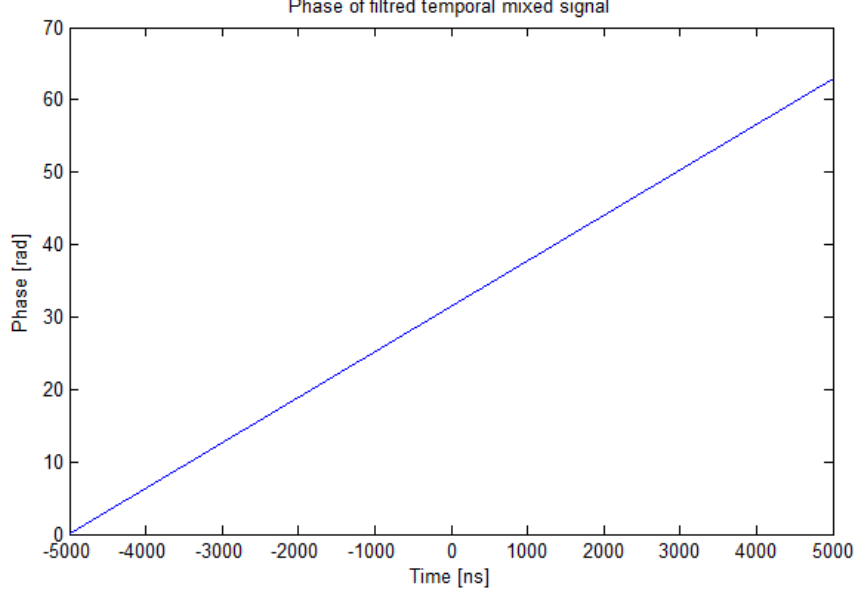


Figure 1.6: Temporal phase of filtered temporal mixed signal.

The slope m of this temporal phase is $m = 2\pi\Delta f$, and the phase offset $b = \Delta\Phi$. A linear fit $\phi_f = mt + b$ therefore extracts $\Delta\Phi$. Removing the linear fit from $\phi_f(t)$ yields $\phi'_f(t) = \phi_f - mt = b$. The effect of 3-dB directional coupler is to change $\phi'_f = \phi'_f + \frac{\pi}{2}$ which is plotted in Figure 1.7. $\Delta\Phi = \phi_s - \phi_o$ is the final quantity determined by optical heterodyne detection, and is the desired phase offset ϕ_s referenced to the phase offset of the local oscillator ϕ_o .

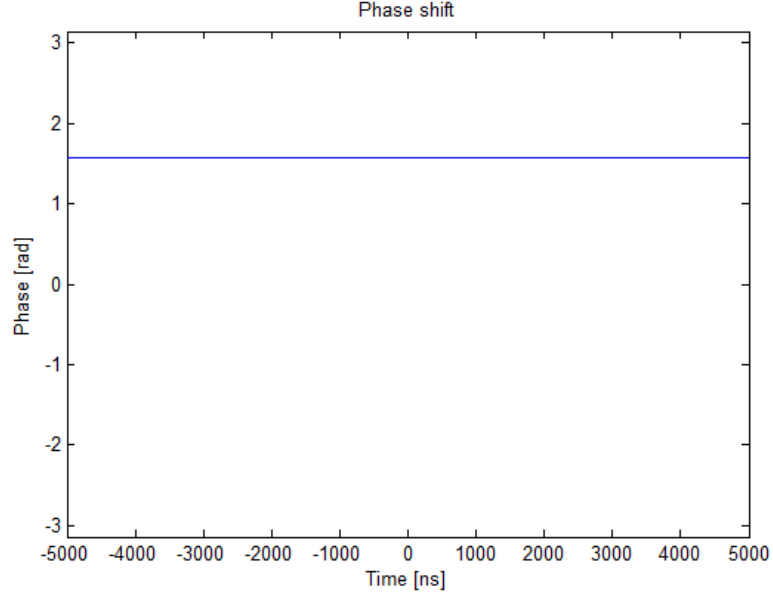


Figure 1.7: Temporal phase of filtered temporal mixed signal with linear part removed.

We note that $\Delta\Phi$ is provided by two steps in the OHD process:

1. $\phi'_f(t)$, Figure 1.7
2. $\phi(f)$, Figure 1.3b

We will continue to look at both sources of $\Delta\Phi$ throughout the thesis.

1.3 Details on Coupling and Mixing

In this section we discuss the optical heterodyne detection operations in greater detail, with an explicit mathematic form for the coupling. As depicted in Figure 1.1 — the basic set-up of optical heterodyne detection — the electric field of the signal $\tilde{E}_s(t)$ with optical frequency ω_s and phase ϕ_s is combined with the electric field of the local-oscillator $\tilde{E}_o(t)$ with optical frequency ω_o and phase ϕ_o :

$$\tilde{E}_s(t) = A_s e^{i\omega_s t + i\phi_s}, \quad (1.27)$$

$$\tilde{E}_o(t) = A_o e^{i\omega_o t + i\phi_o}. \quad (1.28)$$

The 3-dB directional coupler is a four-port device with two input and two output ports, and is used to combine two signals. For the case of only one input signal, the two outputs are equal in power but the coupled output lags behind the direct port by 90° as in Figure 1.8 [5].

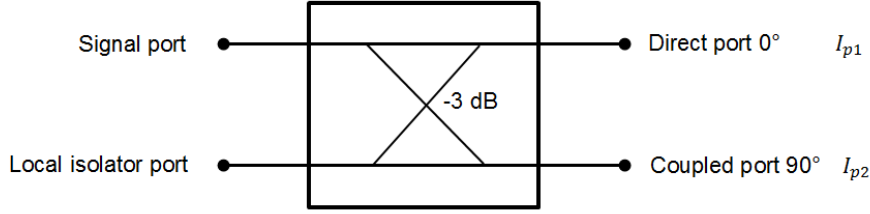


Figure 1.8: 3-dB directional coupler.

The transfer matrix for a 3-dB directional coupler looks like this:

$$\begin{bmatrix} \tilde{E}_1 \\ \tilde{E}_2 \end{bmatrix} = \begin{bmatrix} \sqrt{1-\varepsilon} & i\sqrt{\varepsilon} \\ i\sqrt{\varepsilon} & \sqrt{1-\varepsilon} \end{bmatrix} * \begin{bmatrix} \tilde{E}_s \\ \tilde{E}_o \end{bmatrix}$$

$$\tilde{E}_1 = \sqrt{1-\varepsilon}\tilde{E}_s + i\sqrt{\varepsilon}\tilde{E}_o = \sqrt{1-\varepsilon}A_s e^{i(\omega_s t + \phi_s)} + i\sqrt{\varepsilon}A_o e^{i(\omega_o t + \phi_o)}, \quad (1.29)$$

$$\tilde{E}_2 = \sqrt{1-\varepsilon}\tilde{E}_o + i\sqrt{\varepsilon}\tilde{E}_s = \sqrt{1-\varepsilon}A_o e^{i(\omega_o t + \phi_o)} + i\sqrt{\varepsilon}A_s e^{i(\omega_s t + \phi_s)}, \quad (1.30)$$

where $\varepsilon = 0.5$ for a 3-dB coupler.

After the coupling, the total electrical field is represented as Equation 1.29 or 1.30.

Accordingly, the optical heterodyne detection relationship between photocurrent $I_p(t)$ and phase is based on the following [6]:

$$I_p(t) = \Re|\tilde{E}(t)|^2 = \Re P(t). \quad (1.31)$$

Out of the direct port the photocurrent is:

$$= \Re(\sqrt{1-\varepsilon}A_s e^{i(\omega_s t + \phi_s)} + i\sqrt{\varepsilon}A_o e^{i(\omega_o t + \phi_o)})(\sqrt{1-\varepsilon}A_s e^{-i(\omega_s t + \phi_s)} - i\sqrt{\varepsilon}A_o e^{-i(\omega_o t + \phi_o)}) \quad (1.32)$$

$$\begin{aligned}
&= \Re[\varepsilon A_o^2 + (1 - \varepsilon)A_s^2 - i\sqrt{\varepsilon(1 - \varepsilon)}A_s A_o e^{i[(\omega_s - \omega_o)t + (\phi_s - \phi_o)]} \\
&\quad + i\sqrt{\varepsilon(1 - \varepsilon)}A_s A_o e^{i[(\omega_o - \omega_s)t + (\phi_o - \phi_s)]}]
\end{aligned} \tag{1.33}$$

$$= \Re\{[\varepsilon A_o^2 + (1 - \varepsilon)A_s^2 - i\sqrt{\varepsilon(1 - \varepsilon)}A_s A_o e^{i\Delta\omega t} e^{i\Delta\Phi} + i\sqrt{\varepsilon(1 - \varepsilon)}A_s A_o e^{-i\Delta\omega t} e^{-i\Delta\Phi}]\}, \tag{1.34}$$

$$= \Re\{\varepsilon A_o^2 + (1 - \varepsilon)A_s^2 + 2\sqrt{\varepsilon(1 - \varepsilon)}A_s A_o \sin(\Delta\omega t + \Delta\Phi)\}. \tag{1.35}$$

where \Re is the responsivity of the photodiode, ε is the power-coupling coefficient of the optical coupler, $\Delta\omega = \omega_o - \omega_s$ is the frequency difference between the signal and the local oscillator, and $\Delta\Phi = \phi_o - \phi_s$ is the phase difference between phase offset of the signal and the local oscillator. Since $A_o^2 = P_o$ and $A_s^2 = P_s$, we have

$$I_{p1}(t) = \Re\{\varepsilon P_o + (1 - \varepsilon)P_s + 2\sqrt{\varepsilon(1 - \varepsilon)}\sqrt{P_s P_o} \sin(\Delta\omega t + \Delta\Phi)\}. \tag{1.36}$$

For a 3-dB directional coupler, $\varepsilon = 0.5$, which yields

$$I_{p1}(t) = \Re\{\frac{1}{2}P_o + \frac{1}{2}P_s + \sqrt{P_s P_o} \sin(\Delta\omega t + \Delta\Phi)\}. \tag{1.37}$$

For the coupled port, the photocurrent is

$$I_{p2}(t) = \Re\{\varepsilon A_s^2 + (1 - \varepsilon)A_o^2 - 2\sqrt{\varepsilon(1 - \varepsilon)}A_s A_o \sin(\Delta\omega t + \Delta\Phi)\}. \tag{1.38}$$

In terms of the optical power for a 3-dB directional coupler, the photocurrent is

$$I_{p2}(t) = \Re\{\frac{1}{2}P_s + \frac{1}{2}P_o - \sqrt{P_s P_o} \sin(\Delta\omega t + \Delta\Phi)\}. \tag{1.39}$$

Note that the sum of the photocurrents expresses the conservation of optical power

$$I_{p1} + I_{p2} = \Re(P_o + P_s). \tag{1.40}$$

The current recovered at the photodiode is then processed and analyzed. The ratio of the photocurrent I_p to the optical power P is responsivity \Re . Responsivity is a measure of a photodiode's response to light [6].

$$\Re = \frac{I_p}{P}. \tag{1.41}$$

From this we can find the equation for $P(t)$:

$$P(t) = \frac{I_p(t)}{\Re}. \quad (1.42)$$

Combining equations 1.34 and 1.42, we obtain the formula for the optical power:

$$P_1(t) = \varepsilon P_o + (1 - \varepsilon)P_s + 2\sqrt{\varepsilon(1 - \varepsilon)}\sqrt{P_s P_o} \sin(\Delta\omega t + \Delta\Phi). \quad (1.43)$$

$$= \varepsilon P_o + (1 - \varepsilon)P_s + 2\sqrt{\varepsilon(1 - \varepsilon)}\sqrt{P_s P_o} \cos(\Delta\omega t + \Delta\Phi - \frac{\pi}{2}). \quad (1.44)$$

Comparing this expression for $P_1(t)$ with the simple expression Equation 1.1 yields

$$\begin{aligned} P_a &= (1 - \varepsilon)P_s + \varepsilon P_o, \\ P_b &= 2\sqrt{\varepsilon(1 - \varepsilon)}\sqrt{P_s P_o}, \\ \Delta\Phi' &= \Delta\Phi - \frac{\pi}{2}, \end{aligned} \quad (1.45)$$

where $\Delta\Phi'$ is the phase offset difference of the simple approach and is the result of the OHD process. Since the desired $\Delta\Phi = \Delta\Phi' + \frac{\pi}{2}$, $\frac{\pi}{2}$ must be added to the OHD result. This extra $\frac{\pi}{2}$ needs to be added for both techniques of extracting $\Delta\Phi$ — in the temporal and spectral domains. The $-\frac{\pi}{2}$ term exists because ϕ_o is subtracted from ϕ_s , and the local oscillator picks up a $\frac{\pi}{2}$ phase shift from the directional coupler. Thus, we need to add $\frac{\pi}{2}$ in the case of a 3-dB directional coupler in order to cancel the $\frac{\pi}{2}$ shift coming from it, yielding only $\Delta\Phi$.

1.4 Summary of Optical Heterodyne Detection

The steps used to perform optical heterodyne detection are summarized as follows:

1. $P(t)$, using $\Delta f = f_s - f_o$

2. $\tilde{S}(f) = \mathcal{F}\{P(t)\}$

$$\star \Delta\Phi = \phi(\Delta f) = \phi(-\Delta f)$$

$$\star \text{ (with 3-dB directional coupler) } \Delta\Phi = \phi(\Delta f) + \frac{\pi}{2} = \phi(-\Delta f) - \frac{\pi}{2}$$

3. $\tilde{S}_f(f) = \mathcal{F}\{P(t)\} \times \Pi(\frac{f-f_0}{\alpha})$

4. $\tilde{P}_f(t) = \mathcal{F}^{-1}\{\tilde{S}_f(f)\}$

5. $\phi_f(t) = \tan^{-1} \left\{ \frac{\text{Im}\{\tilde{P}_f\}}{\text{Re}\{\tilde{P}_f\}} \right\} = \text{angle}\{\tilde{P}(f)\}$

6. $\phi_f(t) = mt + b$

$$\star \Delta\Phi = \phi_f(t) - mt = b$$

$$\star \text{ (with 3-dB directional coupler) } \Delta\Phi = \phi_f(t) - mt + \frac{\pi}{2} = b + \frac{\pi}{2}$$

Chapter 2

Numeric Computations

Since actual signals are not analytic expression, we need to use the Fast Fourier Transform (FFT) algorithm to perform the Fourier Transform. The MATLAB function *fft* converts a signal with the fixed length N from the time to the frequency domain. In this section we discuss optical heterodyne detection using the FFT algorithm instead of the analytic expression method. Comparisons to analytic expression results will be made along the way.

2.1 Temporal mixed signal

For the computational method there is no need to perform analytic expression calculations. The MATLAB code will find the final solution without knowing the analytic expression solution. The inputs for the code are the equations of the incoming signal and local oscillator. The power detected at the photodiode is the absolute squared value of their sum.

$$\tilde{E}_s(t) = \sqrt{P_s} e^{i\omega_s t + i\phi_s}, \quad (2.1)$$

$$\tilde{E}_o(t) = \sqrt{P_o} e^{i\omega_o t + i\phi_o}, \quad (2.2)$$

$$\tilde{E}_{tot} = \sqrt{1 - \varepsilon} \tilde{E}_s + i\sqrt{\varepsilon} \tilde{E}_o, \quad (2.3)$$

$$P(t) = |\tilde{E}_{tot}|^2. \quad (2.4)$$

The temporal mixed signal with $N = 2^{12} = 4096$ points and the time vector range of 10000 [ns] is depicted in Figure 2.1. This plot is identical to the one shown in Figure 1.2. We take $P_s = P_o = 1$ [mW], $f_s = 1.001$ [GHz], $f_o = 1$ [GHz], $\phi_s = \frac{\pi}{2}$ [rad], and $\phi_o = 0$ [rad]. Here, although $\Delta\Phi = \phi_s - \phi_o = \frac{\pi}{2} - 0 = \frac{\pi}{2}$, the graph includes the phase contribution from the 3-dB coupler, $\Delta\Phi' = \phi_s - \phi'_o = \frac{\pi}{2} - 0 - \frac{\pi}{2} = 0$. Thus, the graph is correctly located at $t = 0$ [ns].

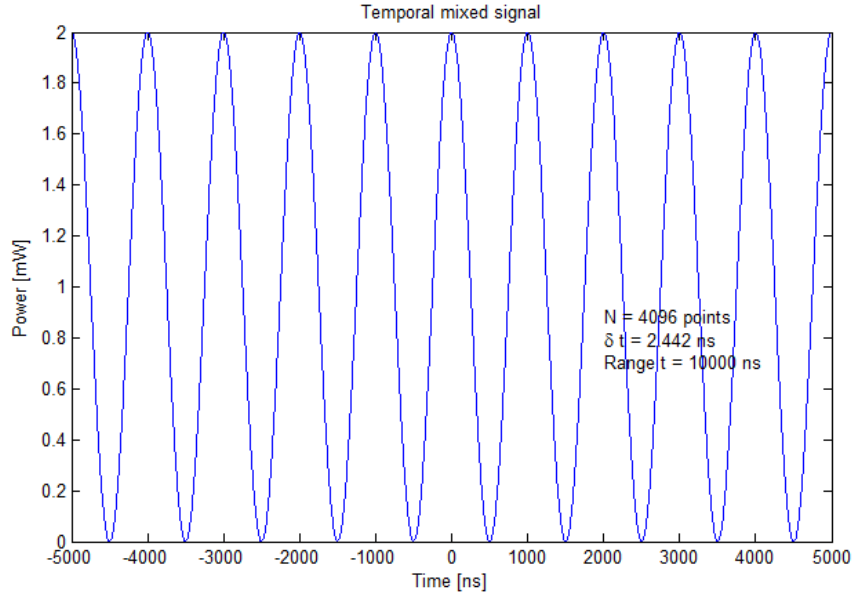


Figure 2.1: Temporal mixed signal.

The text box in Figure 2.1 shows several important quantities. N is the number of points in the time vector. δt is the duration between two points in the time vector; this quantity can be considered to be the sampling period. $Range\ t = t_{max} - t_{min}$ is the range of values of the time vector. The quantity δt can be calculated directly via

$$\delta t = \frac{Range\ t}{N - 1}. \quad (2.5)$$

2.2 Spectral mixed signal

The next step is converting the temporal mixed signal into the spectral mixed signal with the help of the Matlab FFT function. The graphical comparison of the analytic expression and numeric signals is given in Figure 2.2. The spectral mixed signal consists of three spikes with different amplitudes.

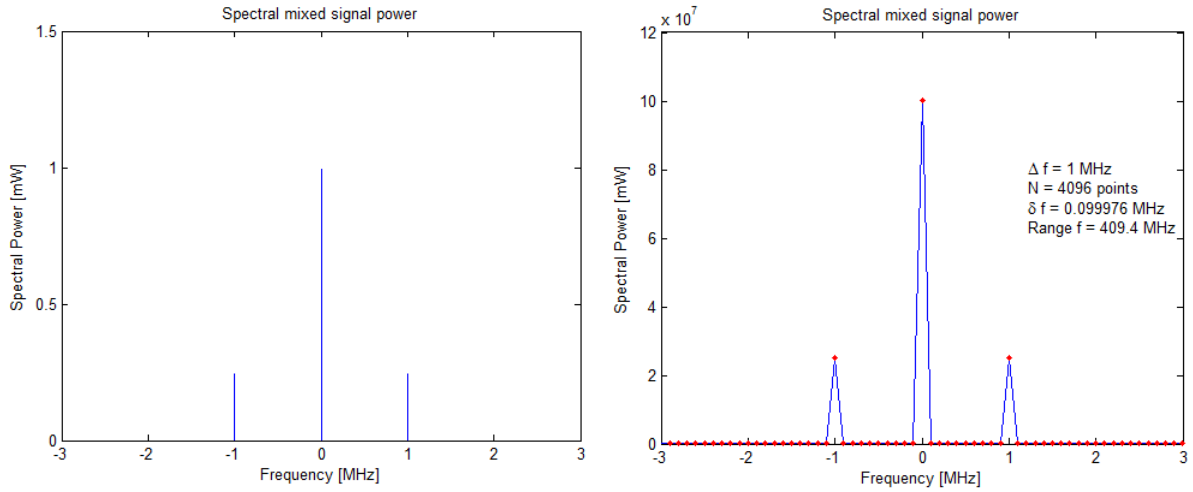


Figure 2.2: Spectral power of mixed signal analytic expression and numeric examples.

The text box in Figure 2.2 shows several important quantities. The frequency difference $\Delta f = f_s - f_o$ defines where the side bands are located, N is the number of points in the frequency vector, δf is the distance between two points in the frequency vector, and $Range f$ is the range of the values of the frequency vector.

The maximum absolute frequency f_{absmax} , which is also known as Nyquist frequency is determined by

$$f_{absmax} = \frac{1}{2\delta t}. \quad (2.6)$$

The vector of frequency values varies from $f_{min} = -f_{absmax}$ to $f_{max} = f_{absmax} - \delta f$, such that the $Range f$ is given by

$$Range f = (f_{absmax} - \delta f) - (-f_{absmax}) = 2f_{absmax} - \delta f. \quad (2.7)$$

Defined this way, f_{min} is the furthest frequency from zero in either the positive or negative frequency direction.

The frequency difference δf is given by

$$\delta f = \frac{\text{Range } f}{N - 1} = \frac{2f_{absmax} - \delta f}{N - 1}. \quad (2.8)$$

If δf is not removed from $2f_{absmax}$ in the numerator, then, the number of points in the denominator increases from $N - 1$ to N , yielding

$$\delta f = \frac{2f_{absmax}}{N}. \quad (2.9)$$

The equations 2.6 and 2.9 provide an insightful relationship:

$$\delta f = \frac{2f_{absmax}}{N} = \frac{2}{N} \times \frac{1}{2\delta t} = \frac{1}{N\delta t}, \quad (2.10)$$

$$\delta f \cdot \delta t \cdot N = 1. \quad (2.11)$$

As an example, if we use the values from the Figures 2.1 and 2.2, where $\delta f = 0.099976$ MHz, $\delta t = 2.442$ ns, and $N = 4096$ points:

$$\delta f \delta t N = 0.099976 \cdot 10^6 \times 2.442 \cdot 10^{-9} \times 4096 = 1. \quad (2.12)$$

There are several differences between the analytic expression and numeric plots in Figure 2.2. One major difference is that the sharp lines have broadened, which is an artifact of using a scatter plot with connected lines. The triangle shape for the numeric case occurs because a large power value only exists at one frequency point. The triangle shape occurs when connecting the dots to two neighboring data points with low or zero power. The width of the triangle spike is therefore approximately the frequency interval δf .

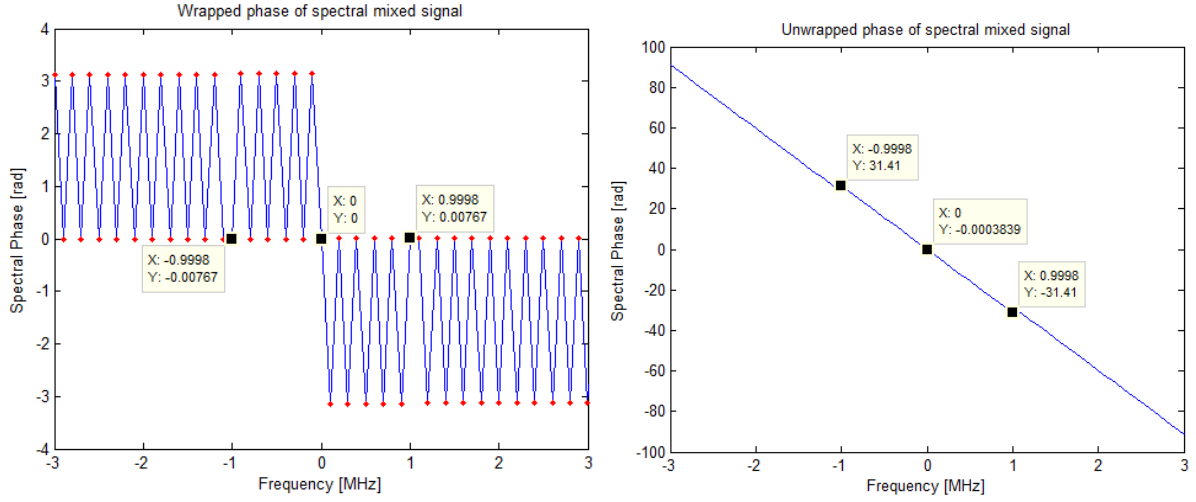


Figure 2.3: Wrapped and unwrapped spectral phase of mixed signal.

Figure 2.3 demonstrates wrapped and unwrapped phase of the spectral mixed signal. In the wrapped case, the peaks give us the phase value 0.00766990394 [rad]; after adding $\frac{\pi}{2}$ because of the 3-dB coupler it goes up to 1.578466231 [rad] with $\Delta = 0.00766990394$. The phase for the unwrapped case is $31.41 - 2 \cdot \pi \cdot 5 + \frac{\pi}{2} = 1.5649$ [rad] which is $\Delta = 0.005926$ [rad] different from the analytic expression result. Although both techniques can be used to find the result, the unwrapped phase has an offset which has to be removed and slows down the computations. Therefore, the wrapped phase detection technique for the spectral mixed signal will be used in further discussions. The saw-tooth nature of the wrapped phase originates from the underlying sinc function of the numeric data (discussed in Chapter 3).

Figure 2.4 compares the analytic expression and numeric phase of the spectral mixed signal. For the numeric case we added $\frac{\pi}{2}$ to the positive frequency value and removed $\frac{\pi}{2}$ from a negative case.

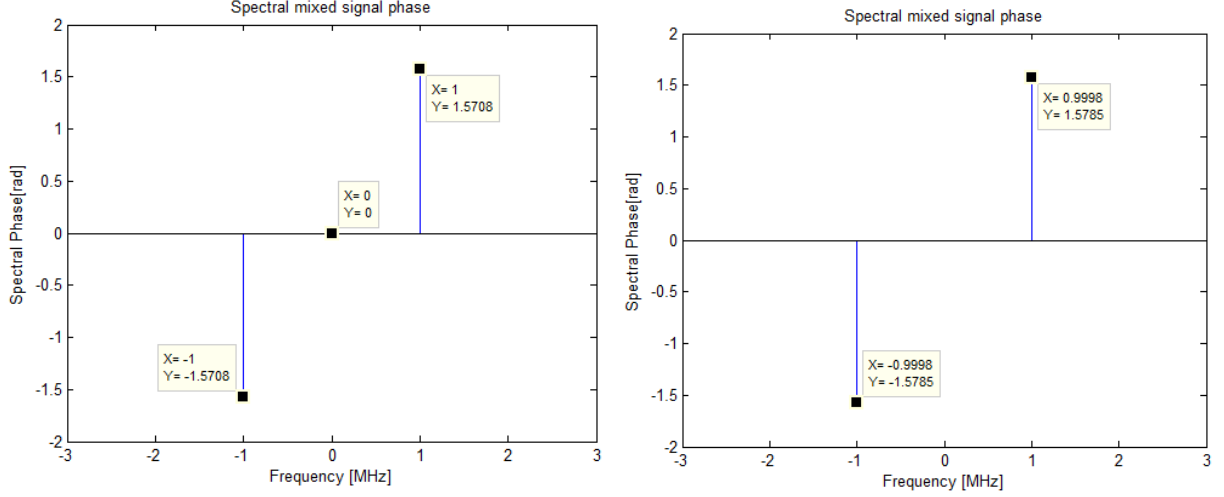


Figure 2.4: Spectral phase of mixed signal analytic expression (a) and numeric (b).

A technique for finding Δf is to use the frequency of the peak of the filtered spectral mixed signal. The location of the peak shows us $\Delta f = 0.9998$ [MHz] for both numerical cases, which is 0.0002 [MHz] decrease from the analytic expression value $\Delta f = 1$ [MHz].

2.2.1 Filtered spectral mixed signal

The highest frequency peak is filtered out by multiplying $\tilde{S}(f)$ by a rectangular function filter. The filter width α is defined manually, but should be wider than the spectral spike. We find that α should be chosen so that $\alpha > 2\delta f = \frac{2}{\delta t N}$. In our case the width of the bottom of the peak is $2\delta f = 0.201$ [MHz] and choosing $\alpha = 0.4$ [MHz] allows to catch all the features of the spike.

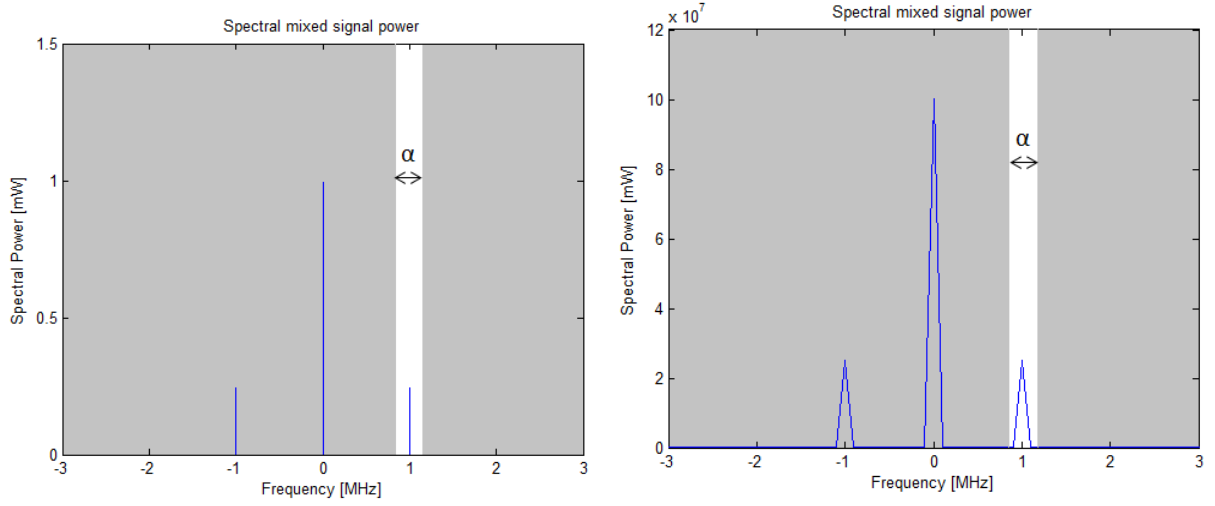


Figure 2.5: Filtered spectral mixed signal analytic expression and numeric.

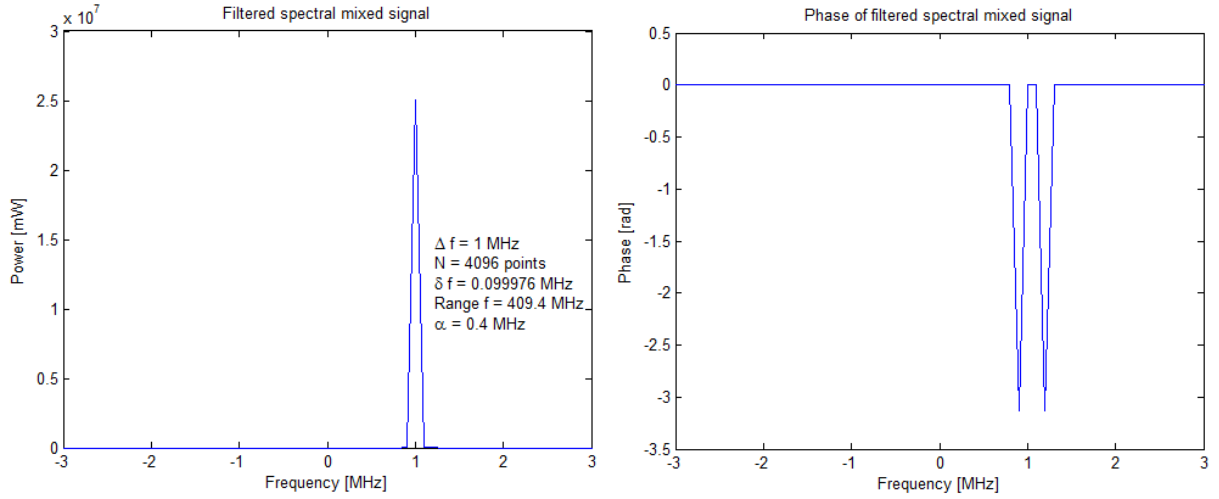


Figure 2.6: Filtered spectral mixed signal.

The filtered spectral mixed signal, as shown in Figure 2.6, has the same number of points N , sampling frequency δf , and $\text{Range } f$ as the unfiltered signal. It contains the highest frequency peak and the rest of the vector is filled with zeroes.

2.3 Filtered temporal mixed signal

After applying the Inverse Fast Fourier Transform (IFFT) algorithm to the filtered spectral mixed signal, we get the waveform very similar to the initial temporal mixed signal as shown in Figure 2.7. However, the power variation is half smaller because of the filtering. This numeric calculation is in-line with the analytic expression solution that $\tilde{P}_f(t) = \frac{P_b}{2}e^{i(2\pi\Delta f t + \Delta\Phi)}$, when the amplitude of the temporal mixed signal changes from P_b to $\frac{P_b}{2}$ after filtering.

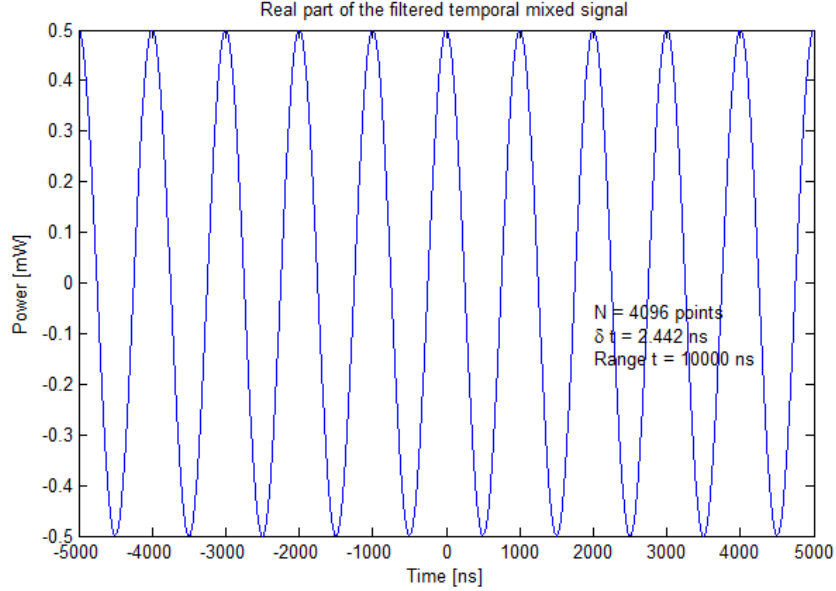


Figure 2.7: Real part of the filtered temporal mixed signal.

2.4 Phase of filtered temporal mixed signal

Figure 2.8 compares wrapped and unwrapped temporal phase of the filtered temporal mixed signal against time. The unwrapped phase is a straight line which makes it easy to pull out the line fit and find the slope. MATLAB function *polifit* allows us to perform a polynomial curve fit and create the line equation of the phase of filtered temporal mixed signal. In order to provide best fitting, we use function $p(t) =$

$\text{polyfit}(t', \text{unwrap}(\text{phaxx}), 6))$ to find coefficients of a polynomial $p(t)$ of sixth degree that fits the data in a least squares sense. The calculated polynomial is $0 \cdot t^6 + 0 \cdot t^5 + 0 \cdot t^4 + 0 \cdot t^3 + 0 \cdot t^2 + m \cdot t + b$, leaving us with $\phi = mt + b = 2\pi\Delta f + \Delta\Phi$, where $m = 0.0062832$ [rad GHz] and $\Delta\Phi = 31.4159$ [rad] as in the text box of Figure 2.8 b. After removing $2\pi k$ from the phase value, where k is an integer, and adding $\frac{\pi}{2}$ to offset the effect of 3-dB directional coupler we get the phase value within 0 and 2π . From this equation, we can find $\Delta\Phi = 31.4159 - 2\pi \cdot 5 + \frac{\pi}{2} = 1.570796327$ [rad] with $\Delta = 2.051034897e^{-10}$ [rad] difference and $\Delta f = \frac{m}{2\pi} = 1.000002338$ [MHz] with $\Delta = 2.338$ [Hz] error. Thus, optical heterodyne detection has successfully found the phase offset difference $\Delta\Phi$ and the frequency difference Δf .

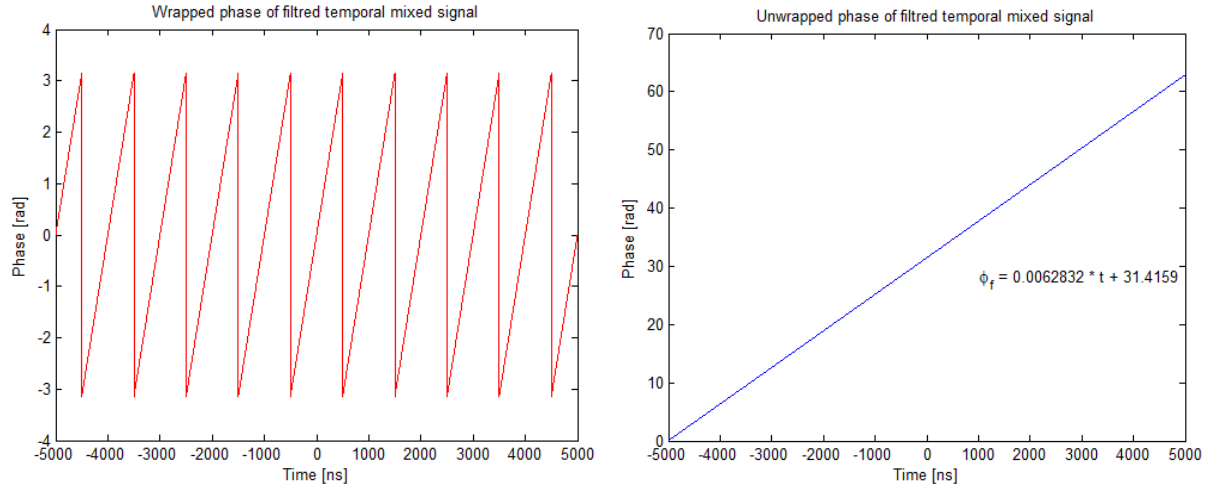


Figure 2.8: Temporal phase of filtered mixed signal.

The wrapped temporal phase is adjusted by multiplying the wrapped phase by $e^{(-i \cdot m \cdot t)}$ and adding $\frac{\pi}{2}$ as a 3-dB coupler correction. The detected phase shift is at 1.570796327 [rad]. The unwrapped temporal phase is adjusted by subtraction of the linear term mt from $y = mt + b$ and addition of $\frac{\pi}{2}$. This gives us the straight line at the phase of 1.570796327 [rad] as shown in Figure 2.9. The phase shift 1.570796327 [rad] has $\Delta = 2.051034897e^{-10} 3.6732e^{-6}$ [rad] difference from $\frac{\pi}{2}$.

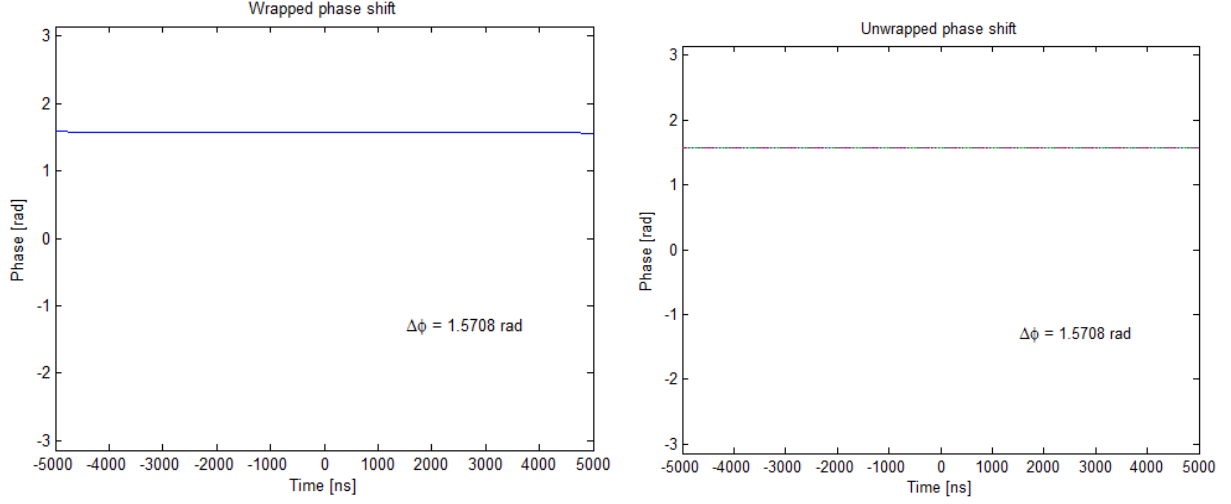


Figure 2.9: Phase without linear portion.

After comparing the wrapped and unwrapped phase for the temporal and spectral mixed signals, we found that the wrapped spectral phase and unwrapped temporal phase provide the best and simplest ways to find the phase shift, although all approaches gave reasonable results as shown in Table 2.1. Thus, these phase quantities will be used in further discussions.

Table 2.1: Phase shift

Source	$\Delta\Phi$	Δ
Actual	$\frac{\pi}{2}$	—
$\phi(f)$ wrapped	1.578466231	0.00766990394
$\phi(f)$ unwrapped	1.5649	0.005896
$\phi(t)$ wrapped	1.570796327	$2.051034897e^{-10}$
$\phi(t)$ unwrapped	1.570796327	$2.051034897e^{-10}$

2.5 Impact of zero padding

In this section we discuss the impact of zero padding on the performance of optical heterodyne detection. The time and frequency domains are interconnected via the following relation $N\delta t\delta f = 1$. Based on this equation, if δt is held constant and N is increased, δf must decrease. Therefore, the addition of zero padding to the temporal mixed signal will improve the spectral resolution and benefit the performance of the spectral mixed signal.

First we compare the example of not having the padding in *case A* and adding the symmetric zero padding to both sides of the temporal mixed signal in *case B*. The number of points in the mixed signal is the same for both cases and equal to $N_{sig} = 2^{12} = 4096$. Additionally, the total number of points in the zero padding case B is $N = 2^{17} = 131072$ making the number of pad points on each side equal to 63488 points. The temporal mixed signal is seen in Figure 2.10. The Fast Fourier transform representations are the most efficient when the length of array N is a power of 2.

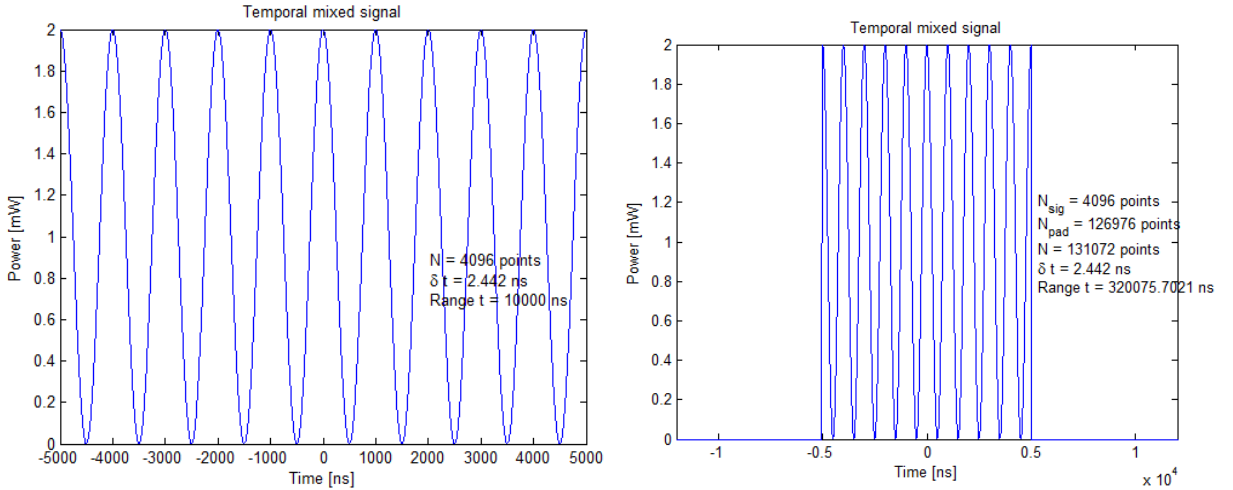


Figure 2.10: Temporal mixed signal with (B) and without (A) zero padding.

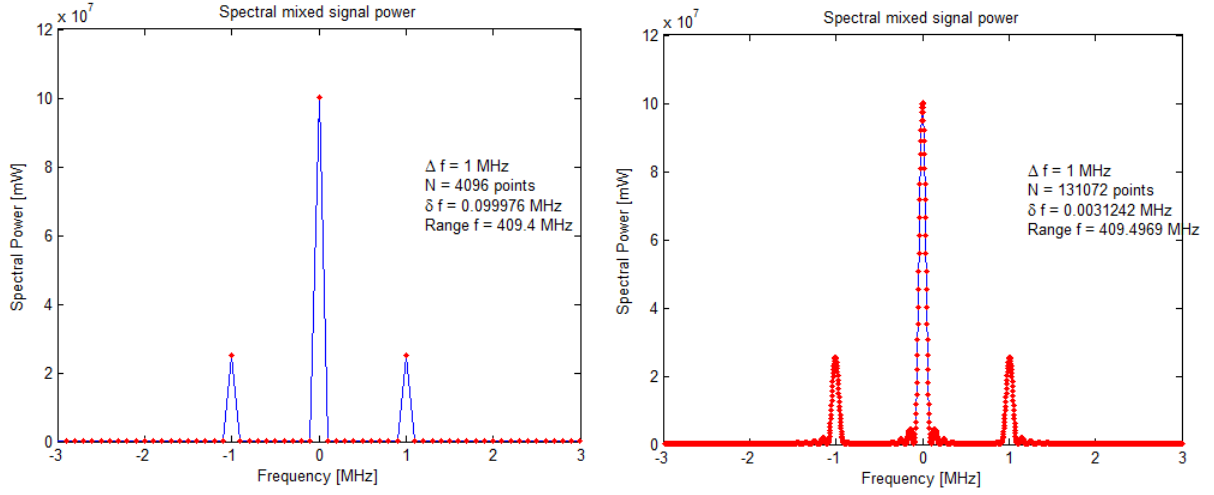


Figure 2.11: Spectral power of mixed signal with (B) and without (A) zero padding.

Figure 2.11 demonstrates the spectral power of the mixed signal for both cases. Zero padding has a noticeable effect on the spectral power graphs, making them more detailed and improving the quality as seen in the figure. Zero padding reduces the bin-size in the frequency domain which graphically reflects as improved resolution. Note that since the time interval δt was held constant, the maximum absolute frequency f_{absmax} stays the same, since $f_{absmax} = \frac{1}{2\delta t}$. The frequency interval δf reduces by the fraction that N increases because $N\delta t\delta f = 1$. Since total number of points N was increased from 2^{12} to 2^{17} (32 times), the sampling frequency δf reduces by 32 times from $9.9976e^{-3}$ to $3.1242e^{-3}$ [MHz]. However, the width of the spectral spike does not decrease by 32 times. It's width is determined by the *Range t* of the sinc term, which is not affected by zero padding.

The non-zero width of spectral power spikes is due to the finite length of the signal vector in time. For the analytic expression case, the modulating temporal power extends infinitely in time. For the numeric case, however, the modulated temporal power $P(t)$ must be truncated in time. The width of this truncation is $Range\ t_{sig} = t_{max_sig} - t_{min_sig}$,

and the actual temporal function can be considered to be

$$P'(t) = P(t) \times \Pi\left(\frac{t - t_o}{Range\ t_{sig}}\right), \quad (2.13)$$

where t_o is the center of the rectangular function and is given by $t_o = \frac{t_{max.sig} + t_{min.sig}}{2}$. The Fourier Transform of $P'(t)$ therefor a convolution:

$$\mathcal{F}\{P'(t)\} = \mathcal{F}\{P(t)\} * \mathcal{F}\{\Pi\}. \quad (2.14)$$

The Fourier Transform of a rectangular function is a sinc function:

$$\mathcal{F}\left\{\Pi\left(\frac{t - t_o}{Range\ t_{sig}}\right)\right\} = Range\ t_{sig} \cdot \text{sinc}(f \cdot Range\ t_{sig}) e^{-i2\pi f t_o}. \quad (2.15)$$

Due to the product $f \cdot Range\ t$ in the sinc argument, as $Range\ t_{sig}$ increases, the impact of f is larger, so the spectral function becomes more narrow. Likewise, as $Range\ t_{sig}$ decreases, the impact of f is lessened, and so the spectral function broadens. The approximate full width half maximum of the sinc function is

$$FWHM \approx \frac{1}{Range\ t_{sig}}. \quad (2.16)$$

The convolution of $\mathcal{F}\{P(t)\}$ with the sinc function will cause the narrow spectral spikes (of the analytic expression case) to broaden. They will broaden to a width of about the width of the sinc function, which is about $1/Range\ t_{sig}$.

For the case shown in Figure 2.11, the width of each spike located at $f = \pm 1$ [MHz] is estimated to be $1/Range\ t_{sig} = 1/10\mu s = 0.1$ [MHz]. The actual half width of the spikes is 0.1042 [MHz]. In case A there are only 3 points per spike, which does not allow the half width to be found accurately. There are about 60 points per spike in case B with zero padding with $N = 2^{17}$ and $N_{sig} = 2^{12}$ which allows to calculate the FWHM.

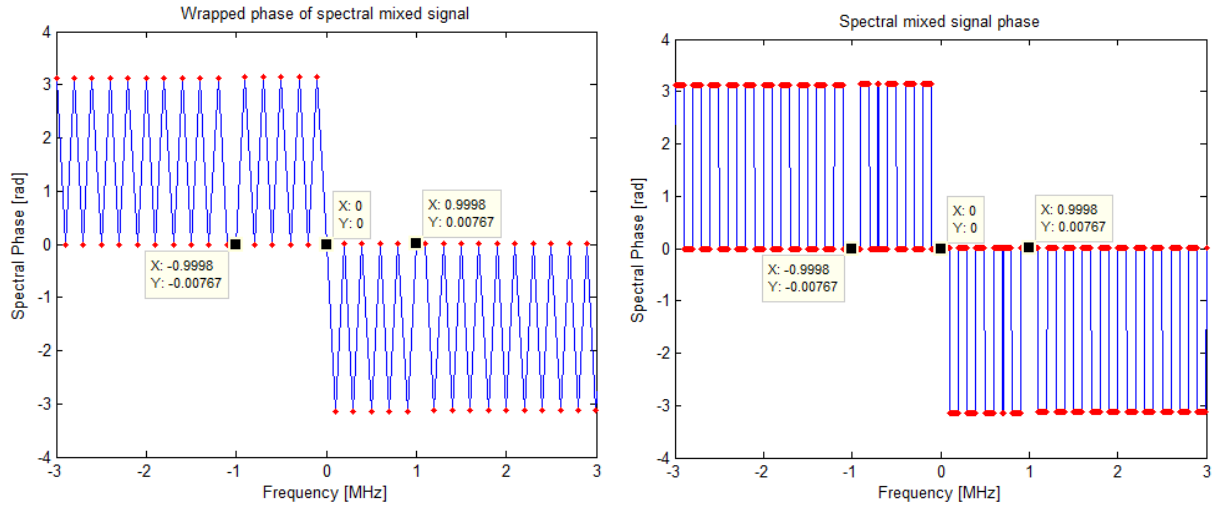


Figure 2.12: Phase of spectral mixed signal with (B) and without (A) zero padding.

Figure 2.12 B allows to see that unwrapped phase is actually consists of squared elements and flat at the top and bottom. We cannot see it in the case without padding due to the lack of points.

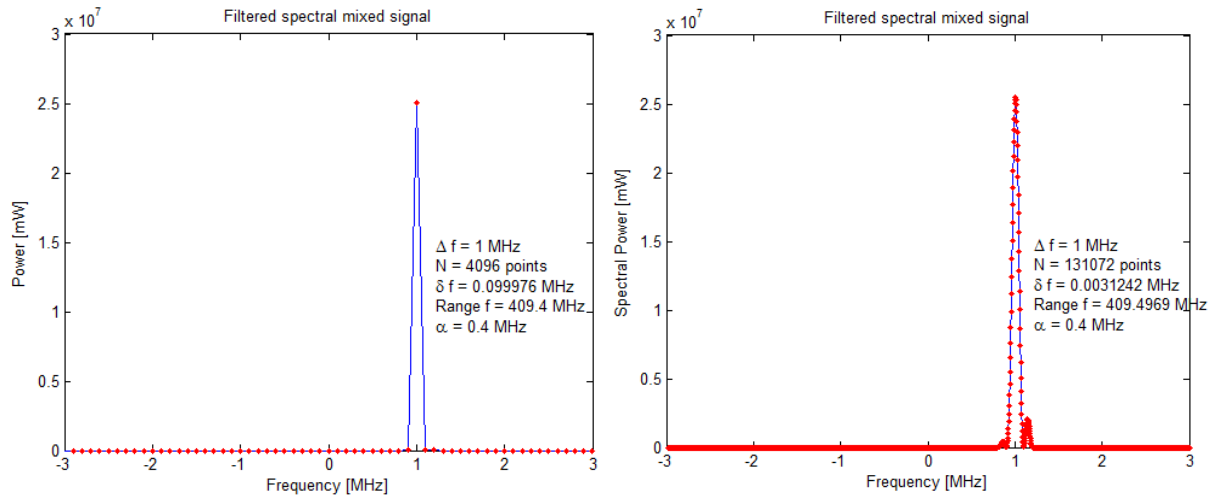


Figure 2.13: Filtered spectral mixed signal with (B) and without (A) zero padding.

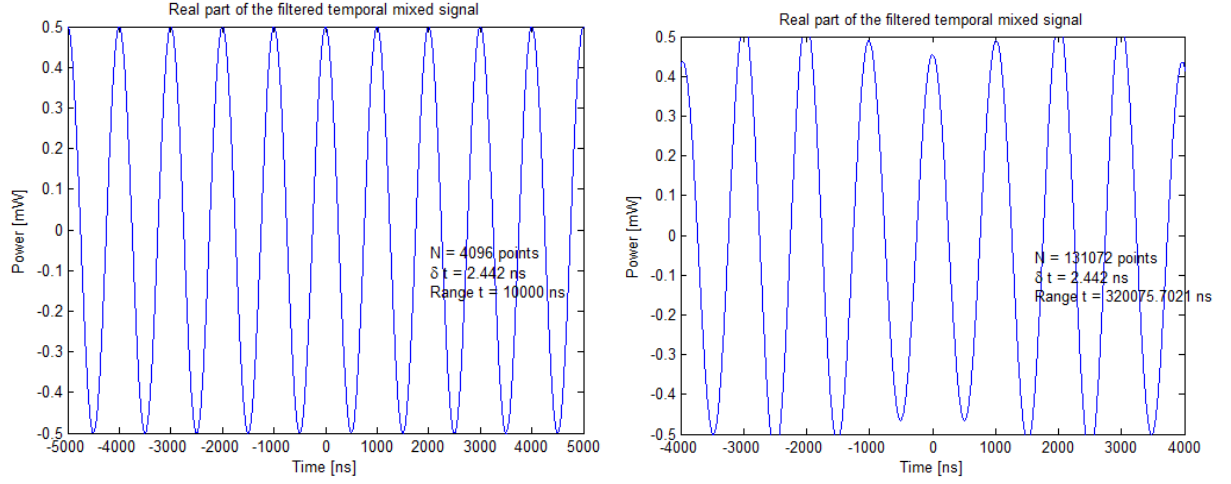


Figure 2.14: Real part of filtered temporal mixed signal with (B) and without (A) zero padding.

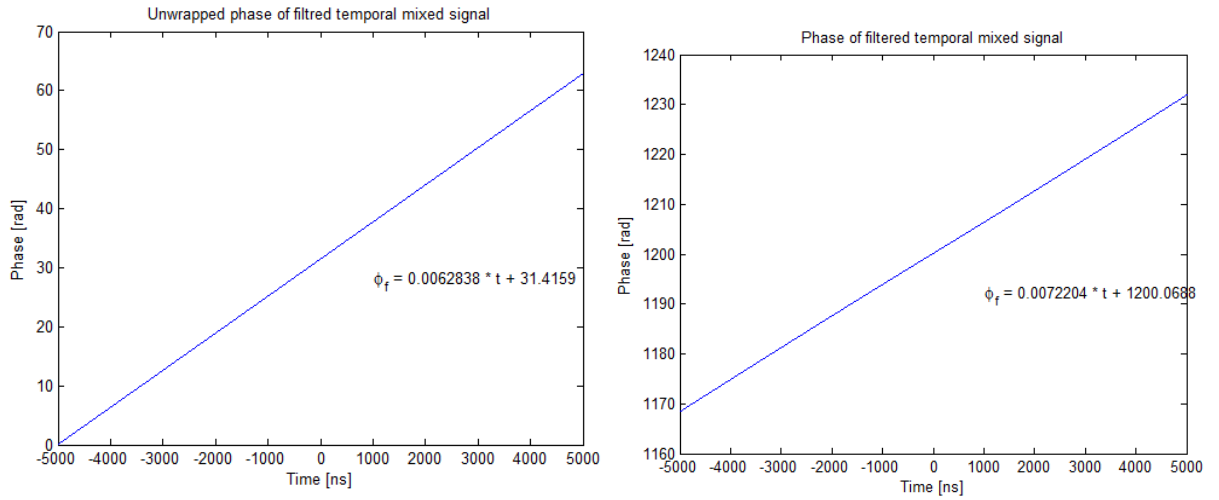


Figure 2.15: Phase of temporal mixed signal with (B) and without (A) zero padding.

Figures 2.12 and 2.15 show the phase of the spectral and temporal mixed signals for both cases. The text box of Figure 2.12 shows that the phase offset of the spectral signal is the same for both cases and yields to $0.00767 + \frac{\pi}{2} = 1.578466327$ [rad] with $\Delta = 0.00767$ [rad]. After removing the linear part and adding $\frac{\pi}{2}$ as a 3-dB coupler effect to the temporal phase in Figure 2.15, we get phase offset of 1.570796327 [rad] with $\Delta = 2.00296e^{-10}$ [rad] and 1.551239063 [rad] with $\Delta = -0.0195572$ [rad] for cases A and

B, respectively as shown in Figure 2.16.

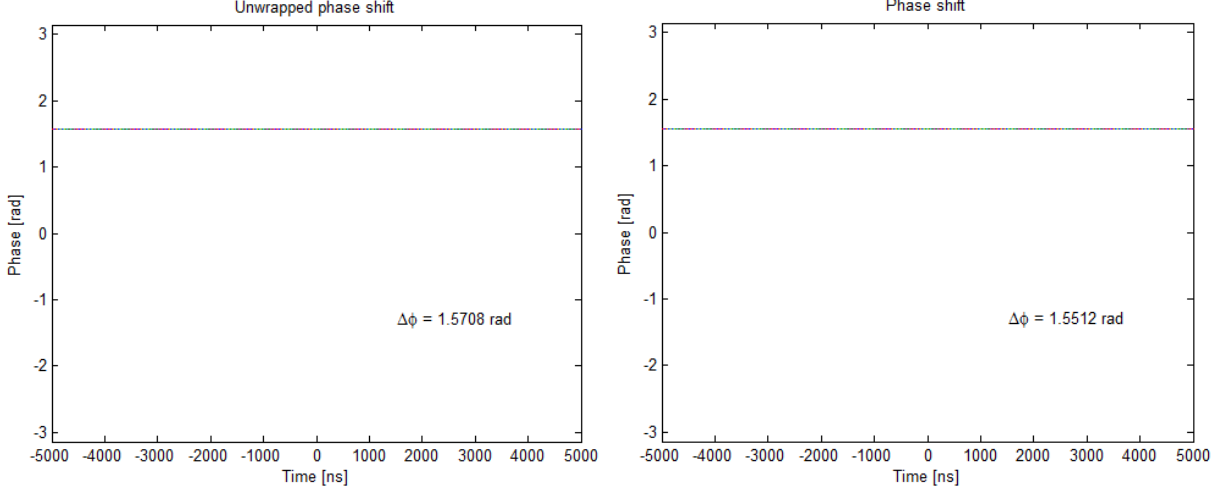


Figure 2.16: Phase of temporal mixed signal with (B) and without (A) zero padding with linear part removed.

In summary, zero padding improves the graphical resolution in the spectral domain, improves the FWHM calculation and captures the same spectral phase shift as the case without padding. It is a useful technique which allows us to maximize the resolution of spectral mixed signal without changing N_{sig} , δt , $Range\ t$ and Δf . Padding, however, does not give a better result in phase and frequency detection in either spectral or temporal domains. Table 2.2 demonstrates the assessed phase difference for wrapped spectral phase and unwrapped temporal phase for cases with and without padding.

Table 2.2: Phase shift

Source	$\Delta\Phi$	Δ
Actual	$\frac{\pi}{2}$	—
$\phi(f)$ without padding	1.578466327	0.00767
$\phi(f)$ with padding	1.578466327	0.00767
$\phi(t)$ without padding	1.570796327	$2.00296e^{-10}$
$\phi(t)$ with padding	1.551239063	-0.0195572

Chapter 3

Important conditions for optical heterodyne phase detection

While this method of phase detection can be applied to a wide range of cases, there are a couple of conditions which have to pass in order for the analysis to work. There are three important aspects that determine the spectral power shape:

- a) δf , the spectral resolution,
- b) $\text{sinc}(f \text{Range } t_{sig})$, the shape of the spectral spike,
- c) Δf , the frequency difference $f_s - f_o$.

Conditions are placed on the frequency difference Δf , the number of temporal periods (which is related to $\text{Range } t_{sig}$), and the number of points in the signal N_{sig} , all of which are discussed in this chapter.

3.1 Frequency difference Δf & δf

As we discussed in Chapter 1, Δf defines where the side bands are located. This condition distinguishes heterodyne detection from homodyne detection:

$$\Delta f = f_s - f_o \neq 0. \quad (3.1)$$

When $\Delta f = 0$ as shown in Figure 3.1, there are no visible side bands which makes filtering impossible. Therefore, one of the must conditions for the optical heterodyne phase shift detection analysis is $\Delta f \neq 0$. In this case, the process of the optical heterodyne detection would be used.

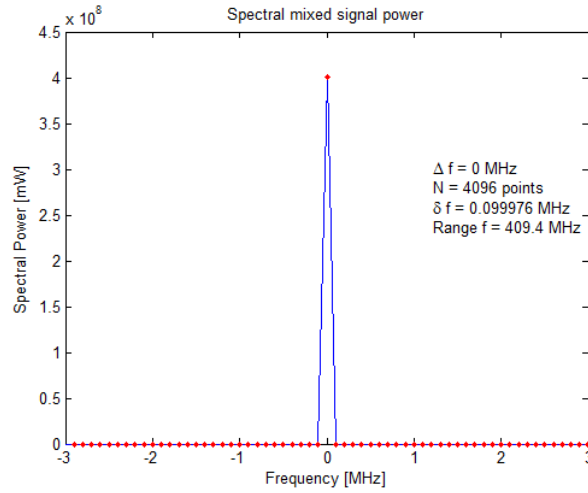


Figure 3.1: Spectral power of mixed signal when $\Delta f = 0$.

The important idea here is that the frequency difference Δf must be larger than the width of the spectral power spike $\Delta f > 2\delta f = \frac{2}{\delta t N}$. Here, the graph is limited by δf , not the sinc function.

3.2 Frequency difference Δf & $\delta t N$

Another important condition is that the number of periods in the temporal mixed signal can influence the power spectrum and produce the same problem as in the previous case

— no side bands in the spectral mixed signal. The number of periods in the temporal mixed signal depends on the frequency difference Δf , the time vector length $Range\ t_{sig}$, and the time interval δt . Here, $Range\ t_{sig}$ is the range of the data and does not include zero padding. For example, one period can be reached by lowering frequency offset Δf as in Figure 3.2 A or by decreasing the length of the time vector as in Figure 3.2 B.

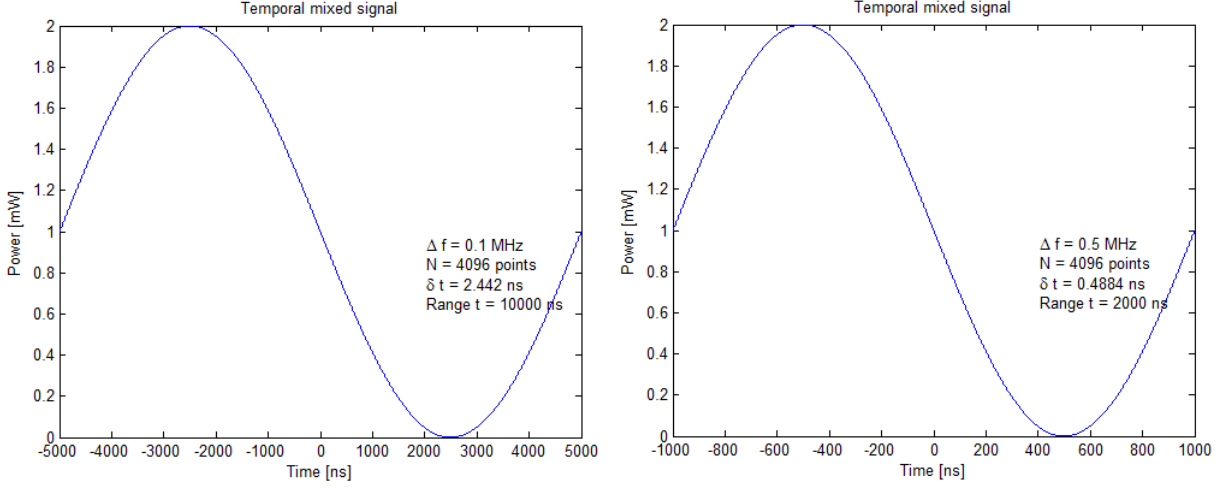


Figure 3.2: Temporal power for A. $\Delta f = 0.1$ MHz, $Range\ t_{sig} = 10000$ ns; B. $\Delta f = 0.5$ MHz, $Range\ t_{sig} = 2000$ ns.

For these examples, the waveform with one period cannot be used for the analysis as it does not have visible side bands in the spectral mixed signal as shown in Figure 3.3. The side bands are essential for the filtering and separating the phase noise in our method of phase shift detection. For case A, $2\delta f = \frac{2}{\delta t N} = 0.12$ [MHz] and is larger than the frequency difference $\Delta f = 0.1$ MHz. Therefore, the side spikes are buried in the width of the central spike. For the case B, $2\delta f = 0.6$ [MHz], which is larger than the frequency offset $\Delta f = 0.5$ [MHz]. Thus, the side bands are not visible.

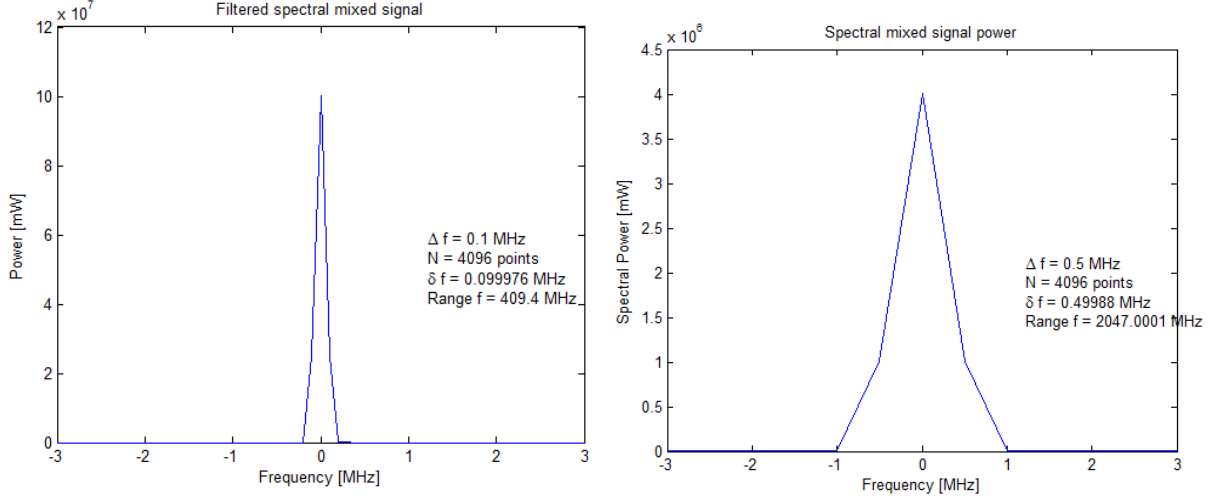


Figure 3.3: Spectral power for A. $\Delta f = 0.1$ MHz, Range $t_{sig} = 10000$ ns; B. $\Delta f = 0.5$ MHz, Range $t_{sig} = 2000$ ns.

Here, we introduce another condition that must be met:

$$1) \text{ Frequency resolution: } \Delta f > 2\delta f = \frac{2}{\delta t N},$$

$$2) \text{ sinc width: } \Delta f > \frac{2}{\text{Range } t_{sig}}.$$

These conditions appear similar, but they are not the same. $\text{Range } t_{sig}$ is the extent of the signal, and does not include zero padding. Thus, while increasing $\text{Range } t_{sig}$ does correspond to an increase in N number of points in the signal, adding zero padding also increases N (assuming δt is fixed), but does not correspond to an increase in $\text{Range } t_{sig}$ of the signal.

Furthermore, the relationship between δf and the width of the sinc function is important too. Under the following conditions, the sinc functions will be resolved:

$$\delta f < \frac{C}{\text{Range } t_{sig}}, \quad (3.2)$$

$$\frac{1}{\delta t N} < \frac{C}{\text{Range } t_{sig}}, \quad (3.3)$$

where C is a constant on the order of 0.5. Range $t_{sig} = \delta t N_{sig} - \delta t$, which yields

$$\frac{1}{\delta t N} < \frac{C}{\delta t N_{sig} - \delta t}, \quad (3.4)$$

$$\frac{1}{N} < \frac{C}{N_{sig} - 1}. \quad (3.5)$$

Since N_{sig} is much greater than 1, this expression simplifies to

$$\frac{1}{N} < \frac{C}{N_{sig}}. \quad (3.6)$$

Without zero padding, $N_{sig} = N$, and

$$1 < C. \quad (3.7)$$

Since C is on the order of 0.5, the sinc function is not resolved well without zero padding.

In the case of zero padding, $N = N_{sig} + N_{pad}$, which yields

$$\frac{1}{N_{sig} + N_{pad}} < \frac{C}{N_{sig} - 1}. \quad (3.8)$$

Again, for simplicity, we approximate $N_{sig} - 1$ by N_{sig} .

$$\frac{1}{N_{sig} + N_{pad}} < \frac{C}{N_{sig}}, \quad (3.9)$$

$$\frac{N_{sig}}{N_{sig} + N_{pad}} < C. \quad (3.10)$$

As N_{pad} increases, it is easier to make the $LHS < C$, and therefore the features of the sinc function can be resolved.

3.3 Number of points N & δt

The number of points in the time vector plays an important role in the process of transformation from the time to frequency domain. Extending the number of points N from 2^{12} to 2^{16} in the temporal domain yields to higher resolution in spectral domain if the

time step δt is held constant. Due to $N\delta t\delta f = 1$, the distance between points δf decreases. Temporal and spectral mixed signal with $N = 2^{12}$ is represented in Figure 3.4, with $N = 2^{16}$ points in Figure 3.5.

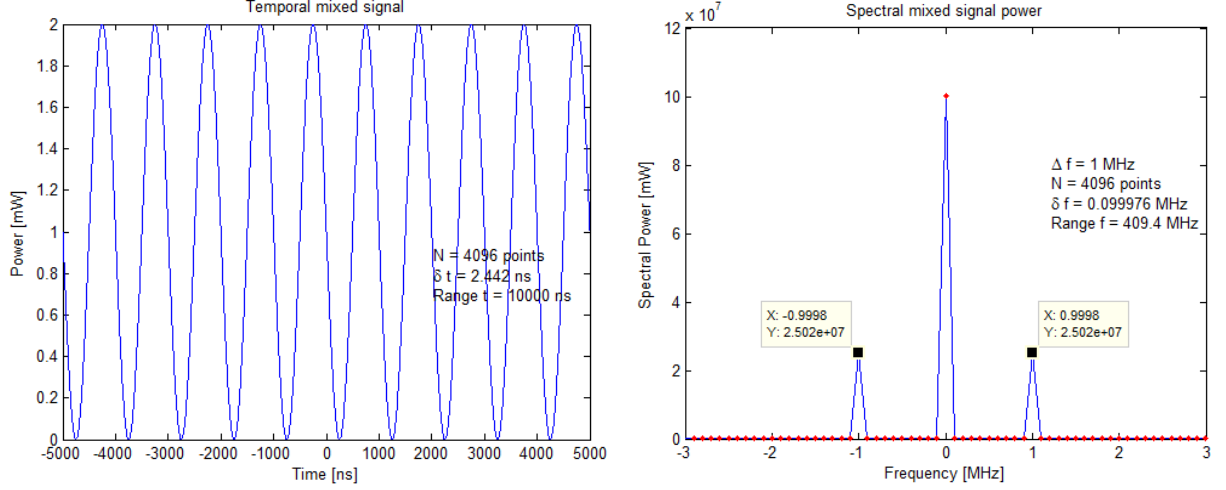


Figure 3.4: Temporal and spectral mixed signal, $N = 2^{12}$

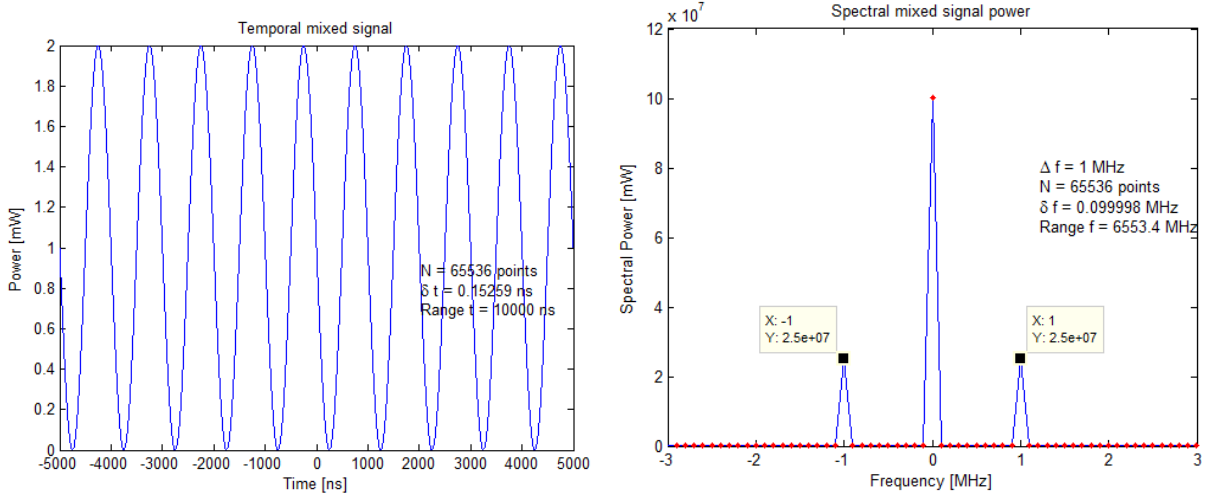


Figure 3.5: Temporal and spectral mixed signal, $N = 2^{16}$

The larger N allows the frequency and height of the spectral spikes to be more accurate. Note that because $Range\ t_{sig}$ is held constant, the width of the spikes doesn't change.

3.3.1 Number of points and zero padding

As discussed previously, zero padding helps to increase the number of points N and reduce the distance between the points in frequency domain if the time interval δt is held constant. Thus, it creates more accurate graphs in the spectral domain. However, increasing the number of points and using zero padding produces even better results. This is because increasing the number of points increases spectral resolution, while using zero padding reduces the impact of windowing the sin wave. The following is a relationship between the number of points in the signal N_{sig} and zero padding.

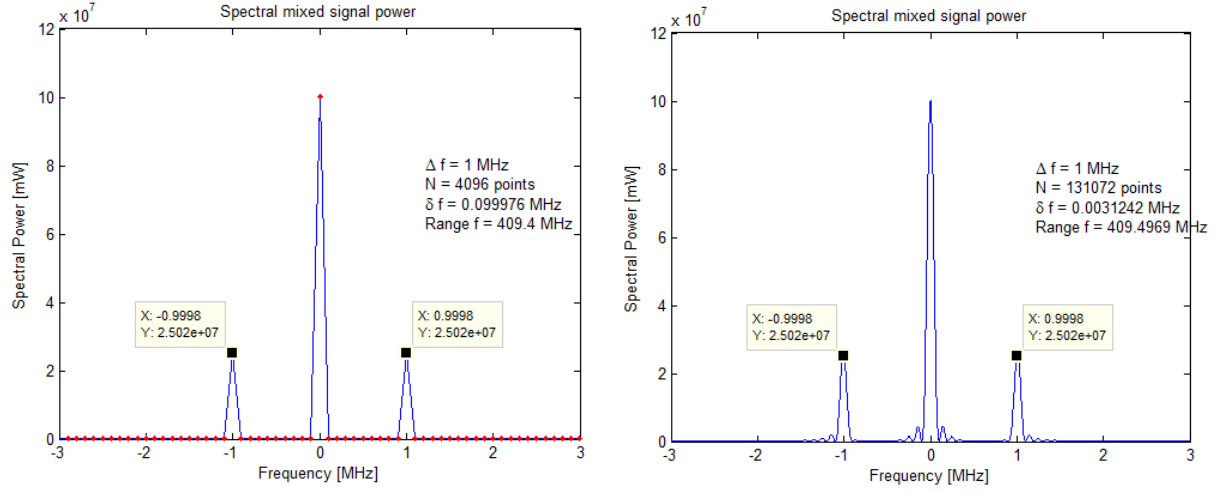


Figure 3.6: Power of spectral mixed signal $N_{sig} = 2^{12}$ without and with zero padding respectively.

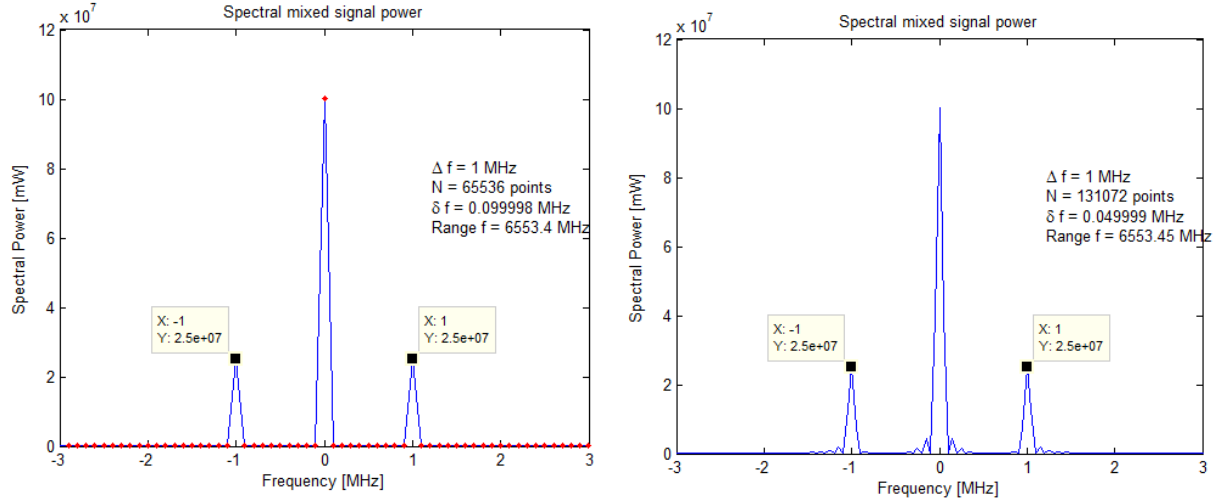


Figure 3.7: Power of spectral mixed signal $N_{sig} = 2^{16}$ without and with zero padding respectively.

The best results are achieved with the number of points in the signal $N_{sig} \geq 2^{16}$ and zero padding used at the same time. This way the frequency offset has the least amount error — $\Delta f = 1$ [MHz] — and the spectral mixed signal has higher resolution.

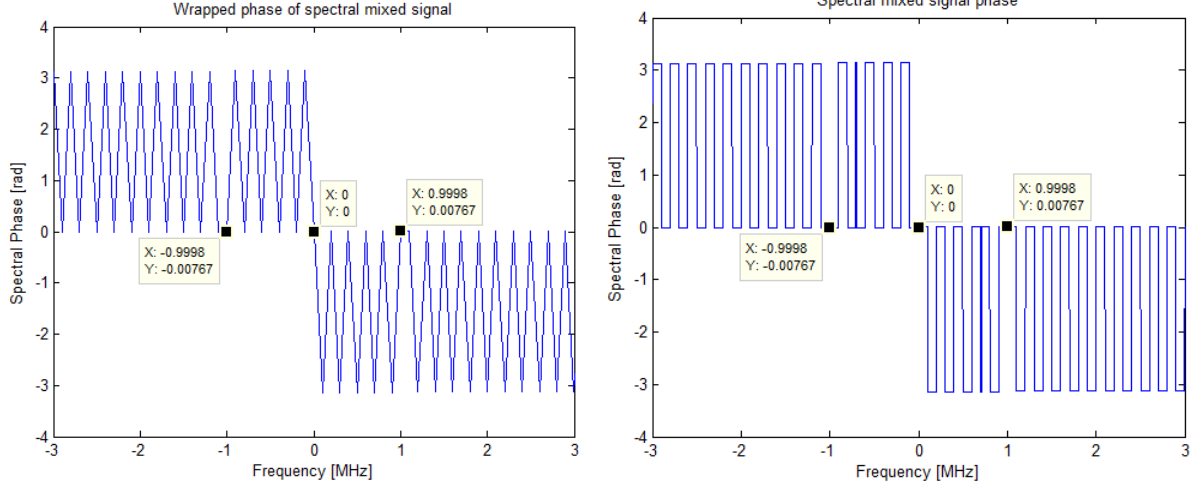


Figure 3.8: Phase of spectral mixed signal $N_{sig} = 2^{12}$ without (A) and with (B) zero padding.

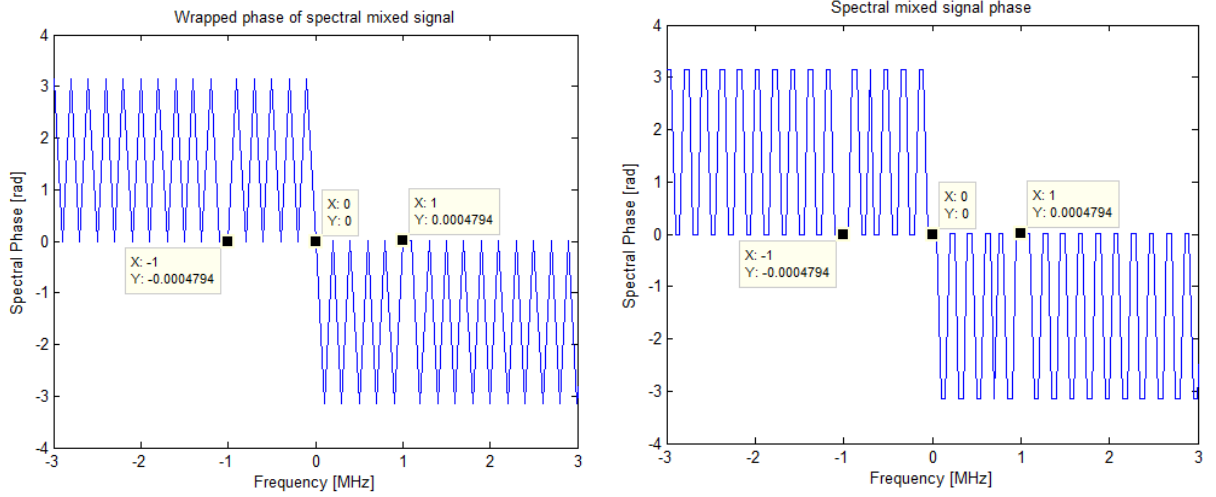


Figure 3.9: Phase of spectral mixed signal $N_{sig} = 2^{16}$ without (A) and with (B) zero padding.

Figures 3.8 and 3.9 compare the phase of spectral mixed signal. The phase offset detected for the case $N_{sig} = 2^{12}$ is $0.00767 + \frac{\pi}{2} = 1.578466327$ [rad] with $\Delta = 0.00767$ [rad]. For the case $N_{sig} = 2^{16}$ it is $0.00047 + \frac{\pi}{2} = 1.571275727$ [rad] with $\Delta = 0.0004794$ [rad] difference from $\frac{\pi}{2}$. Thus, the $N_{sig} = 2^{16}$ case gives better results in estimation of the phase offset difference. Moreover, the Δf is 0.9998 [MHz] in the case $N_{sig} = 2^{12}$ which is

0.0002 [MHz] error from the correct value of 1 [MHz] as detected in the case $N_{sig} = 2^{16}$ points.

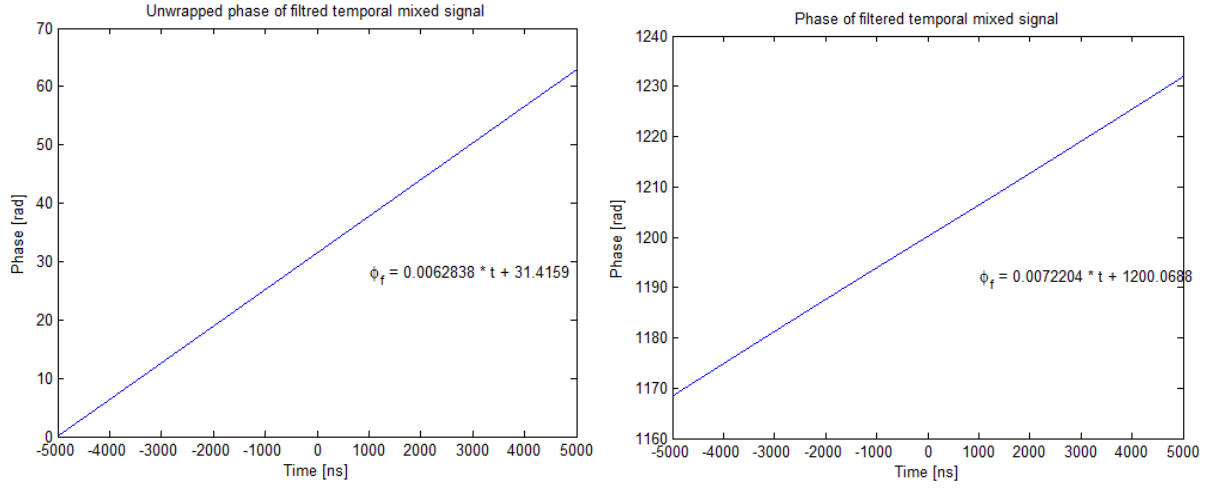


Figure 3.10: Phase of temporal mixed signal $N_{sig} = 2^{12}$ without (A) and with (B) zero padding.

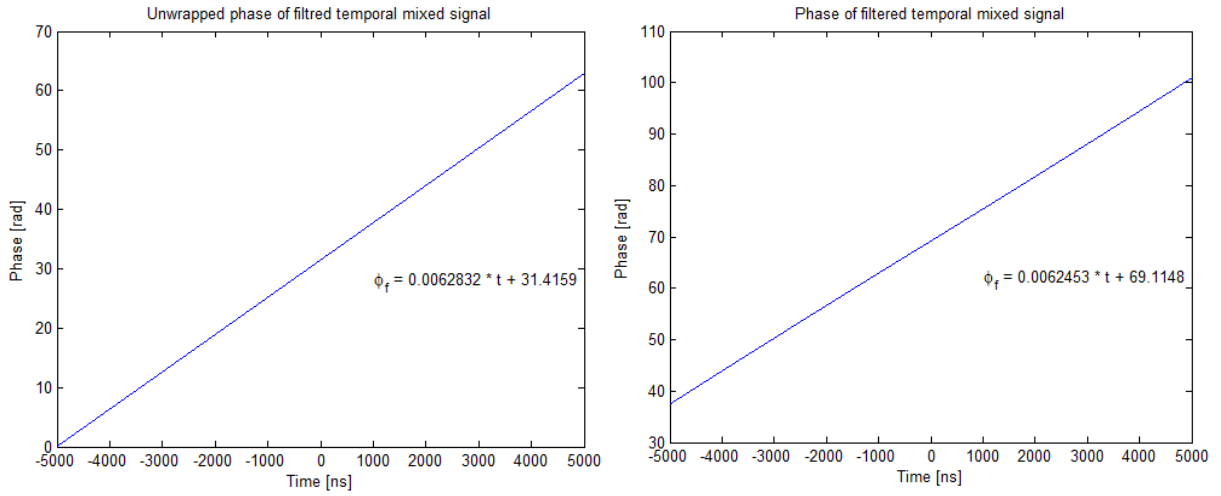


Figure 3.11: Phase of temporal mixed signal $N_{sig} = 2^{16}$ without (A) and with (B) zero padding.

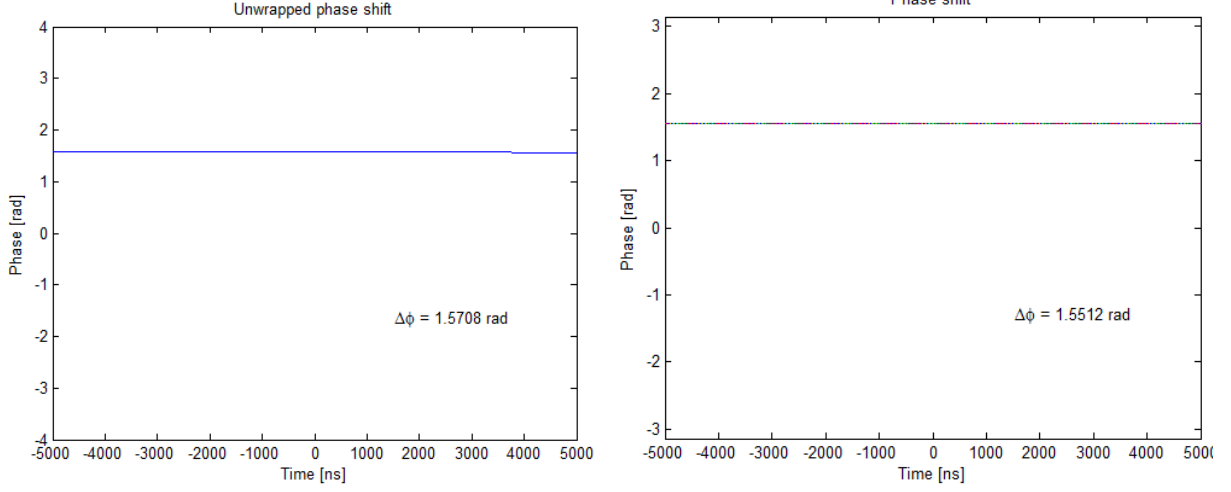


Figure 3.12: Phase of temporal mixed signal with linear part removed and 3-dB coupler correction for $N_{sig} = 2^{12}$ without (A) and with (B) zero padding.

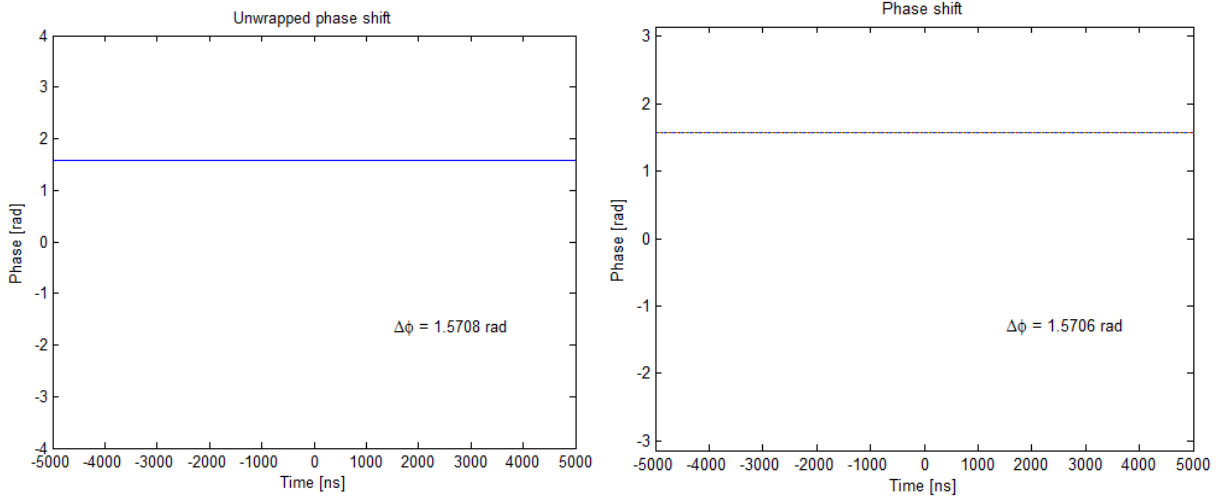


Figure 3.13: Phase of temporal mixed signal with linear part removed and 3-dB coupler correction for $N_{sig} = 2^{16}$ without (A) and with (B) zero padding.

Figures 3.12 and 3.13 show the phase of the temporal mixed signal for $N_{sig} = 2^{12}$ and $N_{sig} = 2^{16}$ points. In the case $N_{sig} = 2^{12}$ without padding, the phase offset is $31.4159 - 2 \cdot \pi \cdot 5 + \frac{\pi}{2} = 1.5708$ [rad] with $\Delta = 2.65358e^{-5}$ [rad] difference from $\frac{\pi}{2}$. The difference in the slope is $6.146928e^{-7}$ [MHz]. In the case $N_{sig} = 2^{12}$ points with padding, the phase offset is 1.5512 [rad] with $\Delta = 0.0195963$ [rad]. In the case $N_{sig} = 2^{16}$ points

without padding, the phase offset is 1.5708 [rad] with $\Delta = 2.65358e^{-5}$ [rad]. In the case $N_{sig} = 2^{16}$ points with padding, the phase offset is 1.5706 [rad] with $\Delta = 1.963268e^{-4}$ [rad].

These results show that we get the biggest improvement when we increase the number of points to $N_{sig} = 2^{16}$. Increase in total number of points N allows to decrease δf without affection the sinc function. Zero padding plays an important role in analyzing signals in the spectral domain, however it does not help to decrease the error of the phase or frequency detection in the temporal domain.

3.4 Conclusion

The important points we can conclude from this chapter are:

- We need to have side bands in the spectral mixed signal, so the restriction is

$$* \Delta f > \frac{2}{\delta t N_{sig}}$$

- The number of points in the signal has a significant effect of the error of detection, therefore we will be using $N_{sig} = 2^{16}$ points in further calculations. Increase of the number of points cause a decrease in δf and the sinc function. Using the conditions $N_{sig} = 2^{16}$ points without padding and $\Delta f = 1$ [MHz], Figure 3.14 shows the data for the assessed $\Delta\Phi$ as markers and the input phase as a line for the temporal and spectral phase shifts.

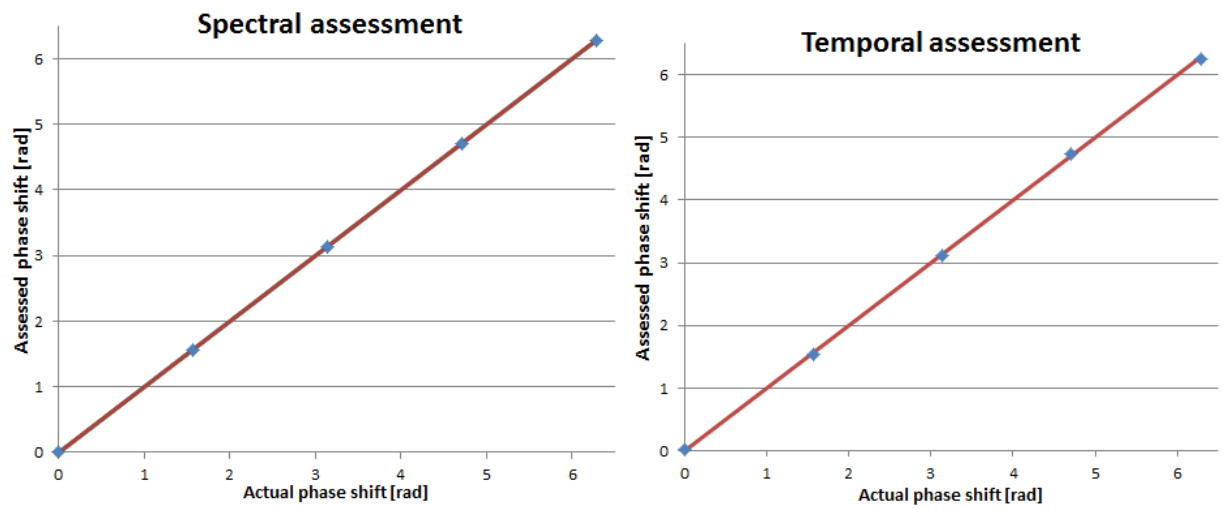


Figure 3.14: Assessed phase versus actual input phase, for spectral and temporal phase assessment techniques.

3.5 Summary of Optical Heterodyne Detection

The steps and conditions used to perform optical heterodyne detection are summarized as follows:

1. $P(t)$, using $\Delta f = f_s - f_o$

$$\star \Delta f > \frac{2}{\delta t N_{sig}}$$

2. $\tilde{S}(f) = \mathcal{F}\{P(t)\}$

$$\star \Delta\Phi = \phi(\Delta f) = \phi(-\Delta f)$$

$$\star \text{ (with 3-dB directional coupler) } \Delta\Phi = \phi(\Delta f) + \frac{\pi}{2} = \phi(-\Delta f) - \frac{\pi}{2}$$

3. $\tilde{S}_f(f) = \mathcal{F}\{P(t)\} \times \Pi(\frac{f-f_0}{\alpha})$

$$\star \alpha > 2\delta f = \frac{2}{\delta t N_{sig}}$$

4. $\tilde{P}_f(t) = \mathcal{F}^{-1}\{\tilde{S}_f(f)\}$

5. $\phi_f(t) = \tan^{-1} \left\{ \frac{Im\{\tilde{P}_f\}}{Re\{\tilde{P}_f\}} \right\} = angle\{\tilde{P}(f)\}$

6. $\phi_f(t) = mt + b$

$$\star \Delta\Phi = \phi_f(t) - mt = b$$

$$\star \text{ (with 3-dB directional coupler) } \Delta\Phi = \phi_f(t) - mt + \frac{\pi}{2} = b + \frac{\pi}{2}$$

Chapter 4

OHD of Phase-Shifted Signals:

Non-Split Signal

In this thesis we are interested in understanding the optical heterodyne detection of phase-shifted signals. We study two basic categories of analyzing the phase-shifted signal. The first category is to process the entire temporal mixed signal with the numerical analysis described in the Chapter 2. This method called the non-split signal method and is the focus of this chapter. The second category is to split the signal at the phase shift into two separate waveforms and then apply the analysis to each segment separately. This method is called the split signal method and is the focus of chapters 5 and 6. In this current chapter we discuss the analysis of phase-shifted signals without splitting the waveform for phase shifts of π , $\frac{\pi}{2}$ and $-\frac{\pi}{2}$ [rad] in detail, and a range of phase shifts in summary.

4.1 Phase shift of π

Temporal mixed signal: The temporal mixed signal in Figure 4.1 has phase shift of π in the middle of the waveform at $t = 0$. We use the number of points $N = 2^{16}$ since it gives less percentage error and compare the signal with and without padding side by side.

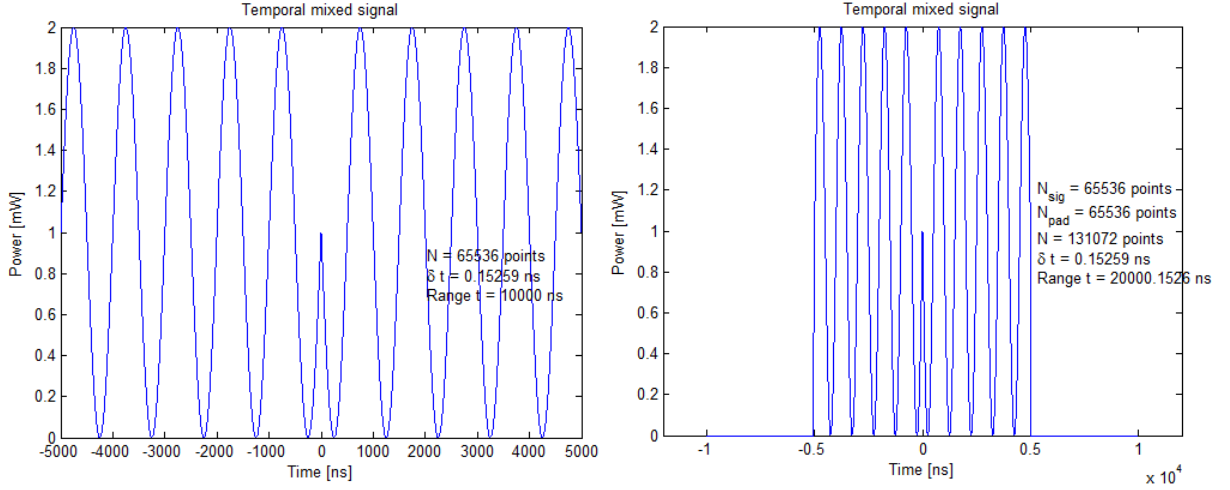


Figure 4.1: Temporal mixed signal with a phase shift of π at $t=0$, with (B) and without (A) padding.

The phase shift $\Delta\phi(f)$ is given by

$$\Delta\phi(f) = \Delta\Phi_2 - \Delta\Phi_1 = \phi_{s2} - \phi_o - (\phi_{s1} - \phi_o) = \phi_{s2} - \phi_{s1}, \quad (4.1)$$

showing that the phase reference of the local oscillator drops out. ϕ_{s1} and ϕ_{s2} are the phase offsets of the signal before and after the phase change.

Spectral mixed signal: Proceeding with the analysis we perform the Fast Fourier transformation on the temporal mixed signal. The power of the spectral mixed signal is represented in Figure 4.2. The power of the spectral mixed signal does not look like that of a single spike anymore. The phase shift of π affects the waveform and cancels out some

of the peak making it reach zero in the middle. Note that the spike is broader than the non-phase shifted case.

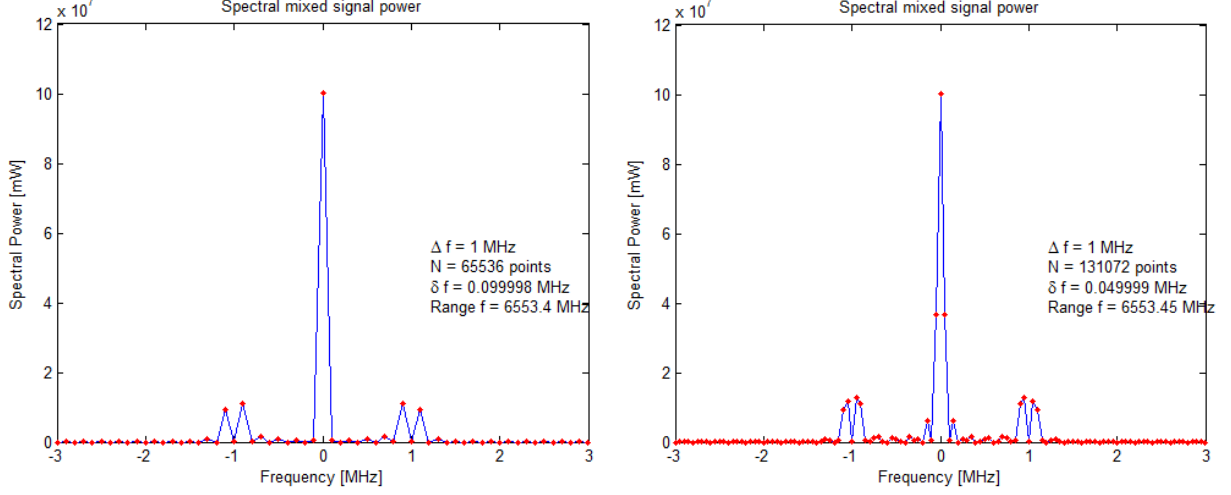


Figure 4.2: Power of spectral mixed signal, with (B) and without (A) padding.

The phase of the spectral mixed signal is different as well. The negative frequency used to provide the negative spike, now it is flipped and the negative frequency has the positive spike as shown in Figure 4.3. The detected phase at $f = 1$ MHz is -3.141 rad, but we still need to add $\frac{\pi}{2}$ to it because of the 3-dB coupler effect.

Analyzing the spectral phase shift, we noticed that the phase shift could be detected using a formula based on the difference of the phase values found at $+\Delta f$ and $-\Delta f$:

$$\Delta\phi(f) = (\phi(+\Delta f) + \frac{\pi}{2}) - (\phi(-\Delta f) - \frac{\pi}{2}) = \phi(+\Delta f) - \phi(-\Delta f) + \pi, \quad (4.2)$$

where $\phi(+\Delta f)$ and $\phi(-\Delta f)$ is phase detected at $\pm\Delta f$. In this case, the assessed phase shift is $\Delta\phi(f) = -3.140633916 - 3.140633916 + \pi = -3.139675178 + 2\pi = 3.143510129$ [rad] with error $\Delta = 1.91747518e^{-3}$ [rad].

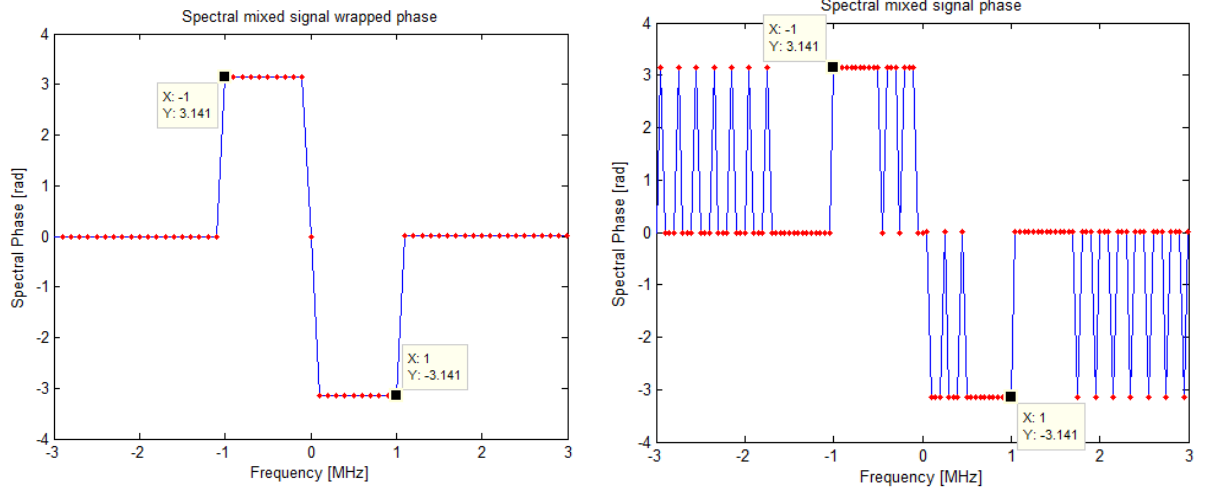


Figure 4.3: Phase of spectral mixed signal, with (B) and without (A) padding.

The width of the filter α was broadened to capture additional features and lower the error. We used $\alpha = 1$ [MHz] and the filtered spectral mixed signal is represented in Figure 4.4.

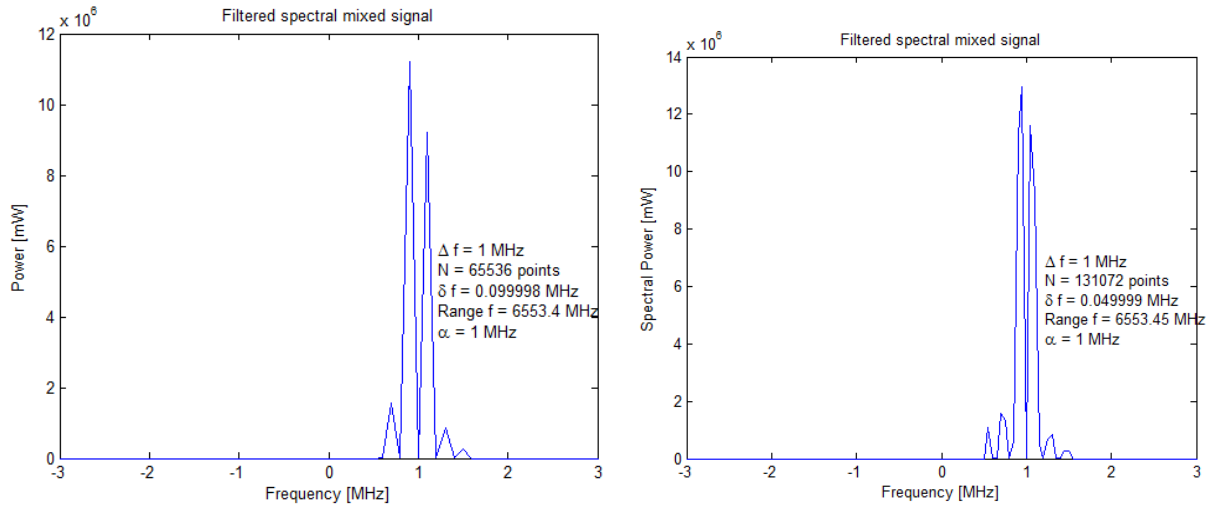


Figure 4.4: Filtered spectral mixed signal, with (B) and without (A) padding.

Filtered temporal mixed signal: Figure 4.5 shows temporal mixed signal with and without padding. For the case with padding, the waveform was zoomed in for the time period from -5000 to 5000.

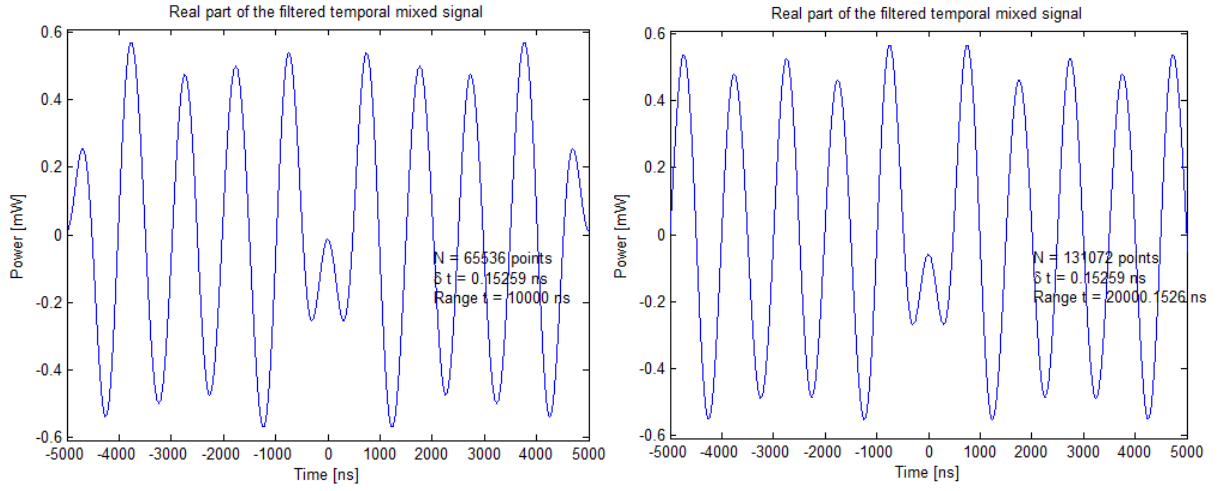


Figure 4.5: Filtered temporal mixed signal, with (B) and without (A) padding.

After applying the filter and inverse FFT, the unwrapped temporal phase of the filtered temporal mixed signal is extracted and represented in Figure 4.6. We can find the polynomial line equation for this waveform, however the resulted waveform is not a straight line anymore. Therefore does not accurately detect $\Delta f = 0.795313166$ [MHz] with error $\Delta = 0.20468683$ [MHz]. The actual waveform has a phase shift and the fitted line is a straight line.

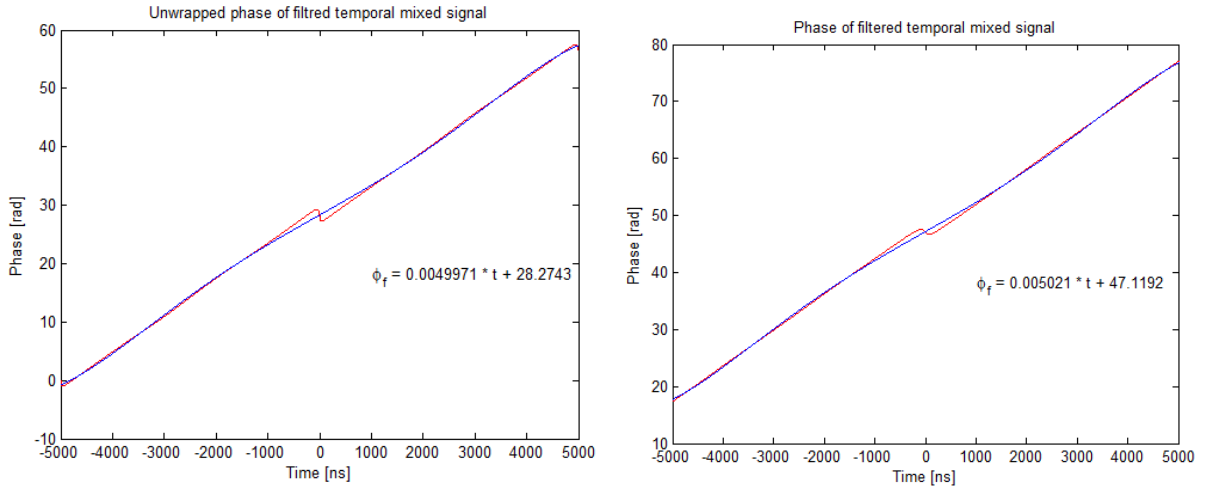


Figure 4.6: Temporal phase of the mixed signal, with (B) and without (A) padding.

In order to find the phase shift, we subtract the linear fit equation ($y = mt + b$) from

the temporal phase waveform. The result is shown in Figure 4.7. The phase distance between two peaks is the phase shift. However, this method does not provide an accurate result. The detected value for the no padding case is 2.568374197 [rad] which is $\Delta = -0.5732184563 \approx \frac{\pi}{6}$ [rad] difference from the original value of π . The case with padding has a phase shift of 2.101947819 [rad] which yields to $\Delta = -1.039644834 \approx \frac{\pi}{3}$ [rad] error.

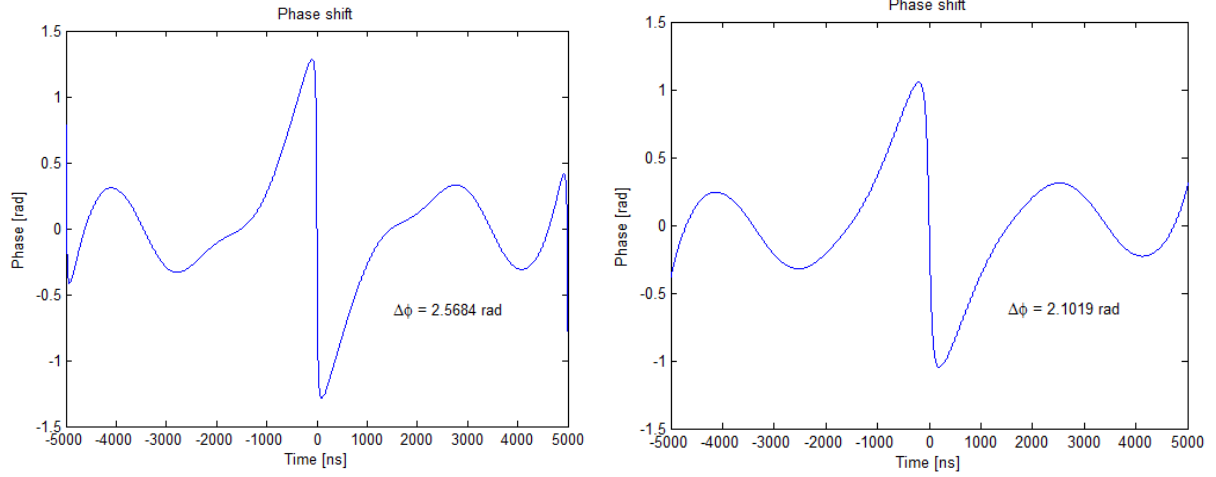


Figure 4.7: Phase of filtered temporal signal, having the linear part removed, with (B) and without (A) padding.

4.2 Phase shift of $\frac{\pi}{2}$

Figure 4.8 shows the temporal mixed signal with a $\frac{\pi}{2}$ phase shift. We proceed with the analysis and find the power and phase of the spectral mixed signal depicted in Figure 4.9.

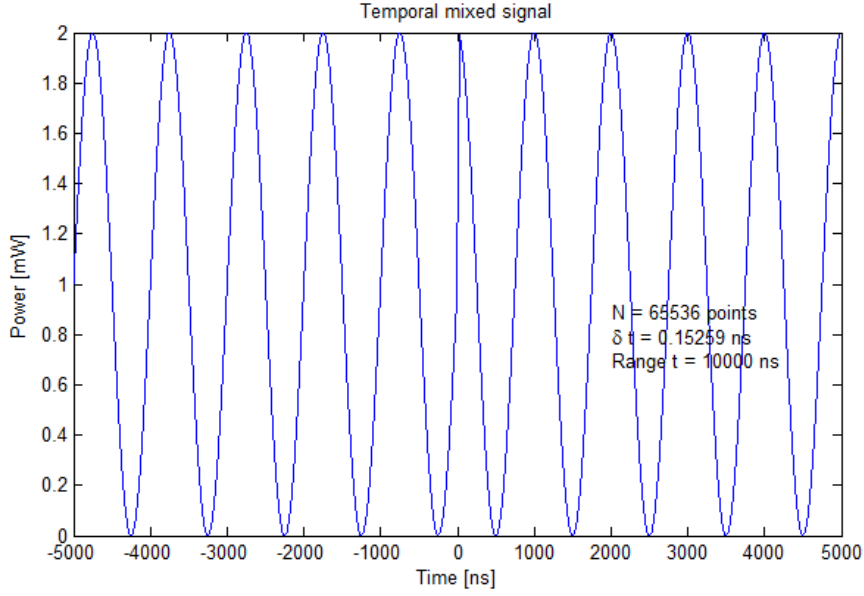


Figure 4.8: Temporal mixed signal with the phase shift of $\frac{\pi}{2}$.

The power of the spectral mixed signal in Figure 4.9 differs from the one in Figure 4.3. The spike does not reach zero in the middle anymore, but it is short and broad. The phase shift $\Delta\phi(f) = \phi(+\Delta f) - \phi(-\Delta f) + \pi$ yields to $-0.7849 - 0.7849 + \pi = 1.571770324$ [rad] with $\Delta = 9.739969006e^{-4}$ [rad] difference from $\frac{\pi}{2}$.

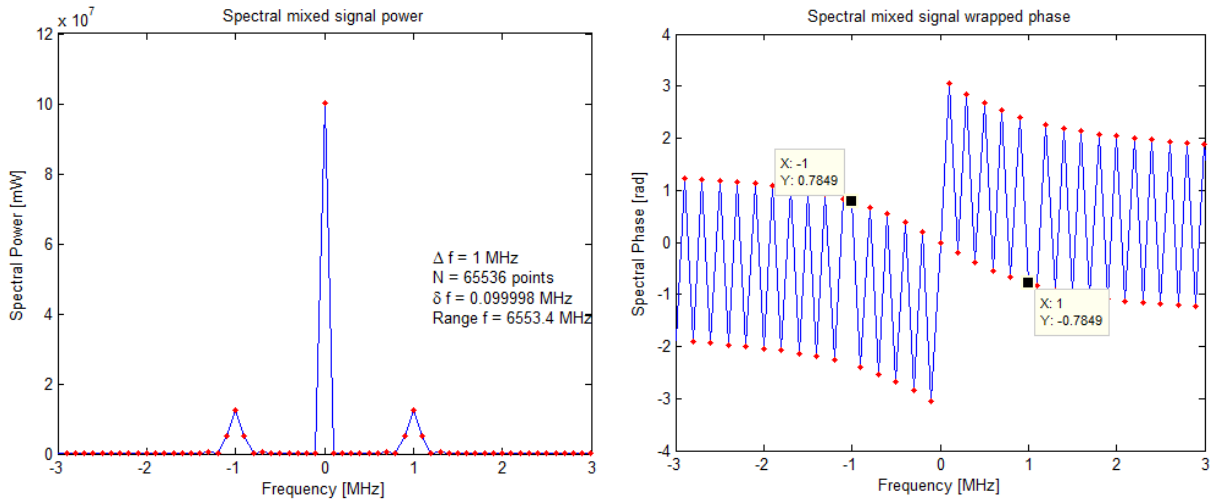


Figure 4.9: Power and phase of the spectral mixed signal.

Figure 4.10 demonstrates filtered spectral and temporal powers.

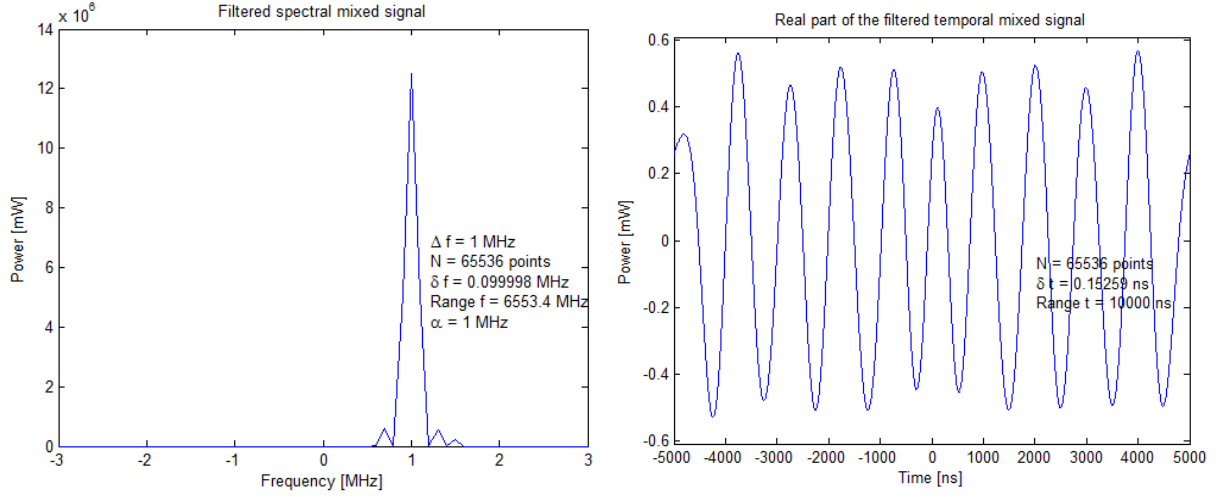


Figure 4.10: Filtered spectral and temporal signals.

Figure 4.11 shows the phase of the temporal mixed signal and the extracted phase shift. However, the error of those calculations is too high being $\Delta = 0.6719963 \approx \frac{\pi}{5}$ [rad] difference between the actual input phase of $\frac{\pi}{2}$ and assessed phase shift of 0.8988 [rad].

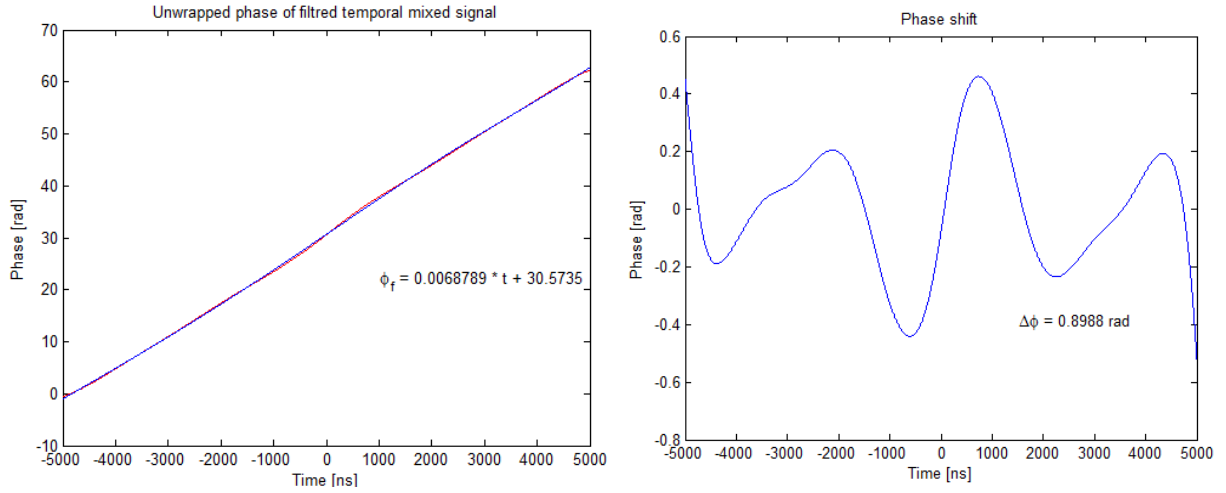


Figure 4.11: Phase of temporal mixed signal.

4.3 Phase shift of $-\frac{\pi}{2}$

In this section we discuss the case of phase change from $\phi_1 = \pi$ to $\phi_2 = \frac{\pi}{2}$, with a total phase shift of $\Delta\phi = -\frac{\pi}{2}$. The power of temporal and spectral mixed signal is displayed

in Figure 4.12.

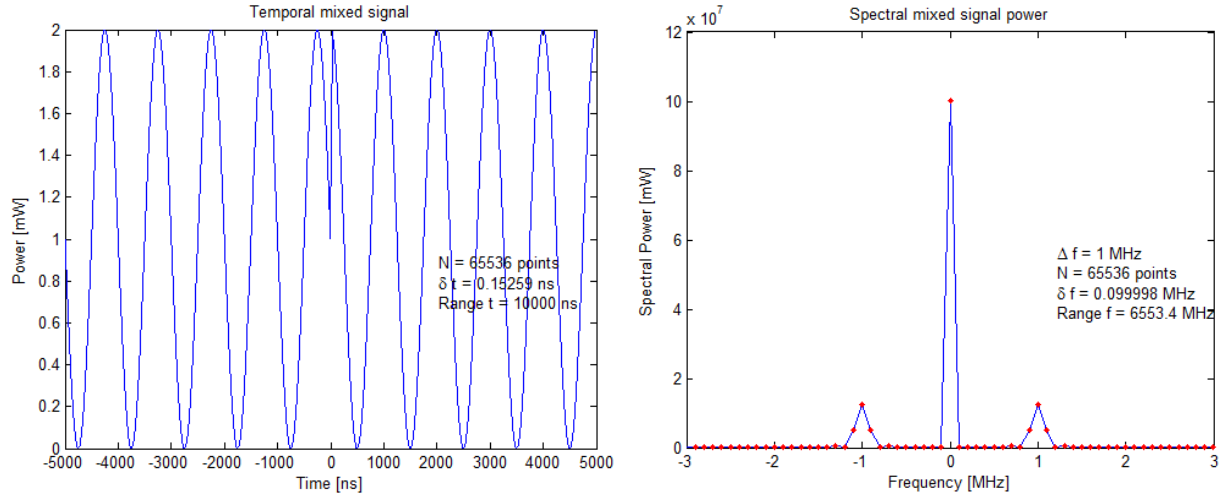


Figure 4.12: Power of temporal (A) and spectral (B) mixed signal.

Figure 4.13 A shows phase of spectral mixed signal. Using $\Delta\phi(f) = \phi(+\Delta f) - \phi(-\Delta f) + \pi$ we get $\Delta\phi(f) = 4.713332459 - 2\pi = -1.569852848$ [rad] with $\Delta = 9.434790845e^{-4}$ [rad] error.

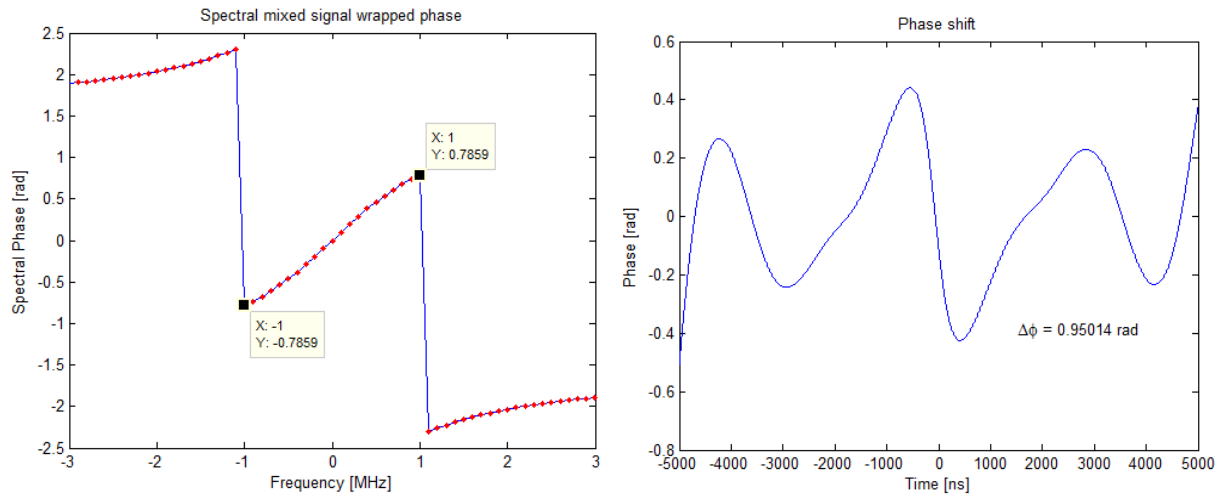


Figure 4.13: Phase of spectral (A) and temporal (B) mixed signal.

The temporal assessment demonstrated in Figure 4.13 B provides an inaccurate result, with $\Delta\phi(t) = 0.95014$ [rad], and error $\Delta = 0.62065632 \approx \frac{\pi}{5}$ [rad].

4.4 Phase shift of 0

In this section we discuss the assessment of the phase shift of 0 [rad]. Table 4.1 shows multiple ways of achieving $\Delta\phi = 0$ [rad] and the assessed spectral and temporal phase shifts. The temporal phase shift shows a good result being assessed with a constant error $\Delta \approx 2.1e^{-4}$ [rad]. However, the spectral phase shift of 0 [rad] does not comply with the equation we were using for the assessment $\Delta\phi(f) = \phi(+\Delta f) - \phi(-\Delta f) + \pi$. It seems like for the case of $\Delta\phi = 0$ [rad] the assessed phase shift is $\phi_{s1} + \phi_{s2}$. Thus, due to the high error of detection and the equation not applicable for all situations, the method of non-split phase shift detection is not recommended for the phase shift assessment.

Table 4.1: Spectral $\phi(f)$ and temporal $\phi(t)$ phase shift assessment of $\Delta\phi = 0$ [rad]

ϕ_{s1}	ϕ_{s2}	Assessed $\Delta\phi(f)$	Assessed $\Delta\phi(t)$
0	0	0.000958738	$2.083520701e^{-4}$
$\frac{\pi}{12}$	$\frac{\pi}{12}$	0.524565143	$2.078515756e^{-4}$
$\frac{\pi}{6}$	$\frac{\pi}{6}$	1.048169504	$2.143091689e^{-4}$
$\frac{\pi}{4}$	$\frac{\pi}{4}$	1.571770324	$2.177939577e^{-4}$
$\frac{\pi}{2}$	$\frac{\pi}{2}$	3.142551392	$2.008806462e^{-4}$
π	π	6.284144045	$2.083520702e^{-4}$
$\frac{3\pi}{2}$	$\frac{3\pi}{2}$	-3.140633916	$2.008806462e^{-4}$
2π	2π	$9.587379934e^{-4}$	$2.083520701e^{-4}$

4.5 Conclusion

After analyzing the technique of processing the temporal mixed signal without splitting it at the phase shift, we were able to achieve good results with spectral phase shift assessment for non-zero phase shifts, however the phase shift of 0 [rad] does not comply the formula used or calculations. The temporal phase shift assessment has a large error for the most of the phase shifts. Figure 4.14 shows the assessed phase versus the input phase for the spectral mixed signal. We got identical results for both cases with and without padding and the largest error yields to $\Delta = 1.00367e-3$ [rad]. Figure 4.15 demonstrates the assessed phase shift of the temporal mixed signal. The temporal assessment results are accurate for the phase shift values of 0 and $\pm 2\pi$, however, they reach the largest error of approximately $\frac{\pi}{3}$ [rad] for the case with padding and $\frac{\pi}{5}$ [rad] for the case without padding.

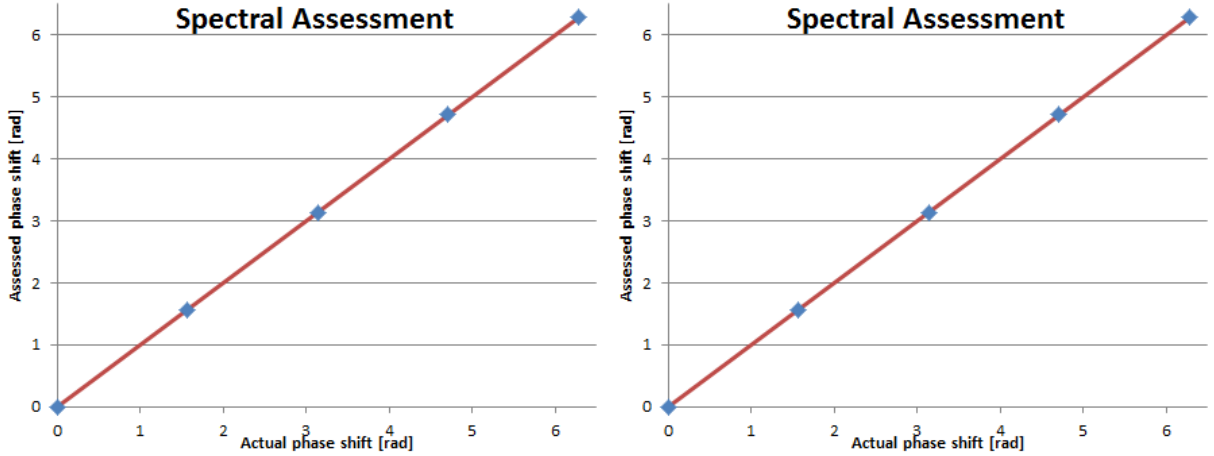


Figure 4.14: Assessed spectral phase shift with (B) and without (A) padding.

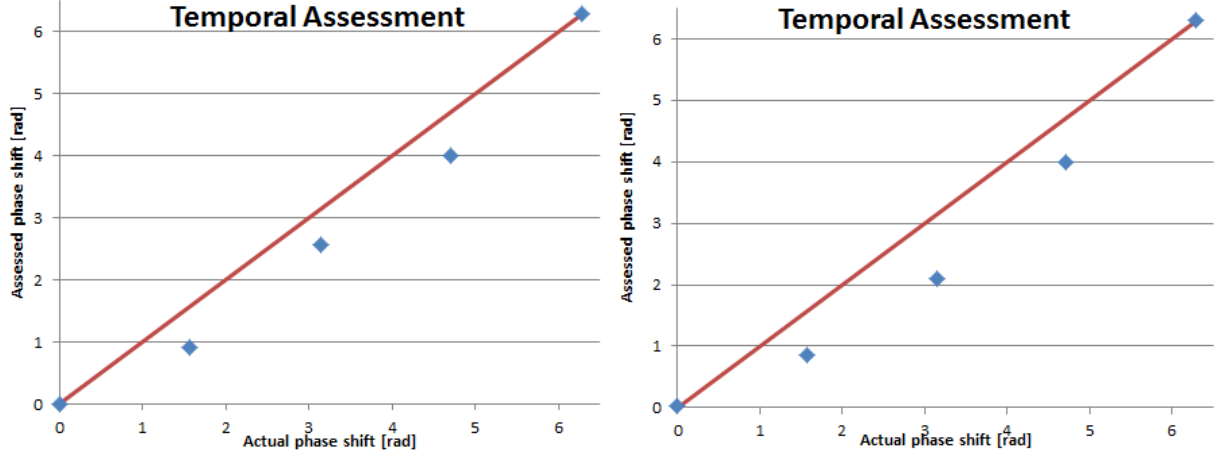


Figure 4.15: Assessed temporal phase shift with (B) and without (A) padding.

Table 4.2: Spectral $\phi(f)$ phase shift assessment [rad] with and without padding

Actual	$\Delta\phi(f)$ without padding	Δ	$\Delta\phi(f)$ with padding	Δ
0	$9.587379924e^{-4}$	$9.587379924e^{-4}$	$9.587379924e^{-4}$	$9.587379924e^{-4}$
$\frac{\pi}{2}$	1.571770324	$9.739969006e^{-4}$	1.571770324	$9.739969006e^{-4}$
π	3.140633916	$9.587379234e^{-4}$	3.140633916	$9.587379234e^{-4}$
$\frac{3\pi}{2}$	4.713332459	$9.434790843e^{-4}$	4.713332459	$9.434790843e^{-4}$
2π	6.282226569	$9.587379929e^{-4}$	6.282226569	$9.587379929e^{-4}$

Table 4.3: Temporal $\phi(t)$ phase shift assessment [rad] with and without padding

Actual	$\Delta\phi(t)$ without padding	Δ	$\Delta\phi(t)$ with padding	Δ
0	$2.083520701e^{-4}$	$2.083520701e^{-4}$	0.2848720012	0.2848720012
$\frac{\pi}{2}$	0.85925701882	-0.5911519235	0.8592570188	-0.711539308
π	2.568374197	-0.5732184563	2.101947819	-1.039644834
$\frac{3\pi}{2}$	4.091730657	-0.6206583234	3.99142327	0.7209657103
2π	6.282976955	$2.083520703e^{-4}$	6.311185307	0.0280701

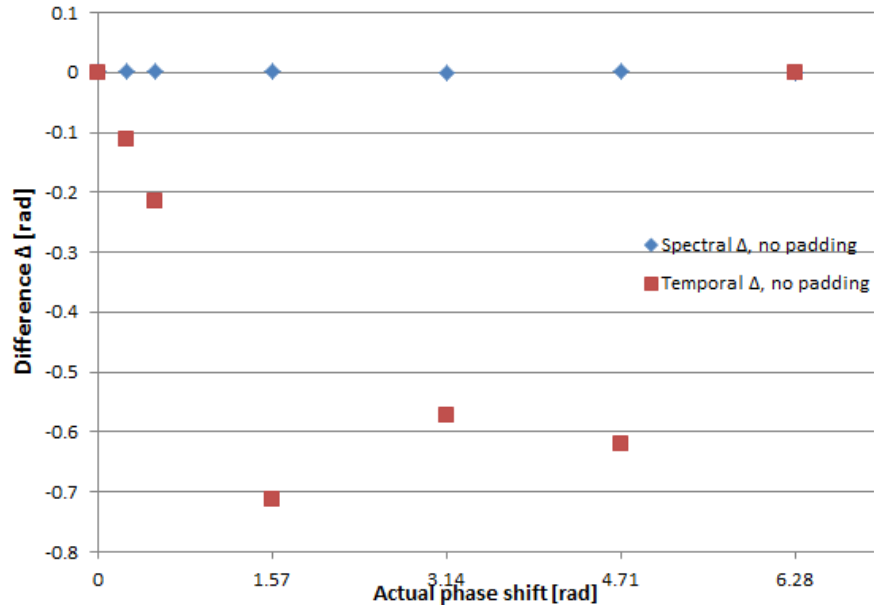


Figure 4.16: Δ difference error.

4.6 Summary of OHD of Phase-Shifted Signals: Non-split Signal

The steps used to perform optical heterodyne detection of phase shifted signals for the non-split signal method are summarized as follows:

1. $P(t)$, using $\Delta f = f_s - f_o$ and $\Delta\phi = \phi_{s1} - \phi_{s2}$

$$\star \Delta f > \frac{2}{\delta t N_{sig}}$$

2. $\tilde{S}(f) = \mathcal{F}\{P(t)\}$

$$\star \text{ (with 3-dB directional coupler) } \Delta\phi = \phi(+\Delta f) - \phi(-\Delta f) + \pi$$

3. $\tilde{S}_f(f) = \mathcal{F}\{P(t)\} \times \Pi(\frac{f-f_0}{\alpha})$

$$\star \alpha > 2\delta f = \frac{2}{\delta t N_{sig}}$$

4. $\tilde{P}_f(t) = \mathcal{F}^{-1}\{\tilde{S}_f(f)\}$

5. $\phi_f(t) = \text{angle}\{\tilde{P}_f(t)\}$

$$\star \Delta\phi = \phi_f(t) - (mt + b)$$

Chapter 5

OHD of Phase-Shifted Signals: Split Signal

In this chapter we discuss our first method of phase shift detection using the split signal. The second method is discussed in Chapter 6. In this current chapter, we consider the phase shift of π in detail and many shifts in summary for the phase-shifted signal split in equal and non-equal parts.

5.1 Impact of time vector zero position

In this section we look at the example of changing time vector zero positions and its effect on the temporal and spectral signals.

For example, instead of defining the time vector from -5000 to 5000 [ns] and centered at $t_o = 0$ as in *case A*, the time vector is changed to -2500 to 7500 and centered at $t_o = 2500$ [ns] as in *case B*. Figure 5.1 shows the temporal signal for cases *A* and *B*. The initial conditions for both cases are defined with $\phi_s = \frac{\pi}{2}$ and $\phi_o = 0$. For both cases N , Δf , $\Delta\phi$ and *Range t* have been defined the same, as indicated in the text box of Figure

5.1.

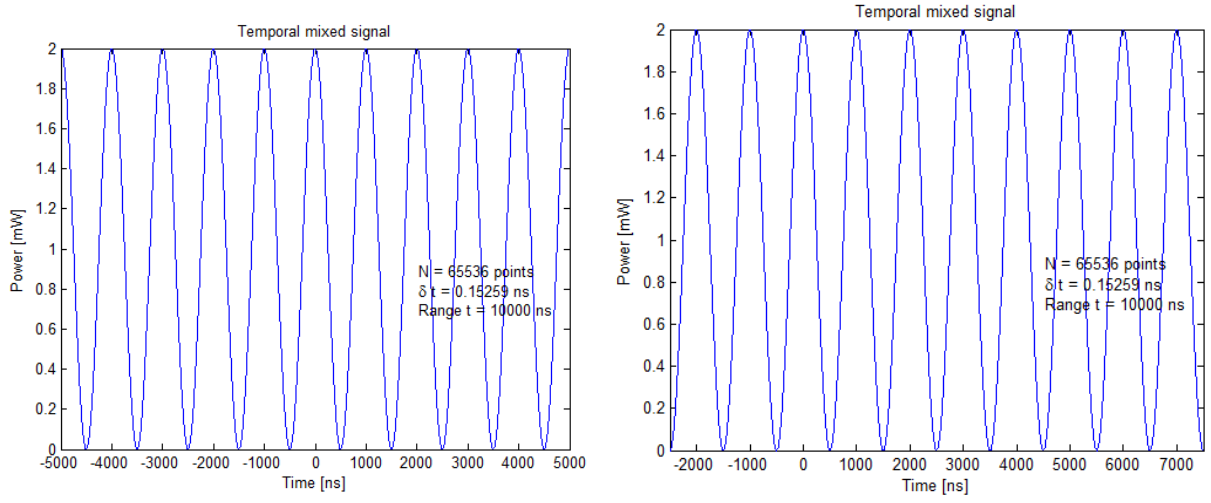


Figure 5.1: Temporal mixed signal for case A and B.

Figure 5.2 displays the power of the spectral mixed signal for the both cases. All the parameters and the form of the peaks remain the same. Shifting the time vector zero position has no effect in the spectral power. Even though the time vector is different, $\delta t N$ and Δf remain the same, so the peaks in the spectral domain appear at the same frequency values.

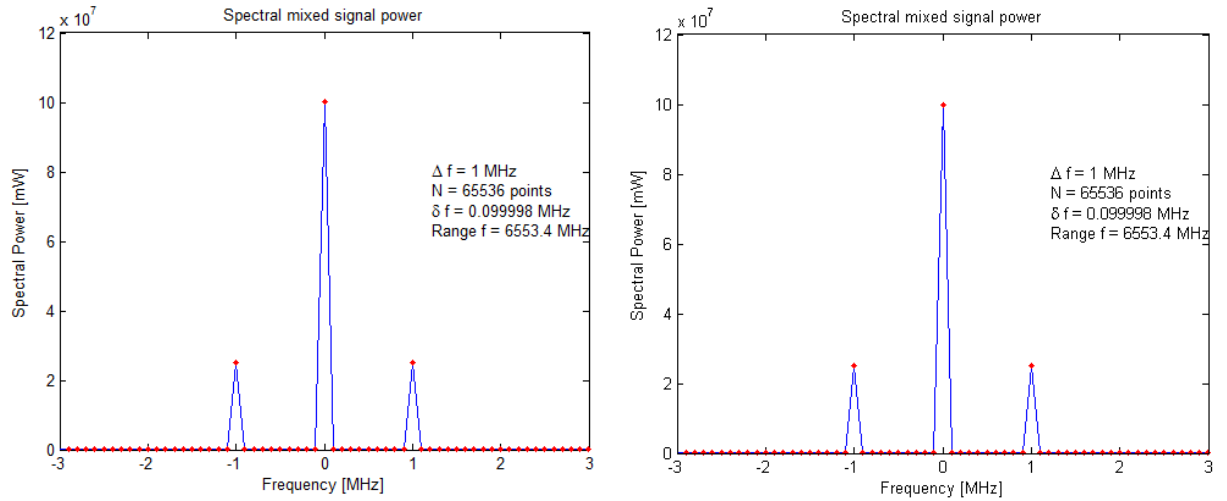


Figure 5.2: Power of spectral mixed signal for case A and B.

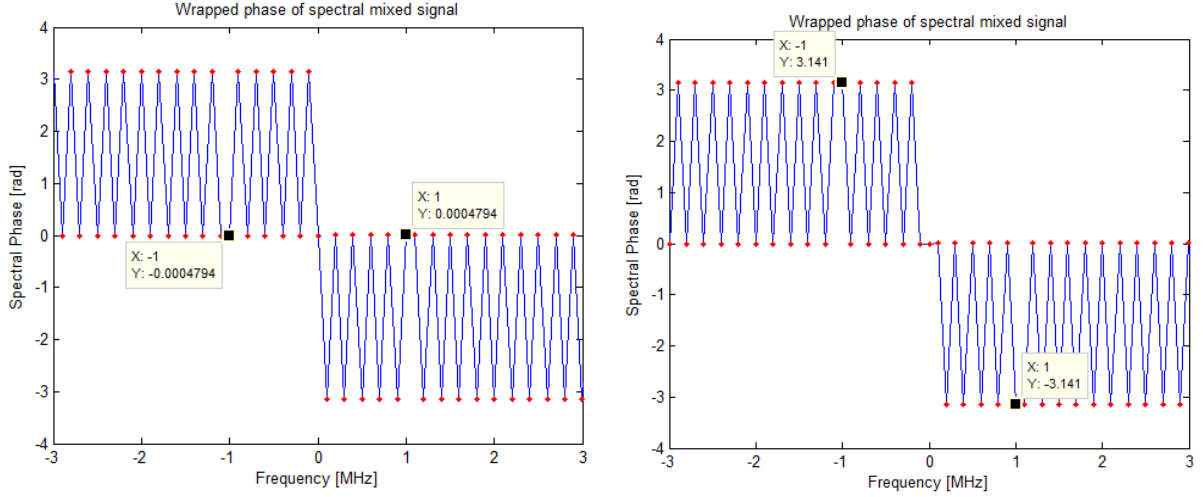


Figure 5.3: Phase of spectral mixed signal for case A and B.

Figure 5.3 displays the phase of spectral mixed signal. This example demonstrates that the spectral phase actually depends on time vector zero position. In case A, after we add $\frac{\pi}{2}$ to the value of the phase located at $f = 1$ MHz and subtract $\frac{\pi}{2}$ from the amplitude of the phase located at $f = -1$ MHz, we get ± 1.5785 [rad] respectively. After we perform the same operations on case B, we get ∓ 1.5632 [rad] respectively. Although the absolute value is approximately the same, the sign has changed.

We need to adjust the spectral phase in order to get the correct value by subtracting $2\pi ft_o$ from the phase value:

$$\phi' = (\phi - 2\pi ft_o) - 2\pi k + \frac{\pi}{2}, \quad (5.1)$$

where t_o is the center of the temporal window and f is the variable of the frequency vector that ranges from f_{min} to f_{max} . The center of the temporal window is the middle of the defined time vector and calculated as $t_o = \frac{t_{max_sig} + t_{min_sig}}{2}$.

The adjustment to the spectral phase expressed by Equation 5.1 forces the data to obey the Fourier Shift Theorem (FST). The FST states that a shift in time relates to a linear spectral phase contribution. The MATLAB FFT is unaware of absolute time

values, and therefore its output data must be corrected.

Figure 5.4 demonstrates the spectral phase adjusted by $(\phi - 2\pi ft_o)$. Spectral phase remains unchanged for case A because at $t_o = 0$ [ns], $\phi = \phi - 2\pi ft_o$. For case B, $t_o = 2500$ [ns] and $\phi' = -18.85 + 2 \cdot \pi \cdot 2 + \frac{\pi}{2} = 1.57057$ [rad] with error $\Delta = -4.440784e^{-4}$ [rad].

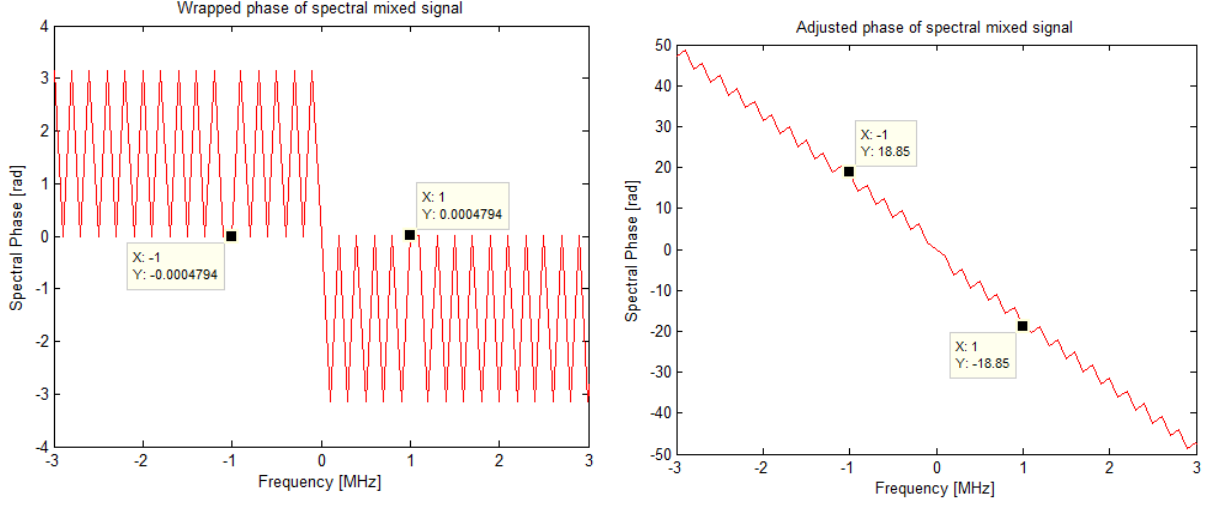


Figure 5.4: Adjusted phase of spectral mixed signal for case A and B.

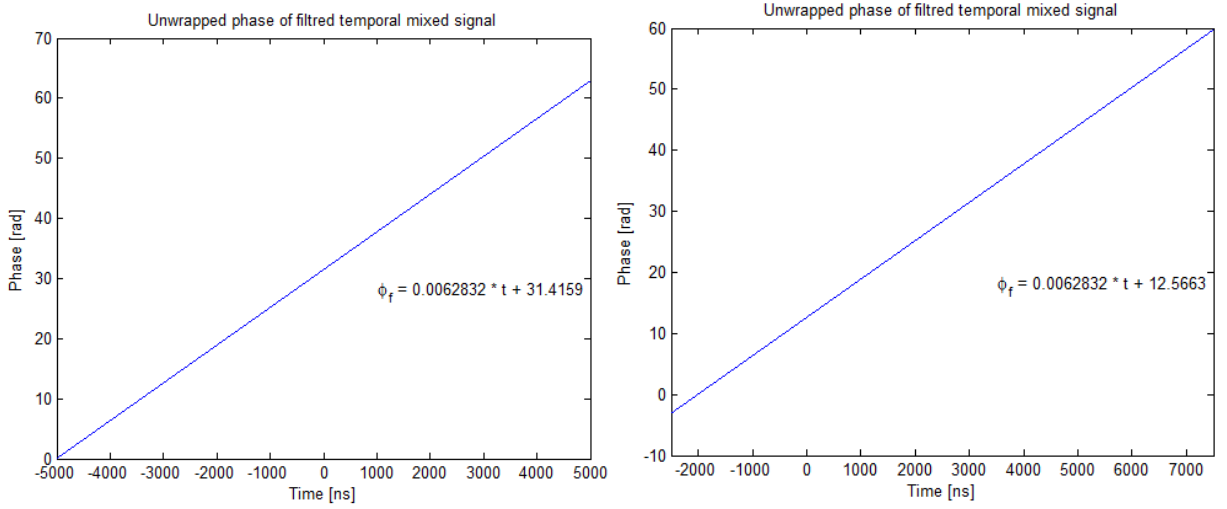


Figure 5.5: Temporal phase of filtered spectral mixed signal for case A and B.

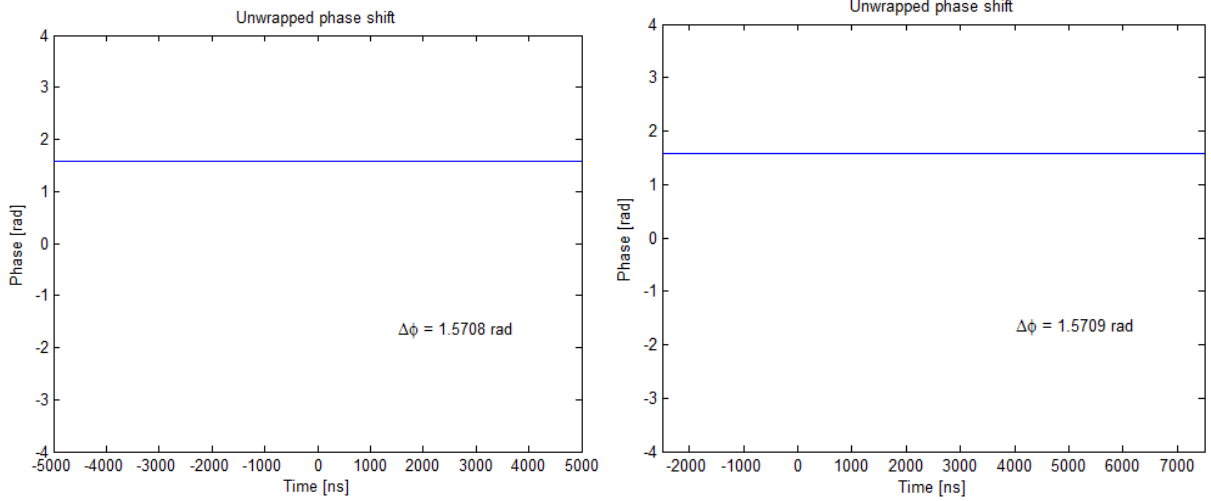


Figure 5.6: Phase of temporal mixed signal with linear part removed and 3-dB coupler correction for case A and B.

Figure 5.6 shows the phase of the temporal mixed signal with the linear part removed and the 3-dB coupler correction applied. The detected phase shift is 1.5708 [rad] for case A and 1.5709 [rad] for case B, which yields to $\Delta_A = 3.6732e^{-6}$ and $\Delta_B = 1.036732e^{-4}$ difference respectively. Note that the FST fix expressed by Equation 5.1 does not have to be applied to the current phase based on the temporal phase.

5.2 Split of phase-shifted signal at equal parts

The phase-shifted signal will be split in two parts, before and after the phase shift, and each part will be processed and analyzed separately side by side. This method allows analysis of multiple phase shifts in one waveform by splitting the waveform at each phase shift. Based on the fact that the temporal phase does not depend on the time vector position and spectral phase needs to be adjusted, we can safely split the waveform.

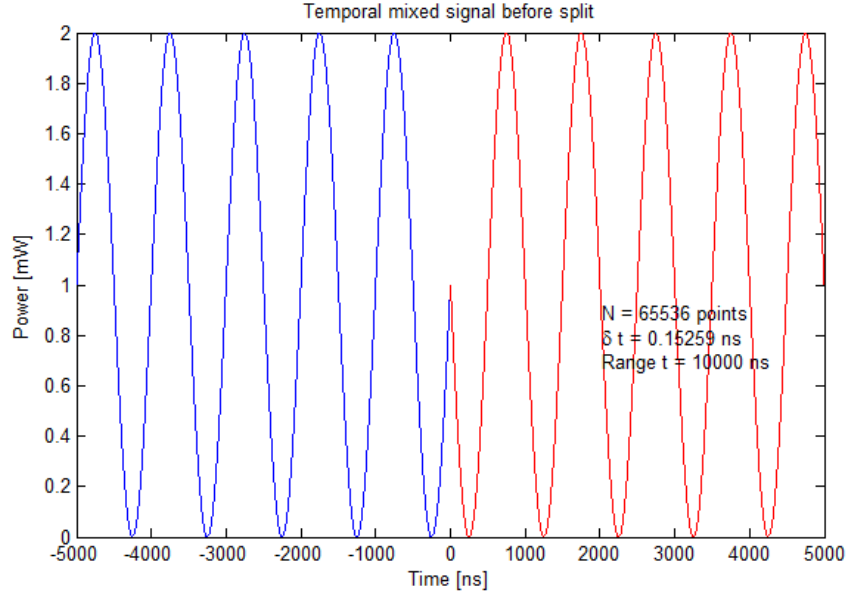


Figure 5.7: Temporal mixed signal before split.

Temporal mixed signal: Figure 5.7 shows the temporal mixed signal with the phase shift at $t=0$. Figure 5.8 demonstrates the splitted temporal mixed signal before (A) and after (B) the phase shift. Comparing to Figure 5.7 the total number of points N and $Range\ t$ split in half, but the time difference δt remains the same. The time vector runs from -5000 to 0 [ns] for case A and from $0 + \delta t$ to 5000 [ns] for case B. Those time vector values are preserved along the analysis. Note that in this example N , $Range\ t$, and δt are identical for both cases. It does not have to be this way, and further on we discuss the case when they are different.

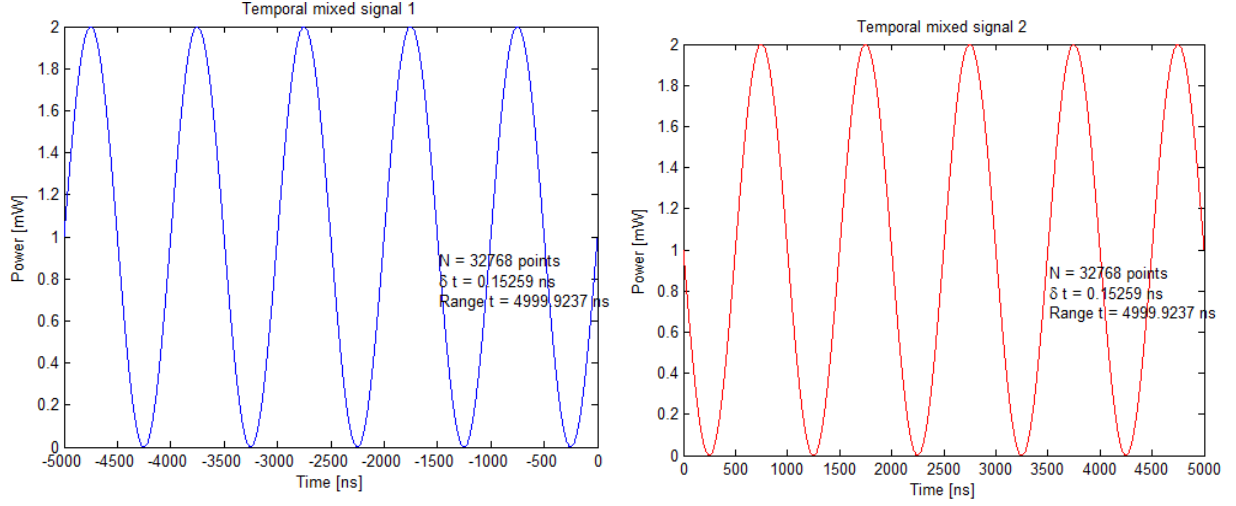


Figure 5.8: Temporal mixed signal, before and after phase shift.

Spectral mixed signal: Figure 5.9 shows the spectral mixed signal. We split the waveform in half, so N becomes a half of the non-split case and the side spikes get wider. The estimated width of each spike is $2\delta f = \frac{2}{\delta t N} = 0.3999938965$ [MHz]. The actual width of the spike is 0.4000 [MHz].

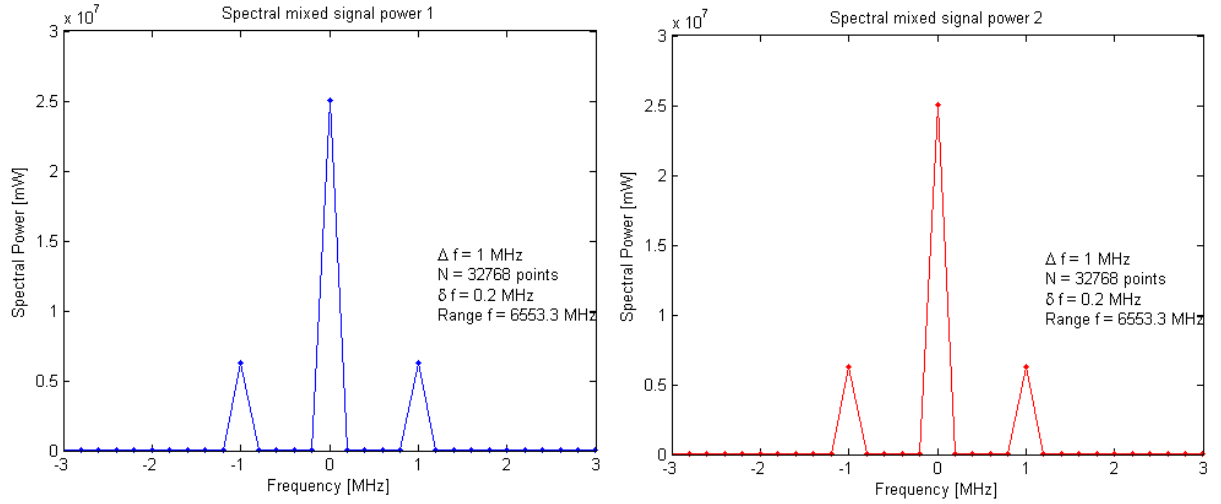


Figure 5.9: Power of spectral mixed signal, before and after phase shift.

The adjusted by $2\pi f t_o$ phase of the spectral mixed signal is represented in Figure 5.10. As we discussed in the last section, it is necessary to adjust the spectral phase by the time vector zero position. t_o is centered at -2500 [ns] for case A and 2500 [ns] for

case B. In case A, the adjusted phase at 1 MHz is $\phi'_{s1} = 17.28 - 2 \cdot \pi \cdot 3 + \frac{\pi}{2} = 1.12404e^{-3}$ [rad]. In case B, the phase is $\phi'_{s2} = -17.28 + 2 \cdot \pi \cdot 3 + \frac{\pi}{2} = 3.14035$ [rad] with error $\Delta = 1.12404e^{-3}$ [rad]. Thus, the phase shift is $\Delta\phi(f) = \phi'_{s2} - \phi'_{s1} = 3.1391096$ [rad] with $\Delta = 2.48305e^{-3}$ [rad] error.

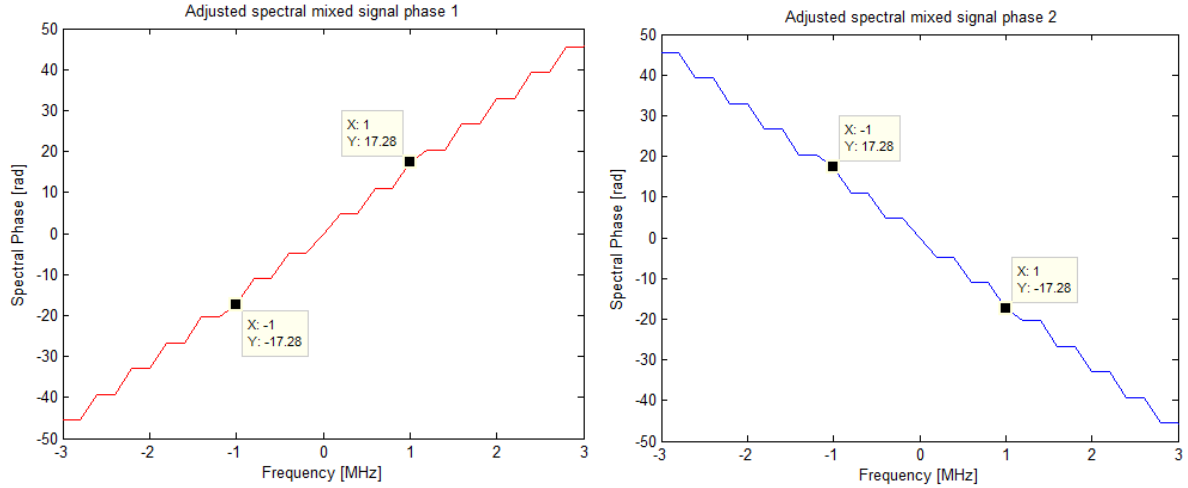


Figure 5.10: Phase of spectral mixed signal, before and after phase shift.

Figure 5.11 shows the filtered spectral mixed signal with $\alpha = 0.4$ [MHz].

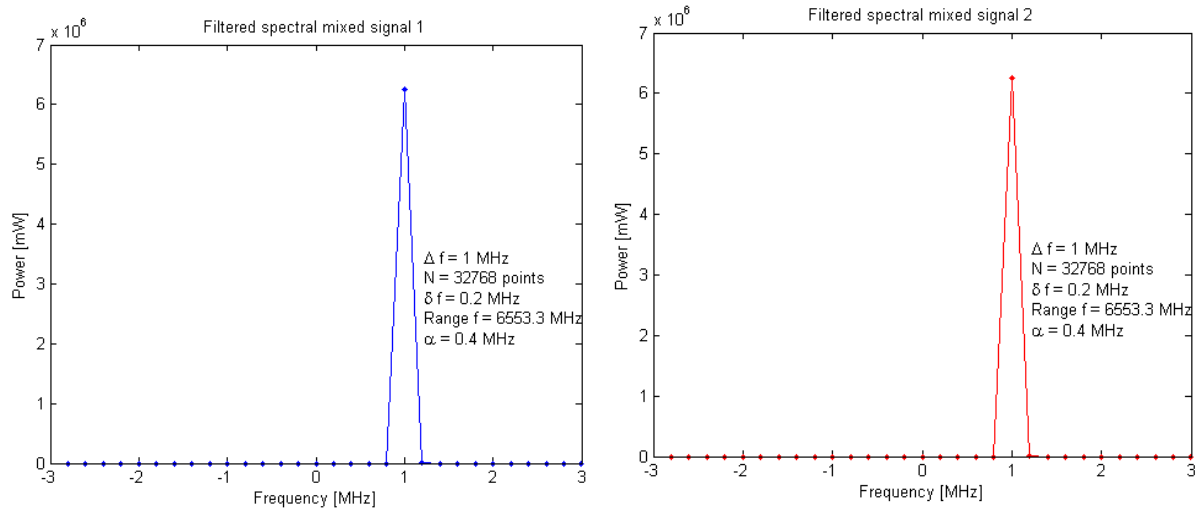


Figure 5.11: Filtered spectral mixed signal, before and after phase shift.

Filtered temporal mixed signal: Figure 5.12 demonstrates the real part of the filtered temporal mixed signal before and after the phase shift. In this case it is similar to

Figure 5.8 — the temporal mixed signal with amplitude being half of that before filtering.

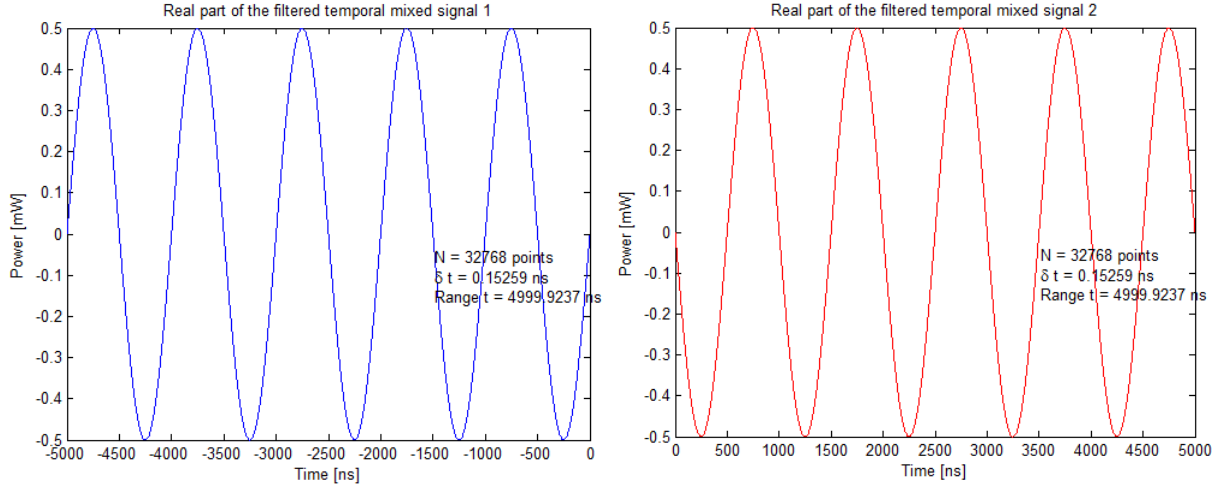


Figure 5.12: Filtered temporal mixed signal, before and after phase shift.

Figure 5.13 shows the phase of the temporal mixed signal. First, let's determine the phase for the each case. In case A, $\phi_{s1} = 29.8449 - 2 \cdot \pi \cdot 5 + \frac{\pi}{2} = -2.3021e - 04$ [rad]. In case B, $\phi_{s2} = 1.571 + \frac{\pi}{2} = 3.1418$ [rad]. Individually, these two phase values are correct. The assessed phase shift is $\Delta\phi(t) = \phi_{s2} - \phi_{s1} = 3.14203021$ [rad], which is $\Delta = 4.375564102e^{-4}$ [rad] accurate in reference to π . The angular frequency is the same for both cases and equal 0.006283 [rad-GHz] which is $\Delta = 2e^{-7}$ [rad-GHz] accurate compared to $2\pi\Delta f = 0.0062832$ [rad-GHz].

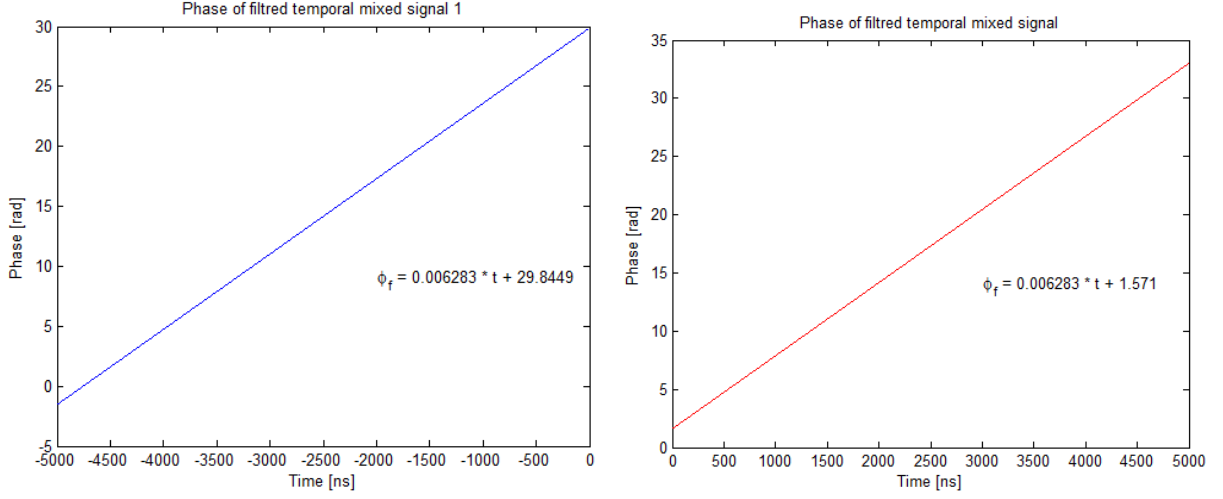


Figure 5.13: Phase of temporal mixed signal, before and after phase shift.

Figure 5.14 shows the phase shift of filtered temporal mixed signal with the linear part removed and 3-dB coupler correction applied. The detected phase shift is $\Delta\phi(t) = 3.142069389$ [rad] with $\Delta = 4.767351611e^{-4}$ [rad] error.

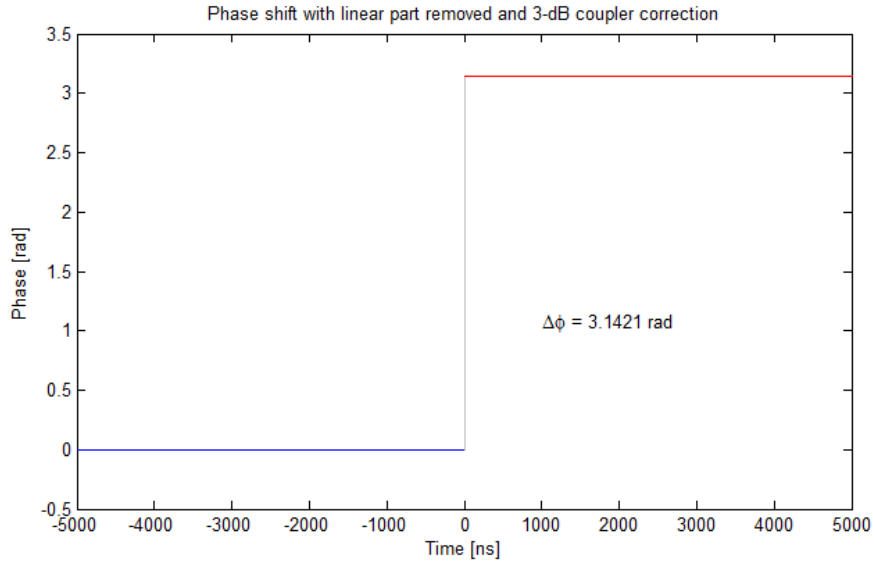


Figure 5.14: Phase of temporal mixed signal with linear part removed and 3-dB coupler correction.

Conclusion: The techniques of splitting the signal at the phase shift and analyzing each part of it separately provides the best results in the phase detection. Figure 5.15

shows the correlation between assessed and inputted phase shift for spectral and temporal phase shifts. At $N = 2^{16}$ points the largest error was $-4.793836081e^{-4}$ [rad]. Thus, we can conclude that this method of phase detection is successful for both spectral and temporal phase assessment.

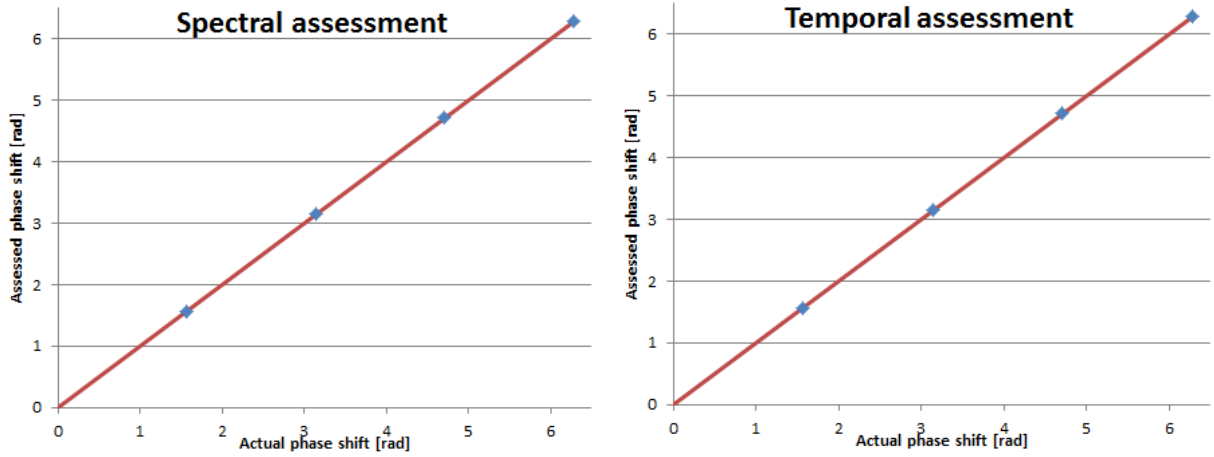


Figure 5.15: Assessed phase shift.

Table 5.1: Spectral $\phi(f)$ and temporal $\phi(t)$ phase shift assessment [rad]

Actual	Assessed $\Delta\phi(f)$	Δ	Assessed $\Delta\phi(t)$	Δ
0	$-4.793836081e^{-4}$	$-4.793836081e^{-4}$	$-4.76735162e^{-4}$	$4.76735162e^{-4}$
$\frac{\pi}{2}$	1.571275703	$4.793762938e^{-4}$	1.571273269	$4.769421099e^{-4}$
π	3.142072037	$4.793836076e^{-4}$	3.142069389	$4.767351611e^{-4}$
$\frac{3\pi}{2}$	4.712868357	$4.79376293e^{-4}$	4.711912038	$4.769421091e^{-4}$
2π	6.283664691	$4.793835947e^{-4}$	6.282708572	$4.767351622e^{-4}$

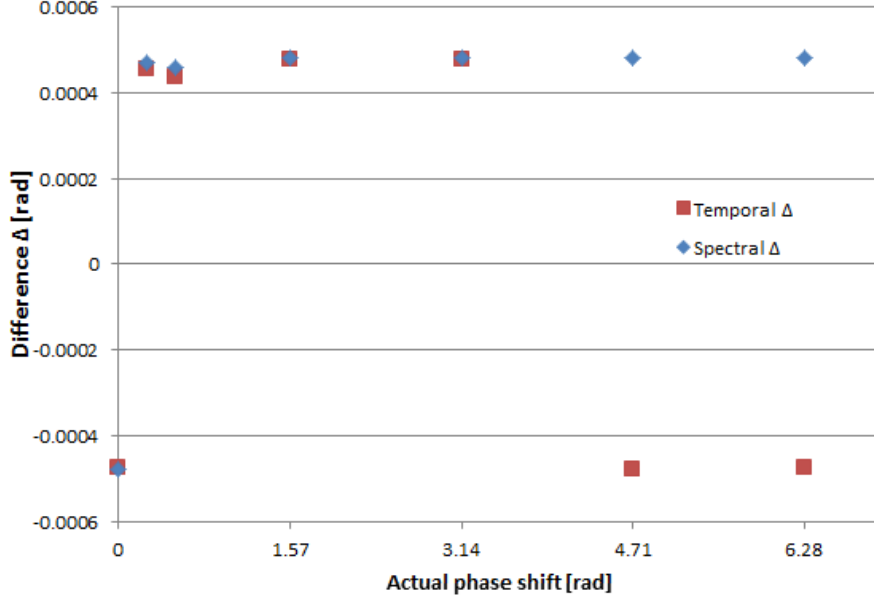


Figure 5.16: Δ difference error.

5.3 Split of phase-shifted signal at not even parts

In the last chapter we have discussed splitting the signal in two even parts. However, it is not always an option. Therefore in this chapter we discuss the case when the phase shift is not at the middle of the waveform. For this example, we picked the signal with the *Range* $t = 20000$ points and $\Delta f = 1$ [MHz], so we have long enough waveform to minimize the errors after splitting.

Temporal mixed signal: Figure 5.17 demonstrates the temporal mixed signal with the phase shift at $t = -5000$ [ns].

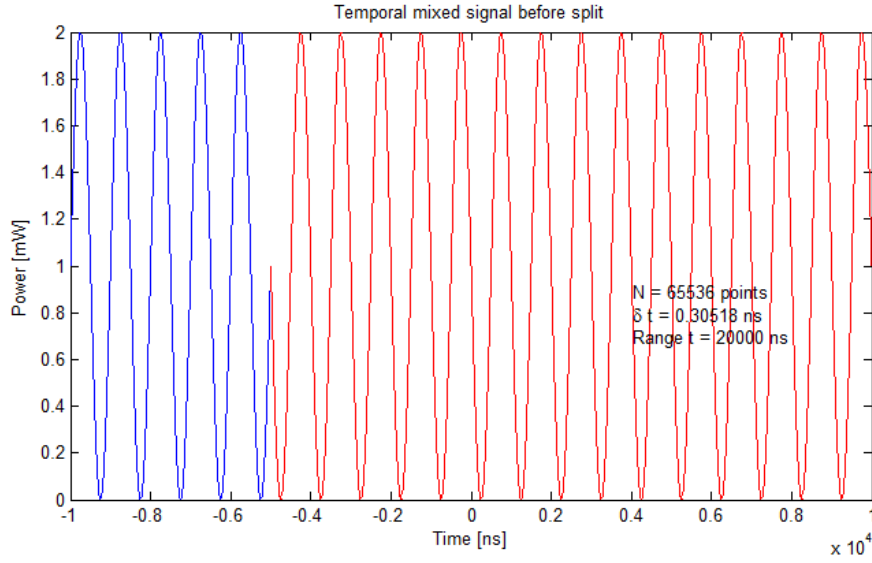


Figure 5.17: Temporal mixed signal before split.

Figure 5.18 shows temporal mixed signal after the split. Temporal mixed signal 2 is 3 times longer and has 3 times more points than signal 1.

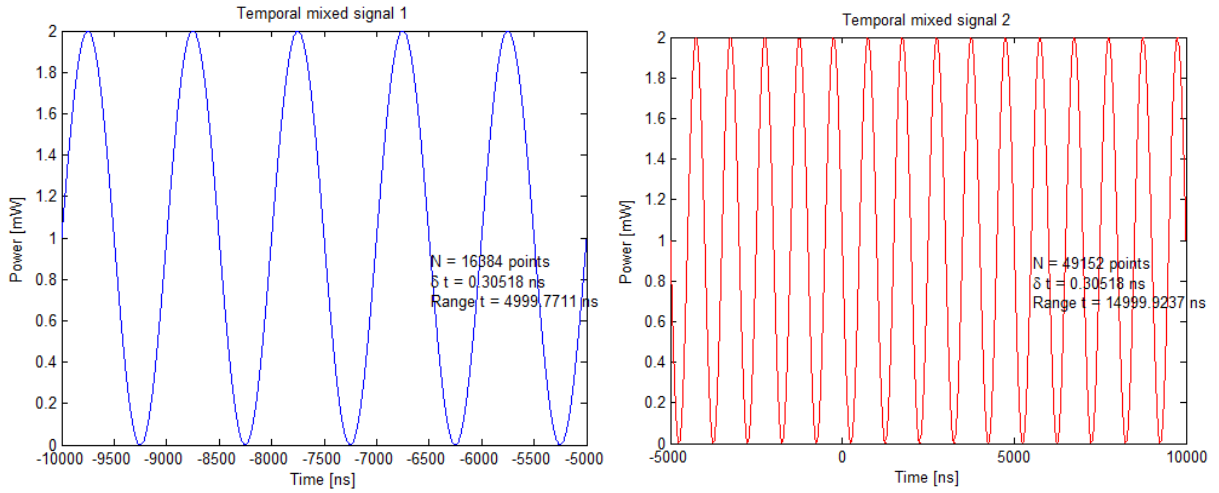


Figure 5.18: Temporal mixed signal after split at the phase shift.

Spectral mixed signal Figure 5.19 displays the power of the spectral mixed signal. The spikes for case A are shorter and wider than case B. It can be explained with the equation $FWHM = \delta f = \frac{1}{\delta t N}$, where δt stays the same, $N_1 = 16384$ points for case A, and $N_2 = 49152$ points for case B. So, the FWHM of the spikes for case A will be 3 times

larger than for case B.

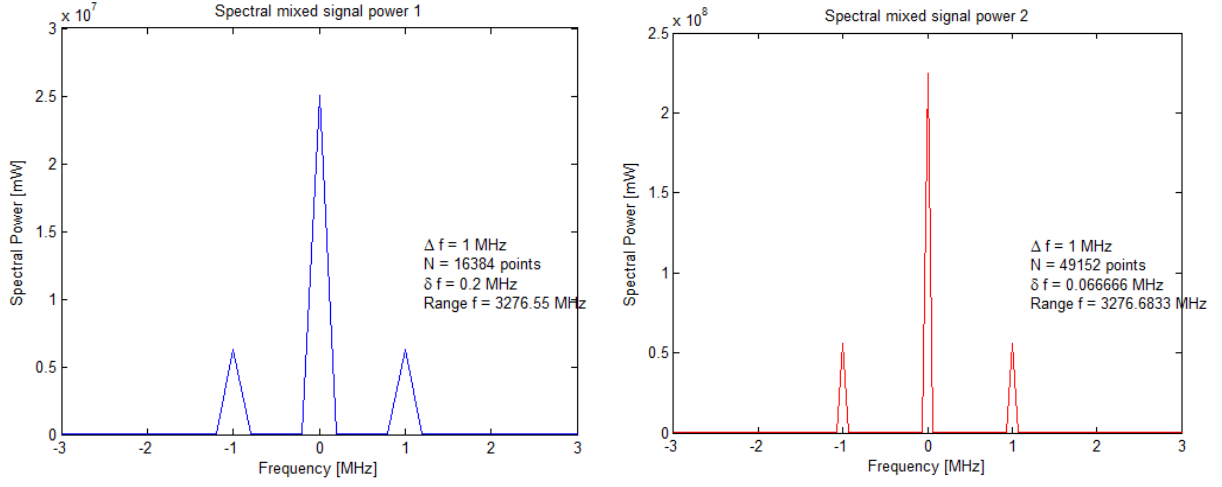


Figure 5.19: Power of spectral mixed signal after split at the phase shift.

Figure 5.20 shows phase of the spectral mixed signal with accounting for the FST. The center of the temporal window is at $t_o = -7500$ [ns] for case A and $t_o = 2500$ [ns] for case B. After adding $\frac{\pi}{2}$ for the each value of the adjusted spectral phase, we get $\phi'_{s1} = 48.68 - 2 \cdot \pi \cdot 8 + \frac{\pi}{2} = -4.686130642e^{-3}$ [rad] for case A and $\phi'_{s2} = -17.28 + 2 \cdot \pi \cdot 3 + \frac{\pi}{2} = 3.140352248$ [rad] for case B. The phase shift $\Delta\phi(f) = 3.145038379$ [rad] which is $\Delta = 3.445725386e^{-3}$ [rad] difference from π .

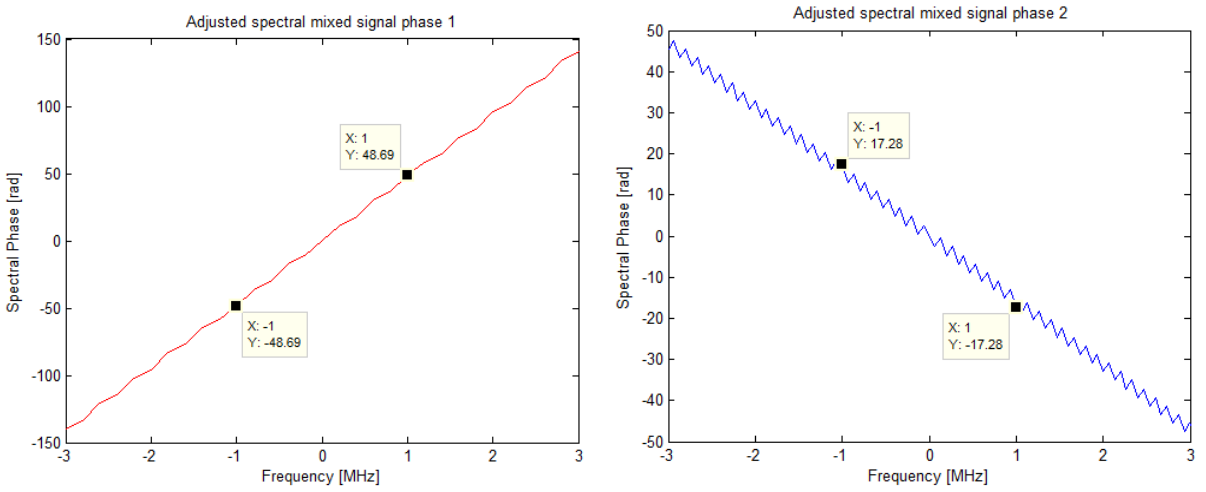


Figure 5.20: Phase of spectral mixed signal after split at the phase shift.

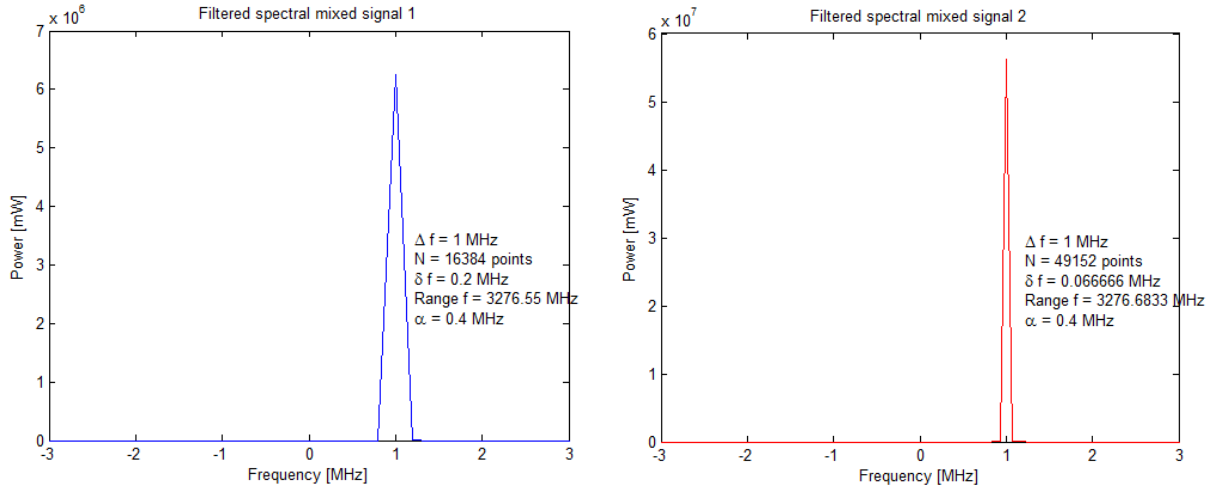


Figure 5.21: Filtered spectral mixed signal after split at the phase shift.

Filtered temporal mixed signal: Figure 5.22 shows filtered temporal mixed signal before and after the split at the phase shift.

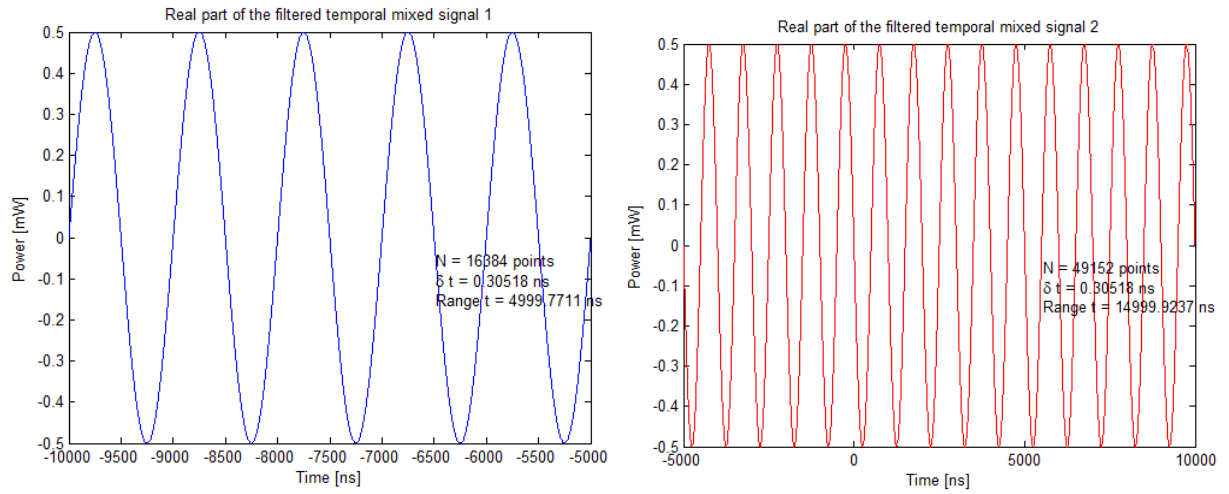


Figure 5.22: Filtered temporal mixed signal after split at the phase shift.

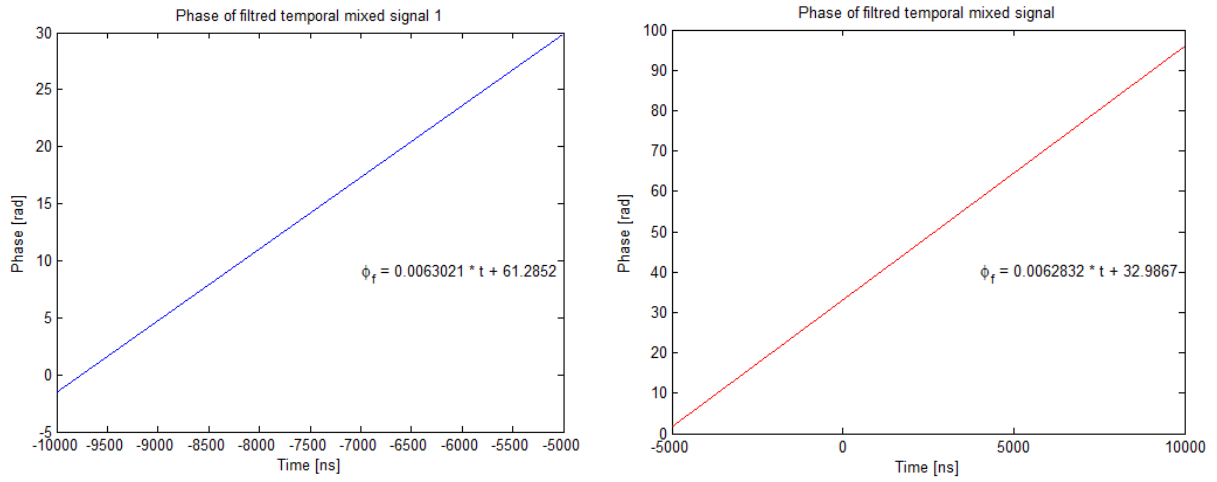


Figure 5.23: Phase of filtered temporal mixed signal after split at the phase shift.

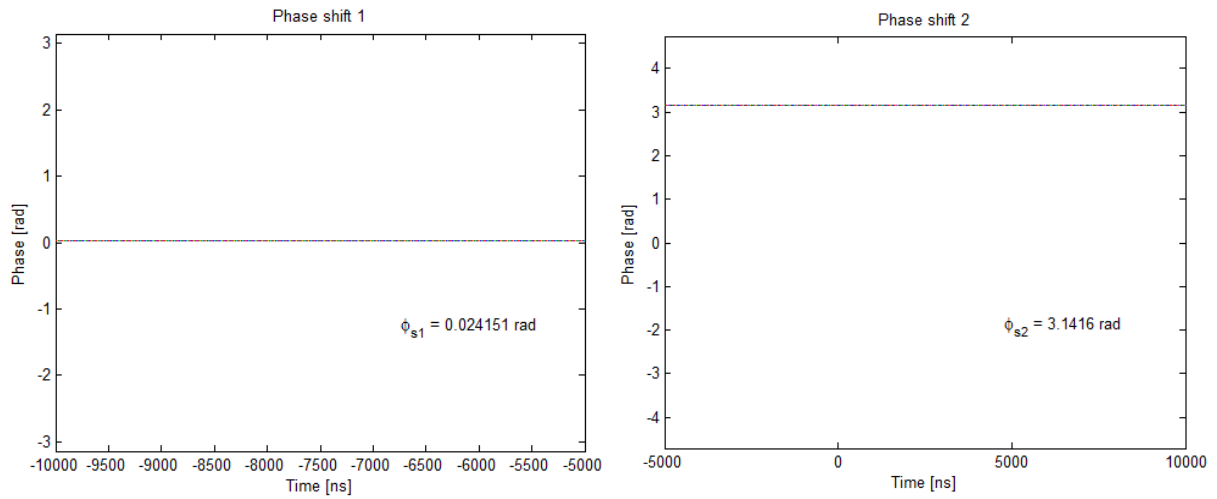


Figure 5.24: Phase of filtered temporal mixed signal after split at the phase shift.

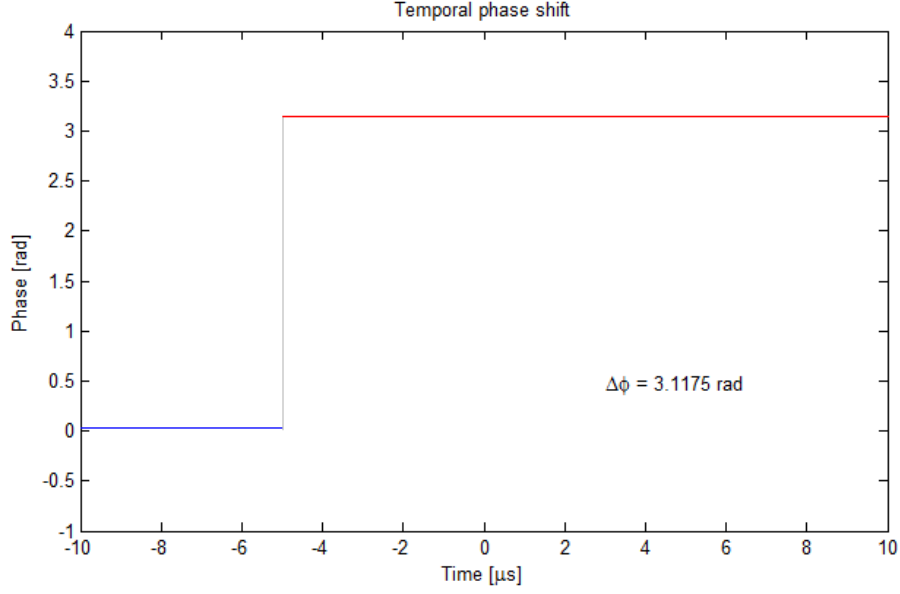


Figure 5.25: Phase of filtered temporal mixed signal with linear part removed and 3-dB coupler correction.

Figure 5.24 shows the phase of the filtered mixed signal with linear part removed and $\frac{\pi}{2}$ added. Case A has a bigger error than case B. It is based on the lower number of points in the first part of the waveform before the shift (case A). Figure 5.25 shows the assessed temporal phase shift $\Delta\phi(t) = 3.11746891$, the error of calculation is $\Delta = -0.02412374376$ [rad].

Conclusion: The method of split signal with non-equal parts is successful. The highest error of the spectral mixed signal is approximately $9.59e^{-4}$ [rad]. Note that there is a constant error of approximately $2.41e^{-2}$ [rad] in the detection of the temporal phase which comes from the ϕ_{s1} assessment. Figure 5.26 shows the assessed phase versus the actual phase for the spectral and temporal phase assessment. The highest error is $2.412374376e^{-2}$ [rad] in the temporal case still allows correct detection of the phase shift.

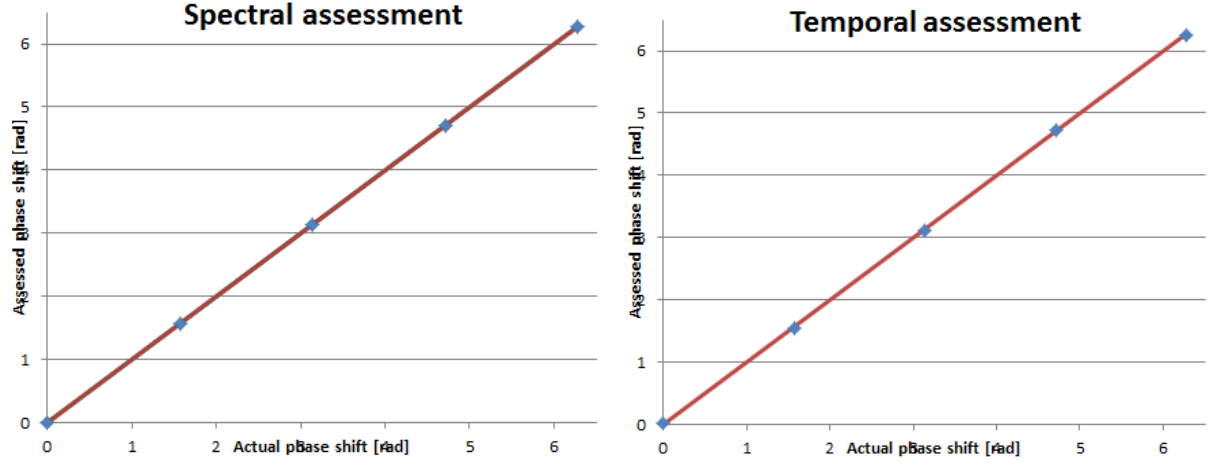


Figure 5.26: Assessed phase.

Table 5.2: Spectral $\phi(f)$ and temporal $\phi(t)$ phase shift assessment [rad]

Actual	Assessed $\Delta\phi(f)$		Assessed $\Delta\phi(t)$	
		Δ		Δ
0	$9.587672198e^{-4}$	$9.587672198e^{-4}$	$2.412374376e^{-2}$	$2.412374376e^{-2}$
$\frac{\pi}{2}$	1.569837567	$9.587599045e^{-4}$	1.546670856	$2.412547115e^{-2}$
π	3.140633886	$9.587672201e^{-4}$	3.11746891	$2.412374376e^{-2}$
$\frac{3\pi}{2}$	4.71143022	$9.587599046e^{-4}$	4.736514452	$2.412547115e^{-2}$
2π	6.28222654	$9.587672192e^{-4}$	6.259061563	$2.412374376e^{-2}$

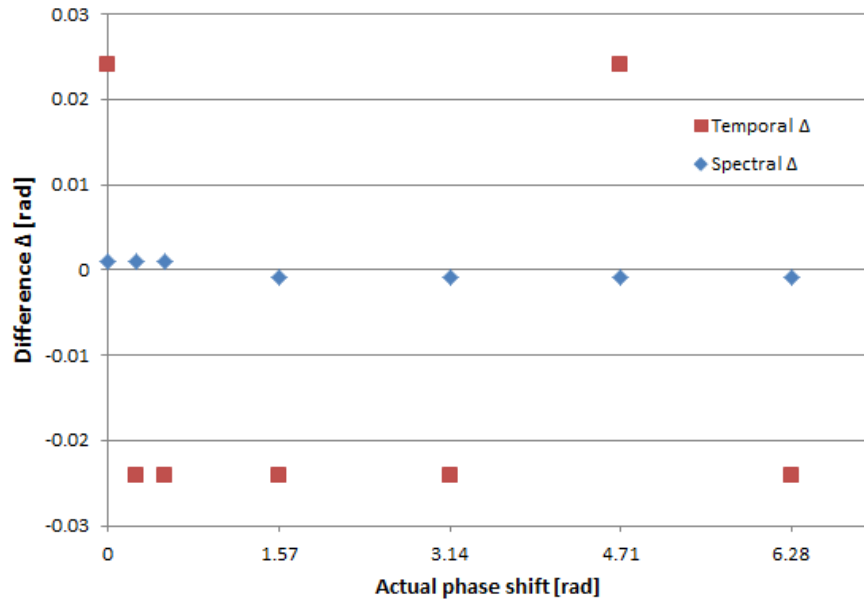


Figure 5.27: Δ difference error.

5.4 Summary of OHD of Phase-Shifted Signals: Split Signal

The steps used to perform OHD of phase shifted signals for the split signal method are summarized as follows:

1. $P(t)$, using $\Delta f = f_s - f_o$ and $\Delta\phi = \phi_{s1} - \phi_{s2}$

$$\star \Delta f > \frac{2}{\delta t N_{sig}}$$

2. Split $P(t)$ at $\Delta\phi$ in $P_1(t_1)$ and $P_2(t_2)$

3. $\tilde{S}_1(f_1) = \mathcal{F}\{P_1(t_1)\}$ and $\tilde{S}_2(f_2) = \mathcal{F}\{P_2(t_2)\}$

\star (with accounting for the FST and 3-dB directional coupler)

$$\phi'_{s1} = \phi_{s1}(\Delta f) - 2\pi f_1 t_{o1} + \frac{\pi}{2} = \phi_{s1}(-\Delta f) - 2\pi f_1 t_{o1} - \frac{\pi}{2}$$

$$\phi'_{s2} = \phi_{s2}(\Delta f) - 2\pi f_2 t_{o2} + \frac{\pi}{2} = \phi_{s2}(-\Delta f) - 2\pi f_2 t_{o2} - \frac{\pi}{2}$$

$$\star \Delta\phi = \phi'_{s2} - \phi'_{s1} = (\phi_{s2}(\Delta f) - 2\pi f_2 t_{o2}) - (\phi_{s1}(\Delta f) - 2\pi f_1 t_{o1})$$

$$\Delta\phi = \phi_{s2}(\Delta f) - \phi_{s1}(\Delta f) - 2\pi(f_2 t_{o2} - f_1 t_{o1})$$

4. $\tilde{S}_{f1}(f_1) = \mathcal{F}\{P_1(t_1)\} \times \Pi_1(\frac{f-f_0}{\alpha})$ and $\tilde{S}_{f2}(f_2) = \mathcal{F}\{P_2(t_2)\} \times \Pi_2(\frac{f-f_0}{\alpha})$

$$\star \alpha > 2\delta f = \frac{2}{\delta t N_{sig}}$$

5. $\tilde{P}_{f1}(t_1) = \mathcal{F}^{-1}\{\tilde{S}_{f1}(f_1)\}$ and $\tilde{P}_{f2}(t_2) = \mathcal{F}^{-1}\{\tilde{S}_{f2}(f_2)\}$

6. $\phi_{f1}(t_1) = \text{angle}\{\tilde{P}_1(f_1)\}$ and $\phi_{f2}(t_2) = \text{angle}\{\tilde{P}_2(f_2)\}$

7. $\phi_{f1}(t_1) = m_1 t_1 + b_1$ and $\phi_{f2}(t_2) = m_2 t_2 + b_2$

$$\star \Delta\phi = b_2 - b_1$$

Chapter 6

OHD of Phase-Shifted Signals: Split Signal with Zero Out

This chapter discusses a second method that uses the split signal to assess phase shifts. In this method the Fourier Shift Theorem (FST) is enforced by setting the unwanted part of the waveform to zero. It maintains the initial time vector to detect the phase shift for temporal and spectral analysis. We discuss the phase shift of π in detail and a variety of phase shifts in the summary at the end of the chapter.

6.1 Split signal with zero out

Temporal mixed signal Figure 6.1 (A) shows the power of the temporal mixed signal with the phase shift of π [rad] at $t = 0$ [ns]. Exactly the same conditions were discussed in Chapters 4 and 5 which allows us to compare this method to others. Figure 6.1 B demonstrates the vector mask used in MATLAB. The masks are used to modify two replicas of the original signal.

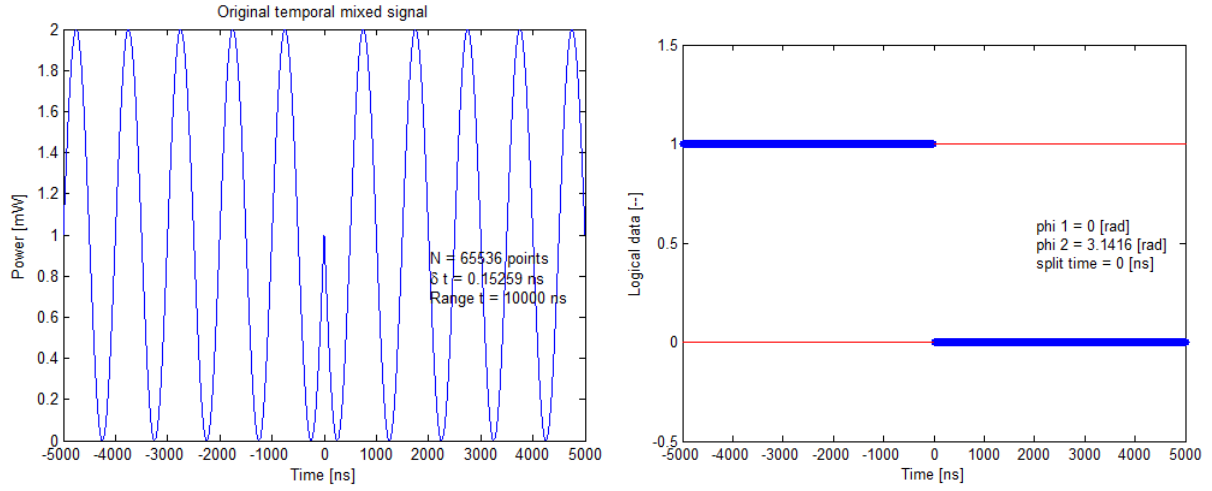


Figure 6.1: Temporal mixed signal.

Figure 6.2 shows the waveforms we work with in this chapter. We use the whole time vector from -5000 to 5000 [ns] but analyze each signal with the unwanted part zeroed out.

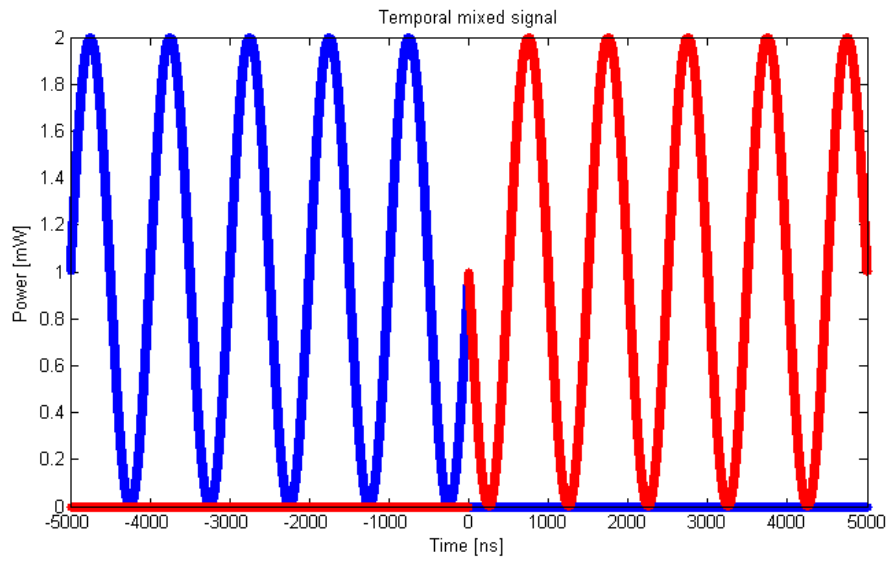


Figure 6.2: Temporal mixed signal.

Spectral mixed signal Figure 6.3 shows the power of spectral mixed signal.

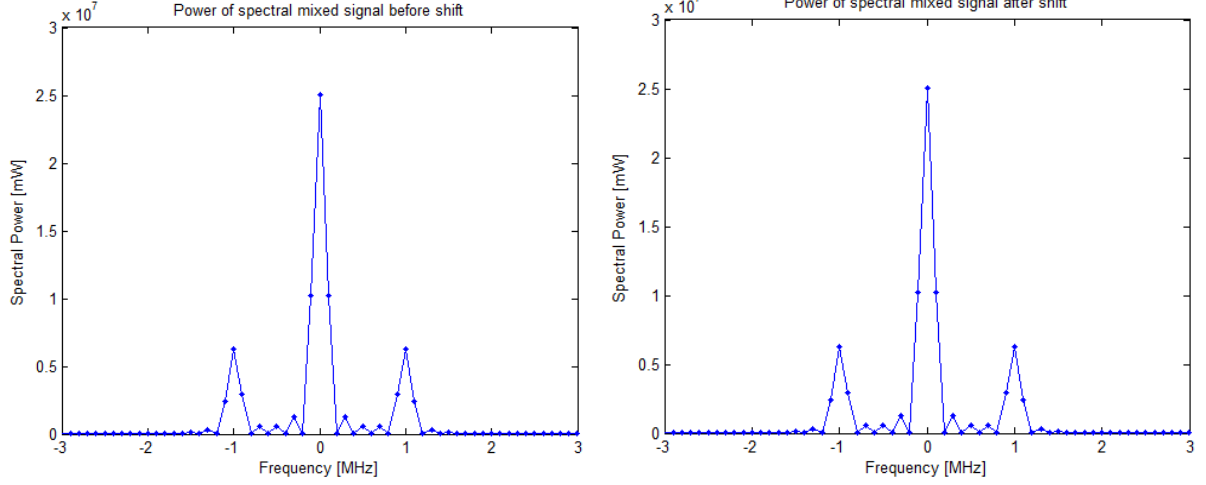


Figure 6.3: Power of spectral mixed signal before (A) and after (B) shift.

Figure 6.4 shows the phase of spectral mixed signal which is detected at $f = 1$ [MHz] as $\phi_{s1} = -1.5705566 + \frac{\pi}{2} = 2.3967718e^{-4}$ [rad] for case A and $\phi_{s2} = 1.571515 + \frac{\pi}{2} = 3.14231171439$ for case B. The assessed phase shift is $\Delta\phi(f) = 3.142072037$ [rad] with error $\Delta = 4.793836232e^{-4}$ [rad]. This method simplifies the detection of the phase of the spectral mixed signal compared to the split signal method discussed in Chapter 5. The current method requires only correction for the 3-dB coupler of the phase assessment.

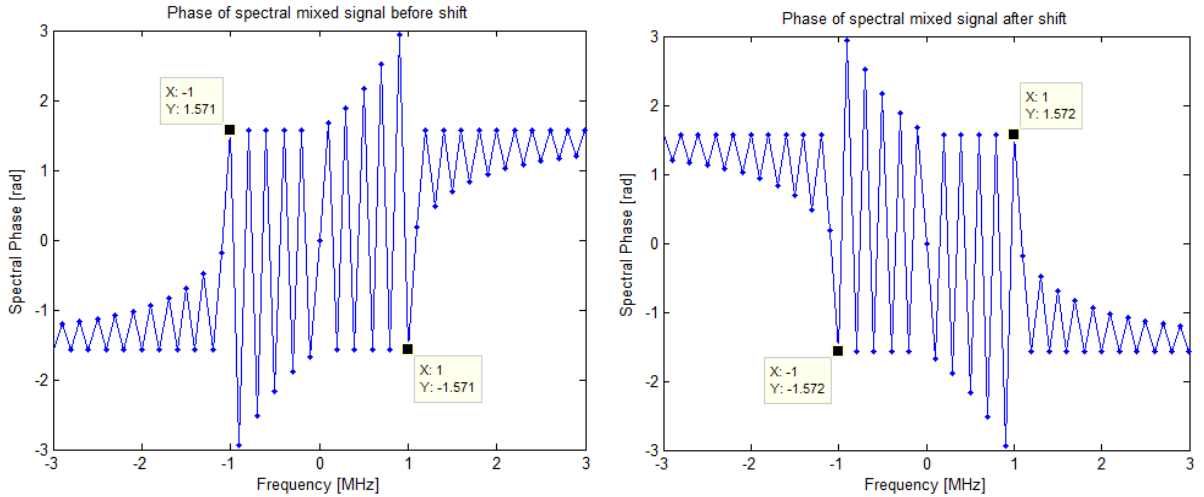


Figure 6.4: Phase of spectral mixed signal before (A) and after (B) shift.

Figure 6.5 displays filtered spectral mixed signal for case A and case B.

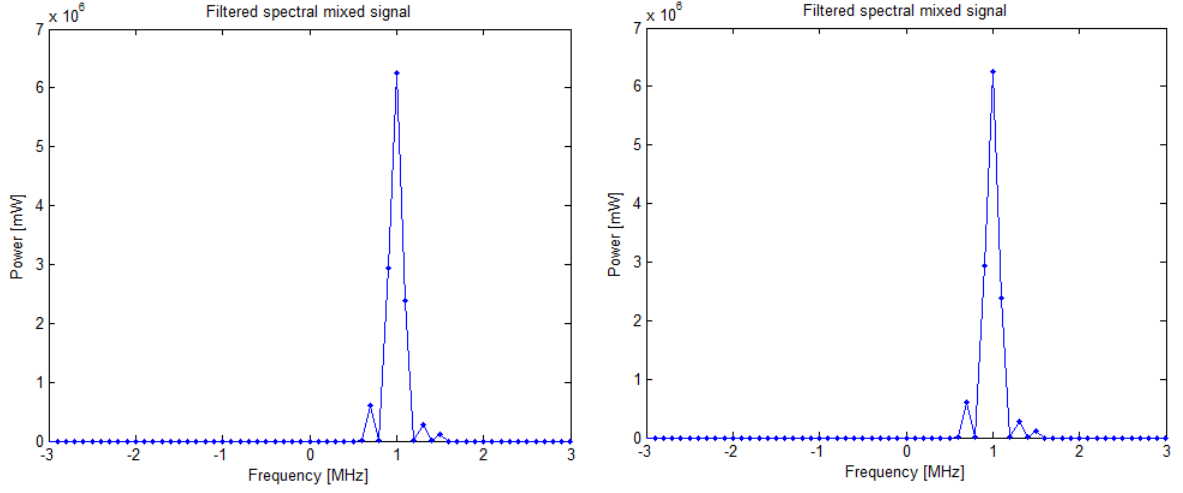


Figure 6.5: Filtered power of spectral mixed signal before (A) and after (B) shift.

Filtered temporal mixed signal After performing the inverse Fourier transformation on the filtered spectral mixed signal, we get the temporal mixed signal displayed in Figure 6.6. Note that due to the filtering, the part of the waveform which was zeroed out has a wavy form. Moreover, the phase of the filtered temporal mixed signal, depicted in Figure 6.7, has a wavy composition as well primarily in the zeroed out part. This creates a sizable error in the temporal phase shift assessment.

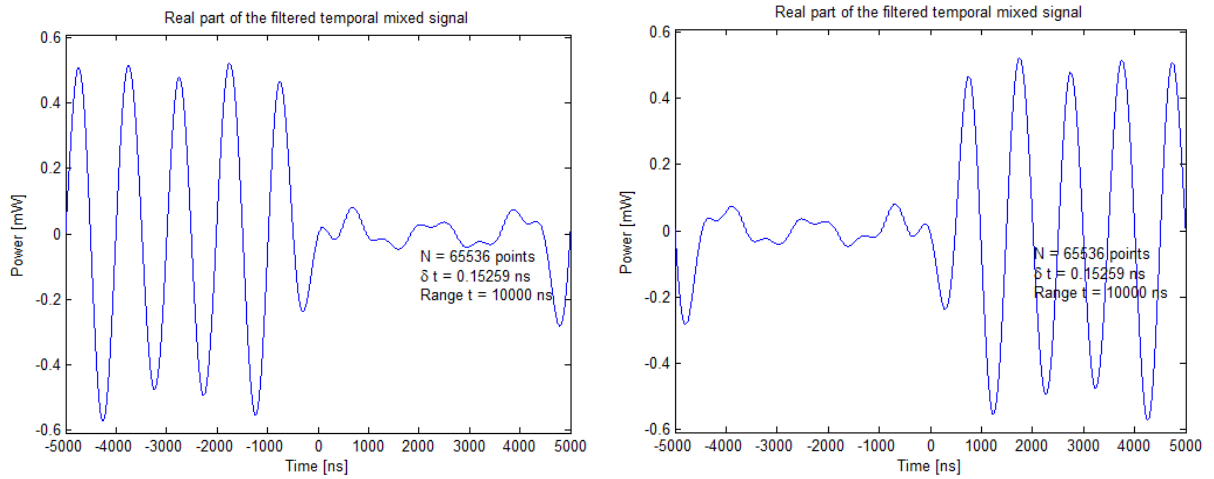


Figure 6.6: Filtered power of temporal mixed signal before (A) and after (B) shift.

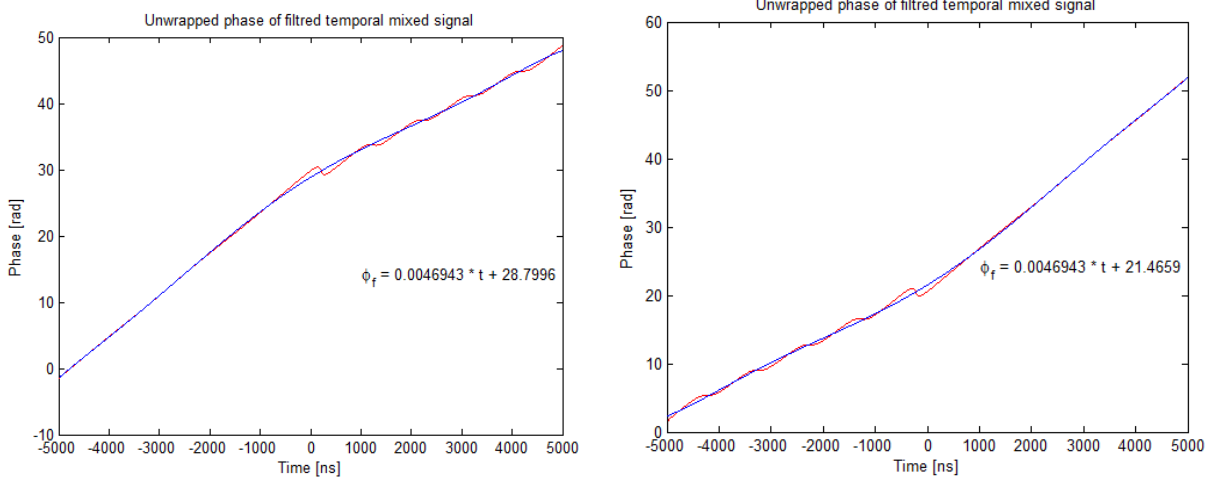


Figure 6.7: Phase of temporal mixed signal before (A) and after (B) shift.

Depicted in Figure 6.8 temporal phase with linear part removed and 3-dB coupler adjustment is estimated as a numeric average at $\phi_{s1} = 2.7215 \approx \frac{\pi}{1.2}$ [rad] instead of 0 [rad] for case A; and $\phi_{s2} = 0.42014 \approx \frac{\pi}{7}$ [rad] instead of π [rad] for case B. The temporal phase shift is assessed at $\Delta\phi(t) = 2.30130975$ [rad] with error $\Delta = 0.840282897 \approx \frac{\pi}{4}$ [rad].

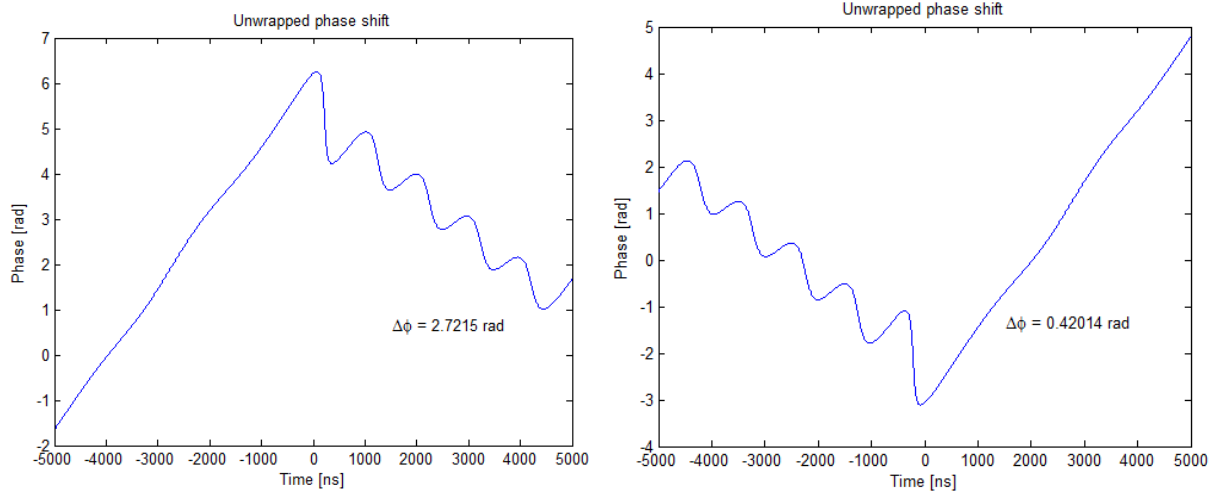


Figure 6.8: Temporal phase with linear part removed and 3-dB coupler correction, before (A) and after (B) shift.

6.2 Temporal phase split

Concerned by poor results in the temporal phase assessment, we decided to use another technique and split the temporal phase shift at the time vector zero position, dropping the part of the waveform which was previously zeroed out. After that a new linear fitting was applied to the temporal phase waveform. Figure 6.9 shows a new phase of the filtered temporal mixed signal. Note that the new fit has better precision.

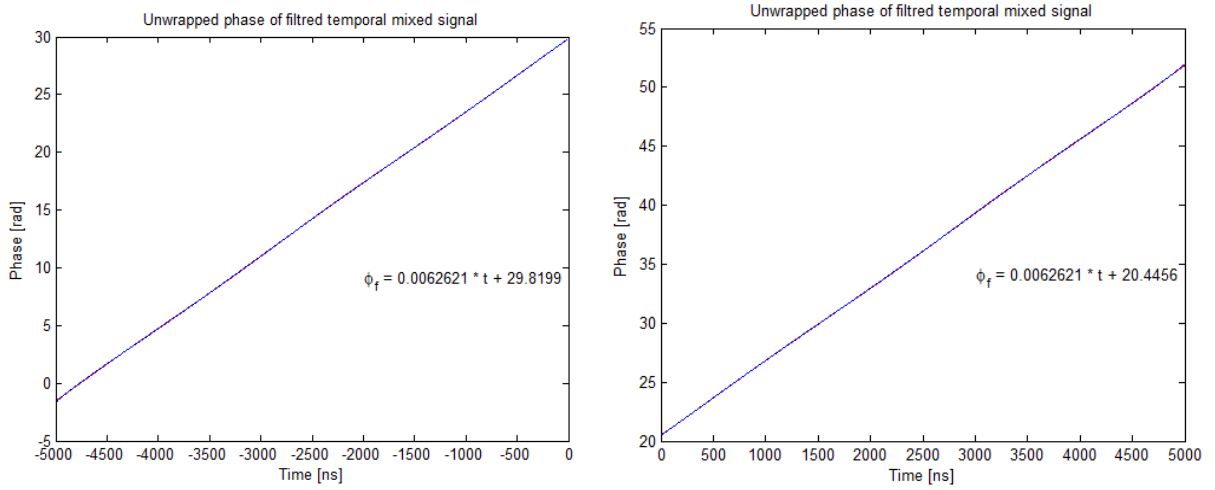


Figure 6.9: Split signal temporal phase, before (A) and after (B) shift.

Figure 6.10 shows the temporal phase with the linear part removed and the 3-dB coupler correction applied. The temporal phase shift waveform is not a straight line either. However, the total assessed phase shift displayed in Figure 6.11 is averaged at $\Delta\phi(t) = 3.27622766$ [rad] with error $\Delta = 0.13463501 \approx \frac{\pi}{23}$ [rad]. These results are considerably better than the ones achieved without phase splitting.

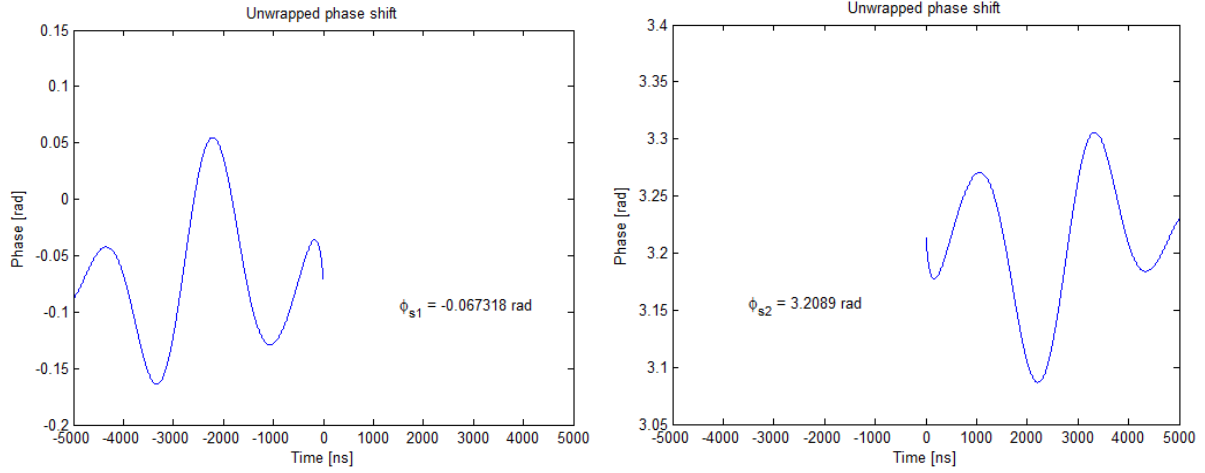


Figure 6.10: Split signal temporal phase with linear part removed and 3-dB coupler correction, before (A) and after (B) shift.

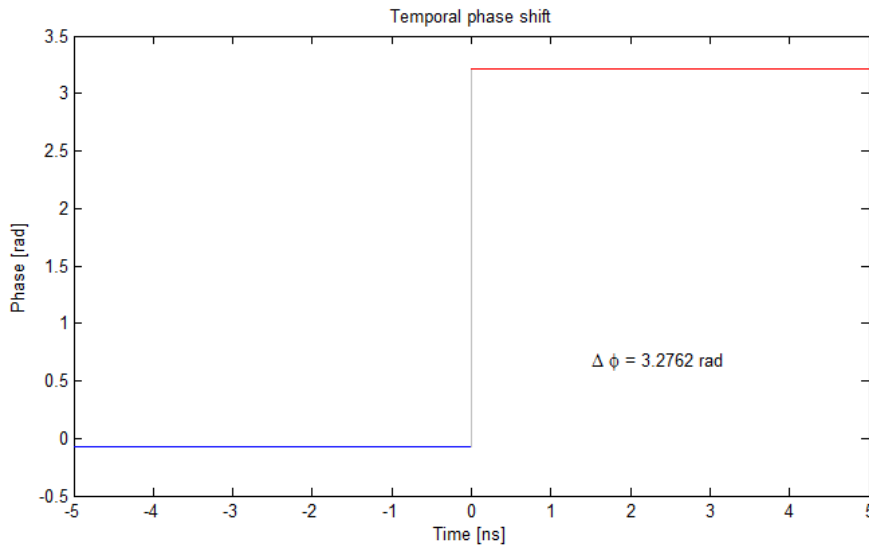


Figure 6.11: Assessed temporal phase shift.

Conclusion: The method of splitting the signal by zeroing out the unwanted part of the waveform demonstrates successful results for the spectral phase analysis. Unfortunately, it provides poor assessment for the temporal phase. Splitting the phase of the filtered temporal mixed signal at the time vector zero position after calculating the spectral phase shift, gives us the benefit of using both techniques discussed in Chapters 5 and

6, and decreases inaccuracy of calculations. However, the results achieved by splitting the waveform in Chapter 5 have higher precision especially for temporal phase shift assessment. In current chapter the highest error reaches $0.747 \approx \frac{\pi}{4}$ [rad].

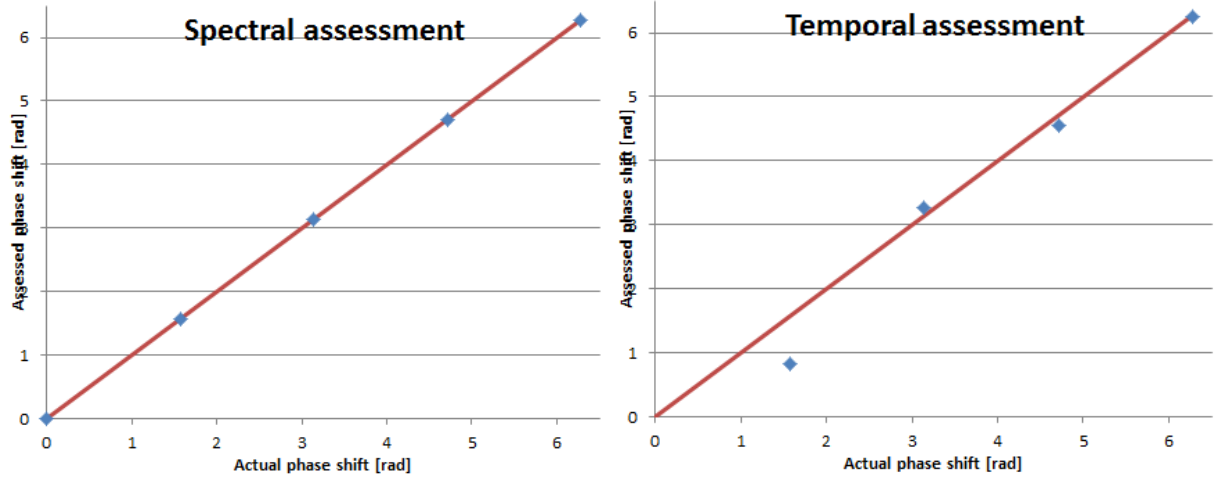


Figure 6.12: Assessed phase.

Table 6.1: Spectral $\Delta\phi(f)$ and temporal $\Delta\phi(t)$ phase shift assessment [rad]

Actual	Assessed $\Delta\phi(f)$	Δ	Assessed $\Delta\phi(t)$	Δ
0	$4.7938362377e^{-4}$	$4.7938362377e^{-4}$	-0.020412189	0.020412189
$\frac{\pi}{2}$	1.571275703	$4.793763093e^{-4}$	0.82287224	0.74792408196
π	3.14207204	$4.793836232e^{-4}$	3.27622766	0.13463501
$\frac{3\pi}{2}$	4.71286835669	$4.7937630865e^{-4}$	4.5618870515	-0.1505019288
2π	6.2827059235	$4.7938362426e^{-4}$	6.2627731177	-0.02041218941

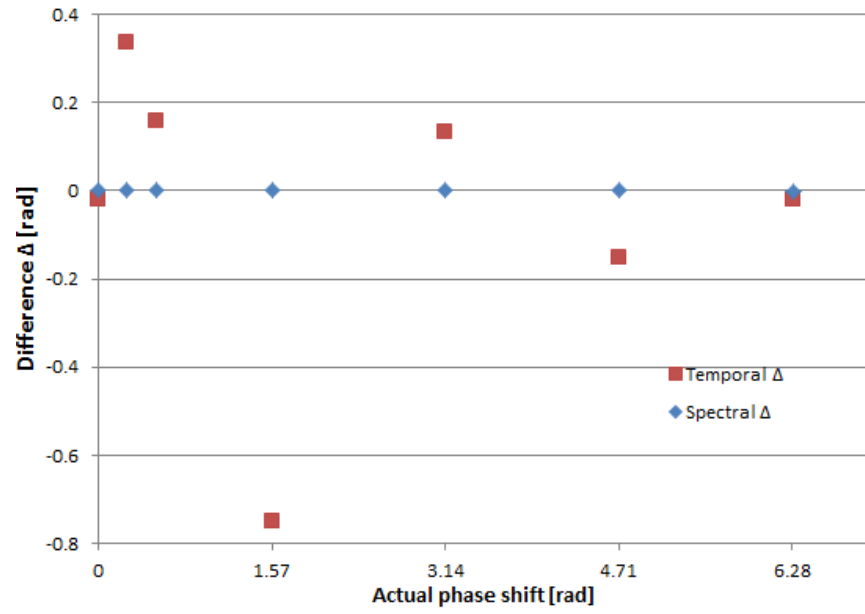


Figure 6.13: Δ difference error.

6.3 Summary of Optical Heterodyne Detection: Split Signal with Zero Out

The steps used to perform optical heterodyne detection of phase shifted signals for the split signal with zero out and split method are summarized as follows:

1. $P(t)$, using $\Delta f = f_s - f_o$ and $\Delta\phi = \phi_{s1} - \phi_{s2}$

$$\star \Delta f > \frac{2}{\delta t N_{sig}}$$

2. Split $P(t)$ at $\Delta\phi$ by zeroing out unwanted part

$$P_1(t) = P(t) \times \text{zero mask}_1 \text{ and } P_2(t) = P(t) \times \text{zero mask}_2$$

3. $\tilde{S}_1(f) = \mathcal{F}\{P_1(t)\}$ and $\tilde{S}_2(f) = \mathcal{F}\{P_2(t)\}$

$$\star \text{ (with 3-dB directional coupler) } \phi_{s1} = \phi_1(\Delta f) + \frac{\pi}{2} = \phi_1(-\Delta f) - \frac{\pi}{2}$$

$$\phi_{s2} = \phi_2(\Delta f) + \frac{\pi}{2} = \phi_2(-\Delta f) - \frac{\pi}{2}$$

$$\star \Delta\phi = \phi_{s2} - \phi_{s1} = \phi_2(\Delta f) - \phi_1(\Delta f)$$

4. $\tilde{S}_{f1}(f) = \mathcal{F}\{P_1(t)\} \times \Pi_1(\frac{f-f_0}{\alpha})$ and $\tilde{S}_{f2}(f) = \mathcal{F}\{P_2(t)\} \times \Pi_2(\frac{f-f_0}{\alpha})$

$$\star \alpha > 2\delta f = \frac{2}{\delta t N_{sig}}$$

5. $\tilde{P}_{f1}(t) = \mathcal{F}^{-1}\{\tilde{S}_{f1}(f)\}$ and $\tilde{P}_{f2}(t) = \mathcal{F}^{-1}\{\tilde{S}_{f2}(f)\}$

6. $\phi_{f1}(t) = \text{angle}\{\tilde{P}_1(f)\}$ and $\phi_{f2}(t) = \text{angle}\{\tilde{P}_2(f)\}$

7. Split the phase vectors $\phi_{f1}(t)$ and $\phi_{f2}(t)$ at the phase shift $\phi_{f1}(t1)$ and $\phi_{f2}(t1)$,

where $t1$ time vector before the shift, $t2$ time vector after the shift

$$\phi_{f1}(t1) = m_1 t1 + b_1 \text{ and } \phi_{f2}(t2) = m_2 t2 + b_2$$

$$\star \Delta\phi = b_2 - b_1$$

Chapter 7







Conclusion

In this chapter we summarize our study of using optical heterodyne detection to assess a phase shift. Table 7.1 provide a high-level summary. The temporal assessment provides a significant error in two methods — the non-split signal method and the split signal with zero out method. However, the temporal assessment provides a low error for the split signal method, and without introducing any FST term.

All spectral assessments yield much lower error. None of the spectral methods require the inverse Fourier transform or curve fitting like in the temporal assessment methods. However, the non-split signal method uses an odd equation which does not work for all $\Delta\phi(f)$. The split signal method requires introduction of Fourier Shift terms, while the split signal with zero out requires zero-out operations.

Based on the following considerations, we recommend using split signal or split signal with zero out for spectral phase shift assessment and split signal for temporal phase shift assessment. However, there is no need to proceed to the temporal phase shift assessment for the successful phase shift detection. Spectral phase assessment provides high precision results with the minimum of calculations.

Table 7.1: Summary of phase shift assessment

Method	Spectral Assessment	Temporal Assessment
Non-split signal	$\Delta\phi(f) = \phi(+\Delta f) - \phi(-\Delta f) + \pi$ $\Delta_{max} = 3.14255 \text{ [rad]}$ 	$\Delta\phi(t) = \phi_f(t) - (mt + b)$ $\Delta_{max} = 0.67 \text{ [rad]}$ 
Split signal	$\Delta\phi(f) = \phi_{s2} - \phi_{s1} - 2\pi(f_2t_{o2} - f_1t_{o1})$ $\Delta_{max} = 4.8e^{-4} \text{ [rad]}$ 	$\Delta\phi(t) = b_2 - b_1$ $\Delta_{max} = 4.7e^{-4} \text{ [rad]}$ 
Split signal with zero out	$\Delta\phi(f) = \phi_{s2}(\Delta f) - \phi_{s1}(\Delta f)$ $\Delta_{max} = 4.8e^{-4} \text{ [rad]}$ 	$\Delta\phi(t) = b_2 - b_1$ $\Delta_{max} = 0.748 \text{ [rad]}$ 

Bibliography

- [1] C. Dorrer, “Interferometric techniques for the characterization of temporal modulators,” *IEEE Photon. Technol. Lett.*, vol. 17, 2688-2690, 2005.
- [2] J. R. Barry, E. A. Lee, “Performance of Coherent Optical Receivers,” *Proceedings of the IEEE*, vol. 78, 1369-1394, 1990.
- [3] O. E. DeLange, “Optical Heterodyne Detection,” *IEEE Spectrum*, vol.57, 77-85, 1968.
- [4] G. D. Goodno and G. Dadusc, “Ultrafast heterodyne-detected transient-grating spectroscopy using diffractive optics,” *Optical Society of America*, Vol. 15, No. 6, 1791-1794, 1998.
- [5] J. Palais, “Fiber optic communications,” *Pearson Education*, Upper Saddle River, N.J, 1998.
- [6] R. Hui and M. OSullivan, “Fiber optic measurement techniques,” *Academic Press*, Salt Lake City, 2008.